Functional genomic approaches to manipulating Bordetella pertussis outer membrane synthesis for vaccine development.

Mcculloch, David

Award date:
2023

Awarding institution:
University of Bath

Functional genomic approaches to manipulating *Bordetella pertussis* outer membrane synthesis for vaccine development.

David John McCulloch MSc

A thesis submitted for the degree of Doctor of Philosophy

University of Bath

Department of Biology and Biochemistry

Table of Contents

Table of Figures

Table of Tables

Abbreviation list

ACT - Adenylate cyclase toxin, **ACV** - Acellular vaccine, **BVG+** - Highly activated state of the BVG two component system, **BVGi** - Intermediately activated state of the BVG two component system, **BVG-** - Inactivated state of the BVG two component system, **CFU** - Colony forming unit, **CR3** - complement receptor type 3, **D-ala** - D-alanine, **D-glu** - D-glutamic acid, **DLS** - Dynamic light scattering, **FHA** - Filamentous hemagglutinin, **FIM2** - Fimbriae type 2, **FIM3** - Fimbriae type 3, **FIOW** - fluorescence intensity over wildtype, **GlcNAc** - N-acetylglucosamine, **HK** - Histidine kinase, **IM** - Inner membrane, **L-ala** - L-alanine, **Lpp** - Brauns lipoprotein, **LPS** - Lipopolysaccharide , **LRI/IAP** - leukocyte response integrin/integrin associated protein complex, **mDAP** - meso-diaminopimelic acid, **MurNAc** - N-acetylmuramic acid , **NTA** - Nanoparticle tracking analysis, **OM** - Outer membrane, **OmpA** - Outer membrane porin A, **OMV** - Outer membrane vesicle, **PG** - Peptidoglycan , **PL** – Phospholipids, **PRN** – Pertactin, **PT** - Pertussis toxin, **TCT** - Tracheal cytotoxin, **Th1** – Type 1 T helper cell , **Th2** - Type 2 T helper cell , **Th17** - Type 17 T helper cell , **TraDIS** - Transposon directed insertion site sequencing, **TRM** - Tissue resident memory T cell, **VFT1&2** - Venus fly trap domain 1 and 2 , **WCV** - Whole cell vaccine

Acknowledgements

I would like to thank my supervisor at the University of Bath, Professor Andy Preston for his advice, support, and guidance during my time in Bath.

I would also like to thank Preston lab group members past and present for their help and expertise over the past three and a half years.

I would like to thank my GSK co-funders and my collaborators at GSK Vaccines Siena, with special mention to Dr Isabel Delany, Dr Scilla Buccato, Dr Daniela Rinaudo and Dr Marco Spinsanti for their help during my secondments in Siena.

I would like to thank my partner for their endless patience, support and letting me bore them with endless venting of experimental trouble shooting.

Finally, I would like to thank all my family, especially my parents, for their encouragement and belief in me during my PhD.

Conflict of interest statement

This research is sponsored by the University of Bath and GlaxoSmithKline Biologicals and may lead to the development of products which may be licensed to GSK, from which I have received funding to cover research costs, a PhD stipend and two three-month secondments at their site in Siena Italy.

Abstract

Bacterial growth and replication are dependent upon the expression of cell wall biosynthesis genes, many of whom are essential for bacterial viability. The *mre/mrd* operon is a set of such genes which carries out synthesis of the peptidoglycan (PG) sacculus during bacterial elongation. The manipulation of the *mre/mrd* operon in gram-negative bacteria is lethal under unmodified growth conditions, resulting in them being classified as essential for bacterial viability. However, this does not appear to be the case in *B. pertussis*

In *B. pertussis* the *mre/mrd* operon is conditionally essential during *in vitro* plate growth, dependent on the activation state of the BVG two component system. This poses the questions of:

- whether *mre/mrd* mutation induces phenotypic changes in *B. pertussis* as observed in other gram-negative bacteria?

- how a fastidious bacteria like *B. pertussis* tolerates the loss of these classically essential cell wall biosynthesis genes?

-whether disruption of the peptidoglycan sacculus in *mre/mrd* mutants results in increased outer membrane vesicle (OMV) production, which have shown promise as vaccine antigens against *B. pertussis*?

Analysis of *mre/mrd* mutant strains growth phenotypes displayed that essentiality was only observed during *in vitro* plate growth under BVG- modulating conditions. Conversely the *mre/mrd* operon was non-essential during bacterial growth in *in vitro* liquid culture independent of BVG activation state. Interestingly, this was despite the change in bacterial morphology, which was observed upon mutation of *mre/mrd* in other gram-negative bacteria, being present in *B. pertussis*.

Utilising transcriptomic profiling of BP536 wildtype *B. pertussis* during growth in plate and liquid culture mediums, I investigated how *B. pertussis* could tolerate the loss of classically essential cell wall biosynthesis genes. This analysis identified genes involved in glycine betaine transport, a well characterised osmoprotectant, to be significantly upregulated during

BVG- broth growth, where mutants are viable, when compared to BVG- plate growth, where mutants are non-viable. This analysis suggests that the bacteria's ability to regulate osmolarity, through betaine uptake, facilitates tolerance of *mre/mrd* mutations. This finding was validated by betaine supplementation rescuing BP_{536}*ΔmreB* BVG- plate viability. However, BP_{536}*ΔmreB* broth viability was not altered upon loss of the ATPase of the betaine glycine uptake system, suggesting conditional viability dependent upon BVG- growth medium is multifactorial.

Characterisation of the vesiculation phenotype of *mre/mrd* mutants displayed hypervesiculation was induced upon loss of elongasome peptidoglycan biosynthesis, with comparable levels of vesiculation to other hypervesiculating *B. pertussis* strains. Characterisation of OMV phenotypes displayed *mre/mrd* mutants OMVs had antigen profiles like that of OMVs produced by wildtype strains. Promisingly, the average size of OMVs produced by mutant strains were in the optimum range for uptake by immune cells. Overall, this analysis suggests that *mre/mrd* mutant strains are promising for OMV production to be utilised as vaccine antigens.

Chapter 1-Introduction

1.1-The gram-negative bacterial cell envelope-

The gram-negative bacterial cell envelope is a multifunctional barrier which shields the bacterium from the external milieu. The cell envelope can facilitate bacterial survival in hostile and rapidly changing environments through the maintenance of cellular physiochemical conditions. Therefore, it is not surprising that gram-negative bacteria have complex envelope architecture, facilitating the balance of protection and interaction with the external environment.

The gram-negative bacterial envelope consists of three layers; the outer membrane (OM), the inner membrane (IM) and situated between the two in the periplasmic space the peptidoglycan (PG) layer (Figure 1.1) (Glauert and Thornley, 1969, Silhavy et al., 2010).

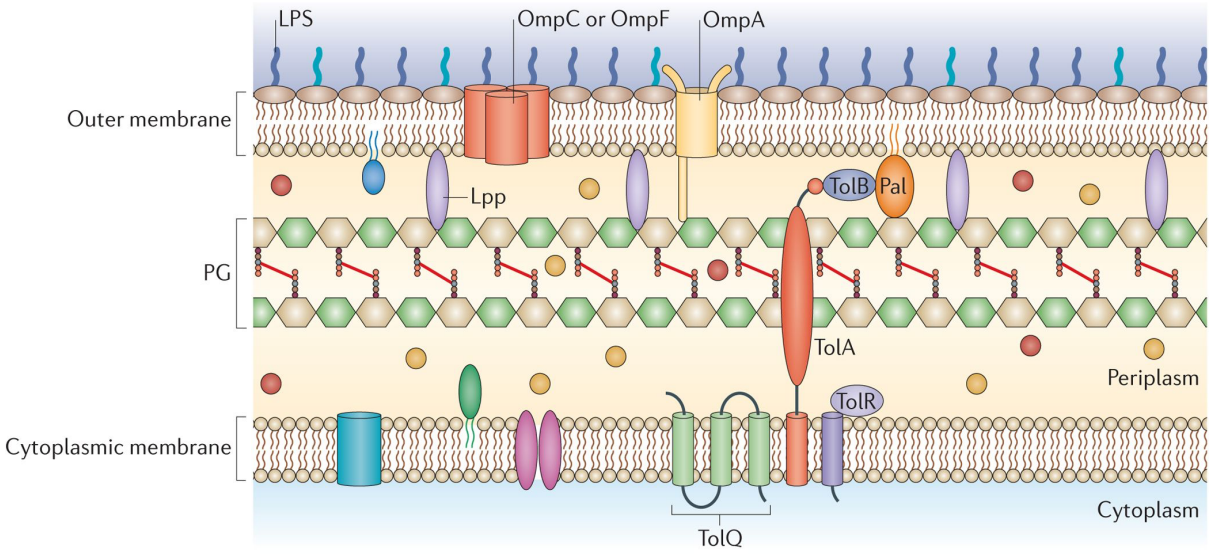

Figure 1.1- Architecture of the gram-negative bacterial cell envelope. The envelope of gram-negative bacteria is made up of two membranes, the outer and the cytoplasmic/inner membrane between which there is a layer of peptidoglycan (PG). Protein crosslinks between the PG layer and the two bacterial envelope membranes are depicted. Figure from Schwechheimer et al., 2015 (Schwechheimer et al., 2015).

1.1.1-The bacterial IM-

The IM consists of a bilayer of phospholipids (PL) (Miura and Mizushima, 1968, Osborn et al., 1972). As this membrane is the interface between the bacterial cytoplasm and the periplasmic space, numerous membrane associated transport systems span the PL bilayer important in nutrient transport, energy production and protein secretion.

1.1.2-The bacterial OM-

The bacterial OM also displays a bilayer architecture with the inner leaf of the membrane consisting of PL (Osborn et al., 1972, Miura and Mizushima, 1968). However, unlike the IM, the outer leaf is made up of a glycolipid called lipopolysaccharide (LPS). LPS acts as a barrier to the entry of both hydrophilic and hydrophobic molecules due to its amphipathic nature (Nikaido, 2003, Carpenter et al., 2016). The selective permeability of the OM is therefore highly reliant on outer membrane porins, which allow the controlled diffusion of environmental hydrophilic molecules into the bacterium.

1.1.3-The PG sacculus-

To maintain the structure and stability of both the IM and OM, gram negative bacteria assemble a large polymer of PG in the periplasmic space (Nanninga, 1998, Mengin-Lecreulx and Lemaitre, 2005). This structure is made up of glycan chains of disaccharide subunits; N-acetylglucosamine (GlcNAc) and N-acetylmuramic acid (MurNAc), and peptide chains (Figure 1.2). Peptide chains are composed of amino acid residues of L-alanine (L-ala), D-glutamic acid (D-glu), meso-diaminopimelic acid (mDAP) and D-alanine (D-ala). Interactions between mDAP residues and D-ala allow for peptide bridge formation between peptide chains of neighbouring glycan strands, facilitating the formation of a large glycoprotein.(Vollmer, 2008).

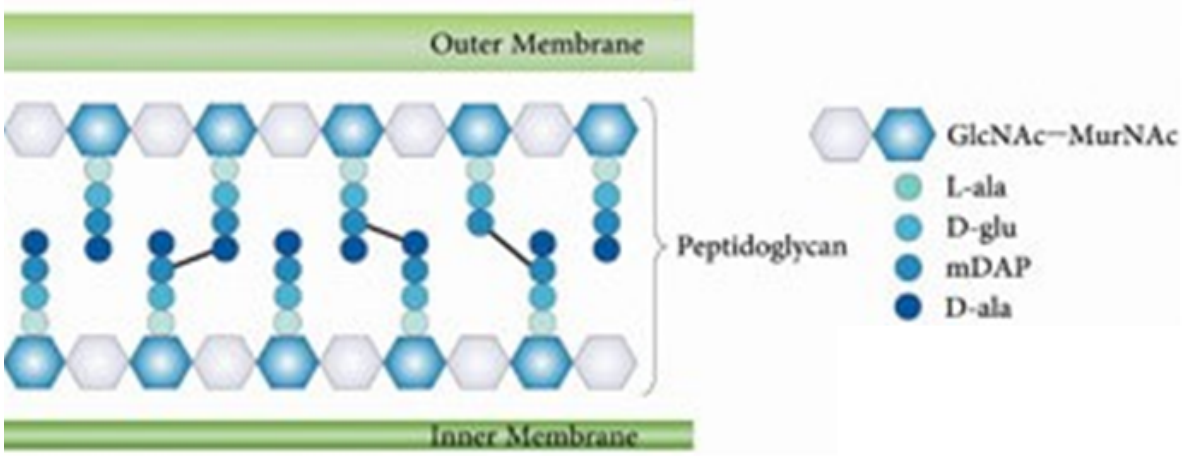

Figure 1.2- PG sacculus composition in gram-negative bacteria. Glycan chains are made up on repetitive units of GlcNAc and MurNAc bound together by glycosidic bonds. Peptide chains composed of L-ala, D-glu, mDAP and D-ala protrude from the MurNAc subunit of the glycan chain. Peptide bonds between the peptide chains form between D-ala and the D-ala or mDAP of neighbouring glycan strands allowing the formation of a sacculus. Figure from Garde et al., 2021 (Garde et al., 2021).

The PG sacculus functions to allow bacteria to maintain cellular integrity against variations in environmental osmolarity which can induce bacterial turgor or swelling. Due to the important role in bacterial viability, PG biosynthesis mechanisms are highly conserved in gram-negative bacteria (Schneider and Sahl, 2010).

PG biosynthesis begins in the bacterial cytoplasm where a complex cascade of enzymatic reactions occurs, changing UDP-GlcNAC to UDP-MurNAc and attaching the pentapeptide chain. UDP-MurNAc is attached to the IM by binding to undecaprenyl phosphate (UDP) (Figure 1.3) (Garde et al., 2021). The bound UDP-MurNAc-pentapeptide is called Lipid I, which then undergoes the addition of a GlcNAC molecule by the *murG* family of enzyme's forming the PG precursor Lipid II. (Kotnik et al., 2007, Walsh, 1989, Neuhaus and Hammes, 1981). Lipid II is then flipped across the IM into the periplasmic space by flippase enzymatic activity (Heijenoort, 2001). In the periplasmic space lipid II is then incorporated into the growing PG sacculus by penicillin binding protein transpeptidase and transglycosylase activity (Figure 1.3) (Den Blaauwen et al., 2008).

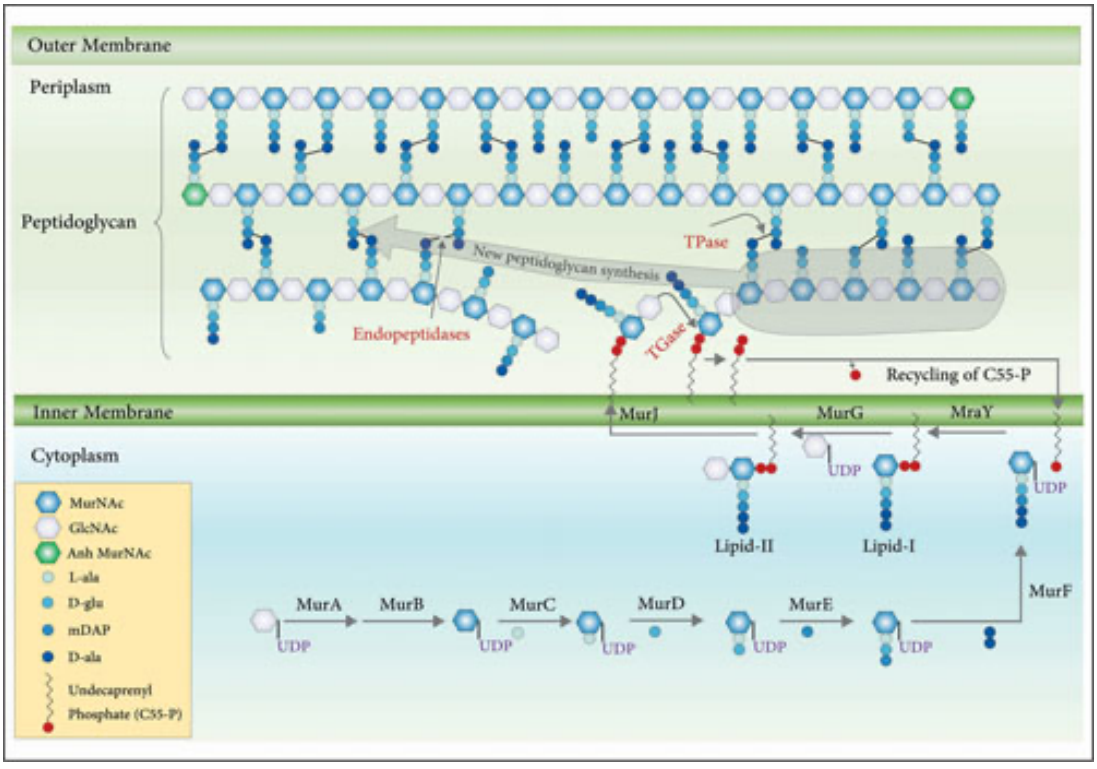

Figure 1.3- The PG biosynthesis pathway. Cytoplasmic stage of PG biosynthesis where UDP-MurNAc-pentapeptide is produced by a series of enzymatic reactions converting UDP-GlcNAc to UDP-MurNAc-pentapeptide catalysed by the Mur family of enzymes. The Inner membrane associated stage of PG biosynthesis where UDP-MurNAc-pentapeptide is converted to Lipid I then Lipid II. After this Lipid II is translocated across the inner membrane into the periplasm by a transmembrane Lipid II flippase. The periplasmic stage of PG

biosynthesis where class I and II penicillin binding proteins polymerise lipid II precursors into the exiting PG sacculus by transglycosylation (TGase) and transpeptidation (Tpase). Figure from Garde et al., 2021 (Garde et al., 2021).

The PG structure is constantly modified by the bacterium via the hydrolysis of existing glycans and the replacement of these with newly synthesised strands (Egan et al., 2020). These processes occur in tandem to limit the effect on neighbouring PG strands stability. Mismanagement of this process can result in cracks in the PG sacculus. This rigid structure determines both the membrane stability and the morphology of the bacterium and is key in bacterial survival and viability.

In rod shaped gram-negative bacteria, two PG biosynthesis pathways have been identified linked to bacterial division during replication and to bacterial elongation, named the divisome and elongasome respectively. These two pathways are highly conserved across gram-negative bacterium with their functions key in bacterial viability (Suzuki et al., 1978a, Denome et al., 1999, Meberg et al., 2001).

1.1.4-Divisome PG biosynthesis-

The bacterial divisome regulates the division of the parent bacterium into the two daughter cells during binary fission (Angert, 2005). During this process, PG synthesis is necessary to form a divisive barrier between the two daughter cells. This barrier is the PG septum (Szwedziak et al., 2014, Chen and Erickson, 2005). At the site of bacterial division, PG synthesis occurs in an inwards direction, forming a ring of PG which enables the bacterium to split into two daughter cells (Gamba et al., 2009, Ma et al., 1996). This process is regulated by the Fts protein family which encodes the divisome apparatus. FtsZ is one such protein that is highly conserved across bacteria. FtsZ is a homolog to tubulin which regulates the location of the septum by associating with the mid-cell cytoplasmic membrane. This association is facilitated by FtsZ interacting with the actin homolog FtsA, which enables the formation of a dynamic structure consisting of proteins related to cytokinesis and the synthesis of PG, named the Z-ring (Ma et al., 1997). When all components have been recruited to the bacterial mid-cell, the Z-ring tightens, pinching the parent bacterium into two identical daughter cells (Bisson-Filho et al., 2017). This tightening process is due to FtsZ treadmilling, where the FtsAZ complex travels around the circumference of the Z-ring, allowing progressive synthesis and incorporation of new PG into the sacculus until the ring is closed.

1.1.5-Elongasome PG biosynthesis-

In rod-shaped gram-negative bacteria, another set of proteins synthesise PG during bacterial elongation. This process is dependent on a five gene operon encoding MreB, MreC, MreD, MrdA (PBP2) and MrdB (RodA) proteins, named the *mre/mrd* operon (Figure 1.4) (Varma and Young, 2009, White et al., 2010). Lipid II is transported to the cytoplasmic side of the IM by MreB. MreB functions as bacterial actin, transporting and coordinating the PG precursors and the PG elongation enzyme complex at the bacterial IM (Colavin et al., 2018). Lipid II is then translocated across the IM into the periplasmic space. This translocation is carried out by MrdB (RodA) via its flippase activity (Tamaki et al., 1980, Sieger et al., 2013). Lipid II precursors are polymerised into a nascent PG chain which is incorporated into the PG sacculus by the transpeptidase activity of MrdA (PBP2) (Figure 1.4) (Den Blaauwen et al., 2003). The precise roles of MreC and MreD are less well defined but they are important in cell wall synthesis in *E. coli,* with MreB failing to form filaments upon depletion of MreC or MreD (White et al., 2010).

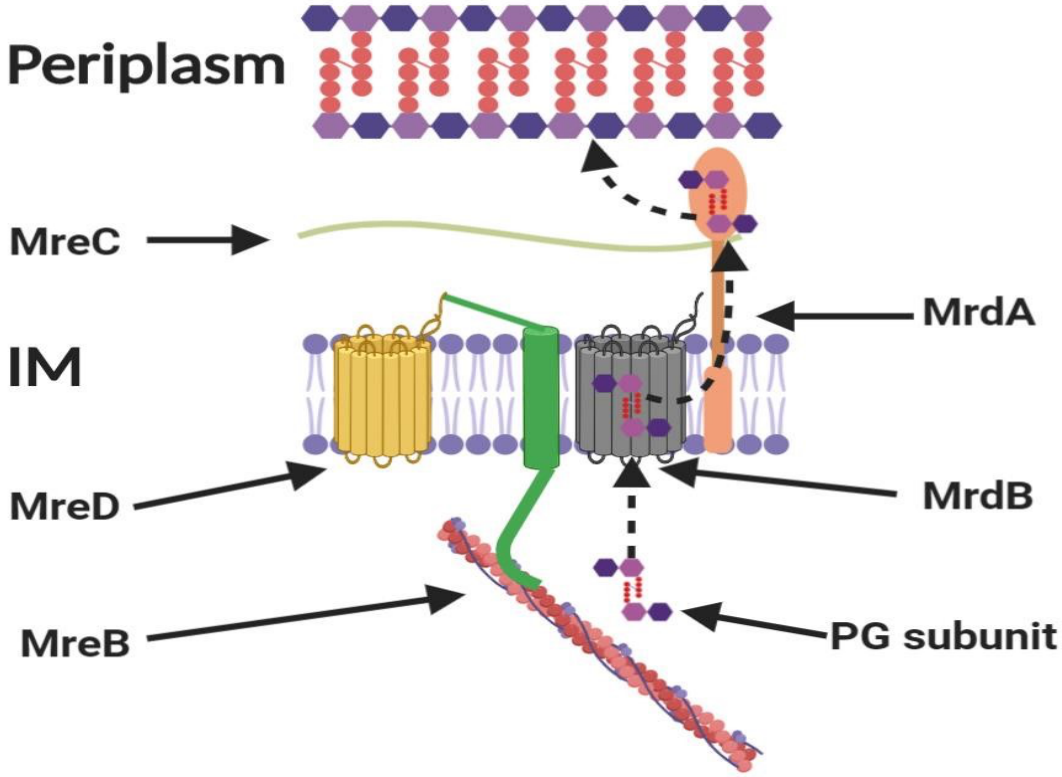

Figure 1.4- The Mre/Mrd protein complex. Function of mre/mrd proteins transporting lipid II precursors across the IM and incorporating it into the PG sacculus. Figure inspired by White and Gober, 2012 (White et al., 2010). Created with BioRender.com

1.1.6- The relationship between PG crosslinking and bacterial viability-

For the PG sacculus to facilitate the bacterium's ability to tolerate osmotic pressures it must provide stability to the OM. This stabilisation is due to PG-protein interactions that link the PG sacculus to both the IM and OM in gram-negative bacteria. Three proteins that are highly conserved in gram-negative bacteria with their interactions with the PG sacculus being key in cell wall stability are; Brauns lipoprotein (Lpp), the Tol-Pal complex and outer membrane porin A (OmpA) (Braun, 1975, Huang et al., 1983, Cascales et al., 2002, Wang, 2002). The importance of these interactions in maintaining bacterial physiology is highlighted by the drastic effect of the knockout of the genes encoding these proteins. Mutation of Lpp, Tol-Pal or OmpA induces OM instability, reducing the bacteria's ability to tolerate OM stress and altering OM morphology (Sonntag et al., 1978, Yeh et al., 2010, Cascales et al., 2002). Mutants displayed an increased sensitivity to detergents and the hydrophobic antibiotic vancomycin, had perturbed growth phenotypes and displayed cell division defects, illustrating the importance of these proteins in the cell envelope structure (Sonntag et al., 1978, Yeh et al., 2010, Cascales et al., 2002).

1.1.7-The relationship between PG biosynthesis and bacterial viability-

With the importance of protein-PG interactions being well characterised, it is not surprising that PG biosynthesis mechanisms are also highly important in maintaining bacterial physiology. FtsZ, the key protein in the organisation of the divisome PG biosynthesis machinery, is essential for bacterial viability (De Boer et al., 1992).

The elongasome on the other hand has been displayed to be more tractable in comparison to the divisome in gram-negative bacteria. The function of MreB has been probed by introduction of point mutations into its coding sequence in both *E. coli* and *B. subtilis,* with a variety of effects on cell morphology depending on the region targeted being observed. Mutants displayed alterations in the width, branching and bending of the bacteria (Shi et al., 2017, Morgenstein et al., 2017, Morgenstein et al., 2015, Ouzounov et al., 2016, Kawazura et al., 2017). Interestingly, the growth rate of some of these point mutants was comparable to wildtype, suggesting point mutagenesis by amino acid replacement was not inducing a detrimental phenotype (Shi et al., 2017). However, this is not the case when *mreB* is knocked out in gram-negative bacteria.

In studies looking at the effect of *mreB* mutation in *B. subtilis*, *C. crescentus* and *E. coli* it was observed that mutation of *mreB* in *B. subtilis* and *C. crescentus* was lethal, whereas in *E. coli* lethality was dependent upon growth conditions (Wachi et al., 1987, Kruse et al., 2003,

Soufo and Graumann, 2003, Lee and Stewart, 2003, Kobayashi et al., 2003, Bendezú and de Boer, 2008).

In *E. coli,* upon the knockout of *mreB, mreC* or *mreD* expression, cells became turgid spheres prone to lysis. This was independent of whether genes were knocked out individually, or as an operon, displaying that all three genes are essential in *E. coli (*Bendezú and de Boer, 2008). However, despite the dramatic effect of the knockout of these genes on bacterial physiology, tolerance mechanisms were identified. It was found that mutant viability was dependent on the rate of biomass production, with growth in highly nutrient limited conditions allowing mutants to remain viable. Interestingly the overexpression of the divisome genes *ftsQ, ftsA* and *ftsZ* resulted in a restoration of viability, most likely due to the resulting increased levels of divisome PG biosynthesis. Recently a previously uncharacterised mechanism of tolerance to *mreB* disruption in *E. coli* was identified utilising the MreB depolymerisation drug A22. Removal of malate dehydrogenase by mutagenesis resulted in increased tolerance to A22 (Barton et al., 2021). Malate dehydrogenase mutants had an increased level of the PG precursor UDP-GlcNAc when compared to wildtype. This suggests that increased PG biosynthesis due to high concentrations of PG precursors may facilitate tolerance of the loss of elongasome PG biosynthesis.

Overall, this displays that the elongasome is tractable in several bacteria. However, the manipulation of this highly conserved mechanism has a detrimental effect on bacterial physiology, introducing osmotic instability. There have been mechanisms identified that allow bacteria to tolerate the loss of PG biosynthesis during bacterial elongation, namely the upregulation of alternate PG biosynthesis mechanisms or increased availability of PG precursors.

1.2-*Bordetella pertussis*-

B. pertussis is a gram-negative bacteria which colonises the upper respiratory tract of humans and is the main causative pathogen of whooping cough; (Bordet and Gengou, 1906, de Greeff et al., 2010). *B. pertussis* is part of the genus *Bordetella* from which only a handful of species have adapted to cause disease in humans; *B. pertussis, B. parapertussis, B. bronchiseptica, and B. holmesii*. Of these species, *B. pertussis* is by far the most prevalent human pathogen, causing the majority of the disease burden in human populations, with other species limited to opportunistic infections (Hamidou Soumana et al., 2017, Mattoo and Cherry, 2005). Human infections are key in the lifecycle of *B. pertussis* as it is an obligate

pathogen of humans, reliant on effective colonisation and persistence in the upper respiratory tract with humans being the only known reservoir for pertussis (Cotter and Miller, 2001, Mattoo et al., 2001).

1.2.1-Clinical manifestation of *B. pertussis* infections-

B. pertussis transmission is thought to occur via aerosol droplets mechanism, with infection of the upper respiratory tract occurring upon inhalation of droplets released by an infected individual (Warfel et al., 2012). Pertussis, the disease caused upon *B. pertussis* infection, is a disease of four phases.

The initial incubation phase where infection is asymptomatic can occur for 1-2 weeks, during which *B. pertussis* colonises and replicates in the upper respiratory tract of the infected individual. Symptom onset occurs after this incubation period with the patient entering the catarrhal phase of disease (Mattoo and Cherry, 2005). This phase is characterised by fever, a progressive cough and rhinorrhoea. After this the patient enters the spasmodic/paroxysmal phase of disease characterised by the development of a persistent and severe paroxysm, during which serious complications can occur. These complications include acute encephalopathy and pneumonia which can be fatal. This phase can vary greatly in longevity, lasting 1-3 months, after which the individual will enter the convalescents phase of disease.

1.2.2-Pathogenesis of *B. pertussis* infections-

The pathogenesis of *B. pertussis* is dependent on key virulence factors that facilitate bacterial attachment to the upper respiratory tract, modulate the host immune responses and induce damage both at the site of infection and systemically (Mattoo and Cherry, 2005).

Bacterial attachment-

One of the most dominant adhesins for *Bordetella* attachment is Filamentous hemagglutinin (FHA), a hairpin shaped protein which can be presented on the bacterial surface or secreted from the bacterial membrane by the cleavage of the tethering C terminus by a protease, SphB1 (Relman et al., 1989, Coutte et al., 2001, Mazar and Cotter, 2006). OM bound FHA attaches to the host upper respiratory tract through a RGD (Arg-Gly-Asp triplet) domain contained at the proximal portion of the hairpin structure (Saukkonen et al., 1991, Relman et al., 1990, Ishibashi et al., 1994). This domain facilitates bacterial attachment by binding of mammalian OM receptors and protein complexes; complement receptor type 3 (CR3) and the

leukocyte response integrin/integrin associated protein complex (LRI/IAP) (Ishibashi et al., 2002, Ishibashi and Nishikawa, 2002, Van Strijp et al., 1993).

Fimbriae have also been identified to play a role in adhesion to the host epithelium. *B. pertussis* encodes a type 1 pili in the *fimBCD* operon with the major fimbrial subunits encoded by *fim2* and *fim3* (Willems et al., 1992). Analysis of the FimD tip component of the *B. pertussis* fimbriae, displayed an ability to bind heparin, a sugar ubiquitous in the upper respiratory tract (Geuijen et al., 1997). This and the fact that *ΔfimD* strains had a decreased ability to colonise murine respiratory tracts, highlights that *B. pertussis* fimbriae play a role in bacterial attachment during colonisation.

Pertactin (PRN), an autotransporter with a surface exposed β-helix domain, has also been highlighted to play a role in attachment as it contains a RGD motif, the same observed in FHA, suggesting an ability to bind to CR3 and LRI/IAP on the epithelial surface (Emsley et al., 1994).

Modulation of host immune response-

To persist in the upper respiratory tract of humans, *B. pertussis* modulates the host immune response to prevent immune killing. To do this *B. pertussis* exports bacterial toxins which modulate the host cells. Two toxins observed to function in this manner are pertussis toxin (PT) and adenylate cyclase toxin (ACT).

PT is made up of two subunits named A and B. The A subunit is the catalytic part of the toxin with subunit B consisting of membrane binding subunits important in toxin transport (Stein et al., 1994a). PT is assembled in the bacterial cytoplasm, after which it is secreted by the *ptl* type IV secretion system (Kotob et al., 1995). PT binds a broad variety of host receptors through its affinity with sialic acid containing glycoproteins. Upon binding to these receptors, PT is internalised into the host cell by receptor mediated endocytosis (Locht et al., 2011, Stein et al., 1994b). Internalised PT is trafficked through the host cell by a retrograde transport pathway, eventually reaching the host endoplasmic reticulum (ER) (el Bayâ et al., 1999, Plaut et al., 2016). PT is cleaved in the host ER and the A-subunit exits into the host cell cytoplasm (Worthington and Carbonetti, 2007). PT subunit A displays catalytic activity, increasing rate of transfer of an ADP-ribose groups to the internal α-subunit of G proteins (Graf et al., 1992, Katada, 2012, Mangmool and Kurose, 2011). The modification of G proteins has a pleiotropic effect on cellular pathways, meaning the precise roles it plays in facilitating *B. pertussis* infection are difficult to distinguish. However, PT effectively reduces

the production of cytokines and chemokines, reducing the recruitment of immune cells to the site of infection, through modulation of host G protein signalling (Carbonetti et al., 2007, Kirimanjeswara et al., 2005, Andreasen and Carbonetti, 2008, Spangrude et al., 1985).

ACT is made up of two functional domains. The C-terminus of the protein binds to the host cell and generates a cation-selective pore through its haemolysin moiety (Sakamoto et al., 1992, El-Azami-El-Idrissi et al., 2003). The N- terminus is the enzymatic domain, displaying adenylate-cyclase activity facilitating the conversion of ATP to cyclic-AMP (Glaser et al., 1989, Ladant et al., 1989). ACT binds preferentially to CR3 which is highly expressed on phagocytic immune cells (Guermonprez et al., 2001). ACT multimers integrate into the host cells membrane through their C-terminus, forming a pore through which the N terminal domain is translocated (Osicková et al., 1999, Fiser et al., 2012). The ability of ACT to disrupt immune cell's responses is via the adenylate-cyclase activity of its N- terminus, resulting in the elevation intracellular cyclic-AMP concentrations. Through this activity ACT perturbs fundamental immune processes such as oxidative burst, chemotaxis, and phagocytosis (Eby et al., 2014, Paccani et al., 2008, Kamanova et al., 2008, Cerny et al., 2015). ACT multimers have also been observed to play a role in altering the host immune response by inducing immune cell death through apoptosis (Basler et al., 2006). This process is mediated by the formation the ACT cation-selective pores in immune cell membranes. Pore formation results in potassium ion efflux triggering apoptosis. However, this process is of secondary importance *in vivo*, with N-terminus adenylate cyclase activity essential for *B. pertussis* colonisation of murine models but C-terminal haemolysin activity non-essential (Skopova et al., 2017).

Localised damage-

Virulence factors secreted by *B. pertussis* during colonisation and growth in the upper respiratory tract result in damage to the host airways, contributing to disease pathogenesis. The classical symptom of paroxysmal cough if predicted to be due to this damage.

One such toxin is tracheal cytotoxin (TCT). TCT is a by-product of PG biosynthesis that is produced during the remodelling of the bacterial cell (Cookson et al., 1989). This molecule is inefficiently recycled in *B. pertussis,* meaning large quantities are released extracellularly during *B. pertussis* growth and replication (Park, 1993, Mielcarek et al., 2006). TCT is internalised into host cells and induces a proinflammatory response against these cells by binding and activation of the cytosolic pattern recognition receptor NOD1 (Magalhaes et al.,

2005). This inflammatory response results in damage to the airway epithelium by immune killing of host cells that is thought to aggravate disease pathogenesis. This is supported by strains with perturbation of TCT recycling, by the mutation of the permease AmpG, causing significantly increased damage to murine lungs upon infection (Skerry et al., 2019).

PT induced damage to the lung epithelium is also thought to play a role in the pathogenesis of pertussis. Despite the well characterised immunomodulatory effects of PT previously discussed, at the height of infection PT is observed to have a proinflammatory effect (Connelly et al., 2012). The proinflammatory response induced by high levels of PT is characterised by the induction of proinflammatory cytokines IFNγ, TNFα and IL-17 in murine models (Petersen et al., 1992, Andreasen et al., 2009). A study which analysed the transcriptional alterations upon challenge with wildtype and PT deficient *B, pertussis* strains in mice highlighted this further. The majority of differentially expressed gene identified in this study were associated with inflammatory and immune signalling pathways, as well as genes associated with known pulmonary disorders (Connelly et al., 2012). The contribution of these mechanisms to pathogenesis was further displayed in baboon infection studies, where coughing was only induced upon infection with a PT+ strains, with a PT- isogenic strain failing to induce coughing (Warfel et al., 2012).

Systemic effects-

Secreted virulence factors contribution to disease pathogenesis are not restricted to the site of infection, with systemic effects significantly contributing to the pathogenesis of pertussis.

PT has also been displayed to have a robust systemic effect *in vivo,* one of which is the induction of leucocytosis, a term used to describe the presence of high numbers of circulating white blood cells (Hinds et al., 1996). Leucocytosis is inherently linked with poor prognosis of *B. pertussis* infections, with it being a hallmark symptom in fatal cases (Winter et al., 2015). PT is thought to induce leucocytosis through its modulation of G protein signalling, inducing perturbation of chemokine mediated trafficking of leucocytes and reducing leucocyte specific adhesin expression (Hodge et al., 2003, Beck et al., 2014). Other effects of PT have been observed across a broad range of organs in murine models upon administration of purified PT, displayed by its use in the induction of autoimmune diseases in murine models (Su et al., 2001). However, the relevance of these findings to clinical pathogenesis is unknown.

1.2.3- Regulation of gene expression in *B. pertussis* and its contribution to disease-

A common mechanism of gene expression regulation in bacteria is two component phosphorelay systems (Appleby et al., 1996). These systems are primarily involved in the control of gene responses to environmental stimuli, such as the induction of virulence factor expression during colonisation of hosts (Gross, 1993). Two component systems utilise histidine kinase (HK) enzymatic activity to transfer a phosphate group from a sensory component to a response regulator domain, activating expression of controlled genes.

In *B. pertussis* a two-component system has been identified to be a master regulator of gene expression, with more than 550 genes of the 3456 encoded being controlled by this two-component system in the Tohama I strain (Moon et al., 2017). Therefore, there are large scale biological and phenotypic changes in *B. pertussis* dependent on the activation state of the BVG two component system.

The BVG two component system is made up of the BvgS sensory component, displaying HK activity, and the BvgA response regulator component (Figure 1.5) (Hot et al., 2003, Cummings et al., 2006). The gene expression phenotype is regulated by the cellular levels of phosphorylated BvgA, with differing levels resulting in either a highly activated (BVG+), inactivated (BVG-) or intermediately activated (BVGi) phase of gene expression (Boulanger et al., 2013, Williams et al., 2005). The shift between these conditions seems to be due to a conformational change in the BvgS's venus fly trap domains (VFT1&2) initiating the phosphorelay (Dupre et al., 2015). Under unmodulated growth conditions, BvgA is highly phosphorylated with *B. pertussis* being in the BVG+ growth phase (Uhl and Miller, 1996). In this growth phase 245 genes are upregulated including well known virulence associated genes key in *B. pertussis* colonisation of humans, such as PT, ACT, FHA, and FIM (Moon et al., 2017). Therefore, it is well accepted that this growth phase is the virulence phase of *B. pertussis.*

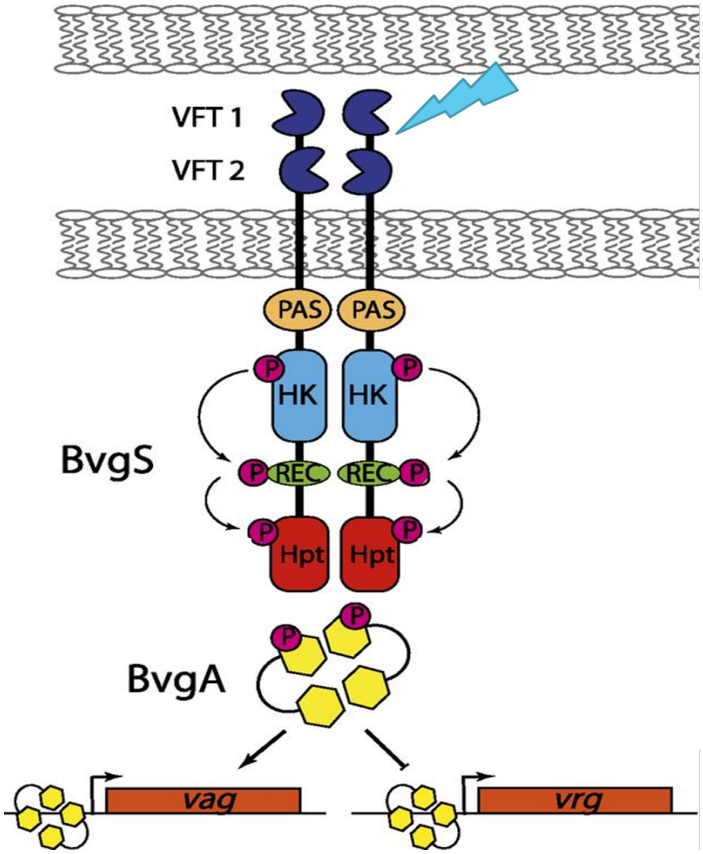

Figure 1.5- The BVG two component system. Conformational changes in VFT1&2 contained in the periplasmic portion of the BvgS sensory kinase results in activation of the HK contained in the cytoplasmic region of BvgS. This activation results in a phosphate group being translocated down BvgS to the Histidine phosphotransferase domain (Hpt). Upon phosphorylation of Hpt its transferase activity shuttles the phosphate group onto the BvgA response regulator. High levels of BvgA phosphorylation initiates expression of virulence associated genes (*vag*) and represses expression of virulence repressed genes (*vrg*). Upon low levels of phosphorylation, the opposite occurs. The role of REC and PAS domains in this process are less well defined. Figure from Bone et al., 2017 (Bone et al., 2017).

The BVG- and BVGi phases are less well understood. In the BVG- phase 326 genes are upregulated with genes involved in metabolic mechanisms enriched such as LPS and capsule biosynthesis genes (Moon et al., 2017). In *B. bronchiseptica,* a closely related species to *pertussis,* the BVG- growth phase has been suggested to be important in the survival of the bacteria out with the host due to the bacteria's ability to survive in nutrient limited conditions (Yuk et al., 1996, Cotter and Miller, 1994). However, this is yet to be proven with the fact that both *B. bronchiseptica* and *B. pertussis* have never been isolated environmentally, casting doubt on this hypothesis. There is also a body of evidence that suggests that the BVG- phase is important in latter stages of infection, where persistence and transmission occurs,

with enrichment of *B. pertussis* BVG- bacterial cells observed in the nasopharynx in rhesus monkey infection models (Karataev et al., 2016).

However, conversely in *B. bronchiseptica* and *B. pertussis,* BVG+ gene expression is necessary and sufficient for efficient colonisation in rabbit and murine models of infection respectively (Martinez de Tejada et al., 1998, Yuk et al., 1996, Cotter and Miller, 1994). These studies utilised BVG+ locked mutants, where they are unable to express BVG- genes, which displayed comparable infection efficiency and persistence as wildtype strains. BVG- locked mutants in these studies displayed decreased levels of infection (Martinez de Tejada et al., 1998, Yuk et al., 1996, Cotter and Miller, 1994). These findings suggests that the BVG- phase is not relevant to the disease caused upon *B. pertussis* infection.

1.2.4-Vaccines against *B. pertussis*-

In the 1940s the Diphtheria Tetanus Pertussis whole cell vaccine (WCV), composed of suspensions of inactivated *B. pertussis* bacteria alongside toxins purified from *Corynebacteriym diptheriae* and *Clostridium tetani,* was introduced (Kuchar et al., 2016, Leslie and Gardner, 1931). WCV introduction significantly reduce pertussis related morbidity and mortality in the following decades (Cherry et al., 1988).

In the 1980s, despite the success of the vaccination scheme and the dramatic reduction in cases, focus shifted to WCV safety. WCV vaccination was associated with localised adverse events at injection sites, such as swelling as well as mild systemic events such as drowsiness (Reyes et al., 2011). However, it was suggested that the vaccine caused severe systemic events in a small subset of infants reported as neurological adverse events such as hypnotic-hyperresponsiveness and convulsions (Reyes et al., 2011). Despite no strong correlation of vaccination to these adverse event significant damage to the WCVs reputation occurred, resulting in increased public vaccine scepticism. These adverse events were later determined to be unrelated to vaccination and linked to a rare epileptic encephalopathy, caused by a mutation in a gene encoding a sodium channel in neurons (Depienne et al., 2009).

Due to reputational damage of the WCV, to maintain vaccine confidence acellular vaccines (ACV) were developed, with many countries switching to these in the late-1980s/early-1990s (WHO, 2015). The pertussis antigens utilised in these vaccines consist of 5 *B. pertussis* proteins key in bacterial virulence, the adhesins PRN, FHA, FIM2 and FIM3, and a detoxified version of the immunomodulatory toxin PT (Liang et al., 2018). These pertussis antigens have been utilised in multivalent vaccines against a number or childhood diseases

(CDC, 2012). Vaccination composition and immunization schedules vary country by country as well concentrations of pertussis vaccine antigens vary by vaccine type (Table 1.1 & 1.2). ACVs used for primary immunization, such as the Diphtheria Tetanus acellular-Pertussis (DTaP) contain the highest concentration of antigens (Table 1.2). ACVs utilised for booster immunisations, such as the Tetanus Diphtheria acellular-Pertussis (Tdap) have lower concentrations of diphtheria and pertussis vaccine components.

Table 1.1 - Immunisation schedules in the USA and UK

	USA	UK
Maternal vaccination	**27-36 weeks of gestation. Tdap** (Adacel (Sanofi Pasteur.,Ltd.), Boostrix (GlaxoSmithKline Biologicals,.plc))	**27-36 weeks of gestation. Boostrix-IPV(**GlaxoSmithKline Biologicals,. plc)
Primary immunisation	**2, 4, 6 months. DTap** (DAPTACEL (Sanofi Pasteur.,Ltd.), Infanrix (GlaxoSmithKline Biologicals,. plc), Kinrix (GlaxoSmithKline Biologicals,. plc), Pediarix (GlaxoSmithKline Biologicals,. plc), Pentacel (Sanofi Pasteur.,Ltd.), Quadracel (Sanofi Pasteur.,Ltd.), Vaxelis (Merck and Sanofi Pasteur Vaccine Company))	**2, 3, 4 months. 6-in-1 vaccine** (Infranix hexa 6-in-1 (GlaxoSmithKline Biologicals,. plc), Vaxelis 6-in-1(Merck and Sanofi Pasteur Vaccine Company))
Primary Booster immunisation series	**15-18 months, 4-6 years. DTaP** (DAPTACEL (Sanofi Pasteur.,Ltd.), Infanrix (GlaxoSmithKline Biologicals,. Plc), Kinrix (GlaxoSmithKline Biologicals,. Plc), Pediarix (GlaxoSmithKline Biologicals,. Plc), Pentacel (Sanofi Pasteur.,Ltd.), Quadracel (Sanofi Pasteur.,Ltd.), Vaxelis (Merck and Sanofi Pasteur Vaccine Company))	**3 years 4 months. 4-in-1 vaccine** (REPEVAX (Sanofi Pasteur.,Ltd.))
Adolescence Booster series	**11-18 years. Tdap** (Adacel (Sanofi Pasteur.,Ltd.), Boostrix **(**GlaxoSmithKline Biologicals,. plc))	**NA**

Table 1.2- Vaccine composition in the USA and UK

Vaccine	Multivalent protection	Use	PRN (µg)	FHA (µg)	PT (µg)	FIM (µg)
Adacel (Sanofi Pasteur.,Ltd.)	Diphtheria, Tetanus, Pertussis	Maternal and adolescent booster USA	3	5	2.5	5
Boostrix (GlaxoSmithKline Biologicals,. plc)	Diphtheria, Tetanus, Pertussis	Maternal and adolescent booster USA	2.5	8	8	NA
Boostrix-IPV (GlaxoSmithKline Biologicals,. plc)	Diphtheria, Tetanus, Pertussis, Polio	Maternal booster UK	2.5	8	8	NA
DAPTACEL (Sanofi Pasteur.,Ltd.)	Diphtheria, Tetanus, Pertussis	Primary immunisation and primary booster series USA	3	5	10	5
Infanrix (GlaxoSmithKline Biologicals,. plc)	Diphtheria, Tetanus, Pertussis	Primary immunisation and primary booster series USA	8	25	25	NA
Kinrix (GlaxoSmithKline Biologicals,. plc)	Diphtheria, Tetanus, Pertussis, Polio	Primary immunisation and primary booster series USA	8	25	25	NA
Pediarix (GlaxoSmithKline Biologicals,. plc)	Diphtheria, Tetanus, Pertussis, Polio, Hepatitis B	Primary immunisation and primary booster series USA	8	25	25	NA
Pentacel (Sanofi Pasteur.,Ltd.)	Diphtheria, Tetanus, Pertussis, Polio, *H. influenzae* type B	Primary immunisation and primary booster series USA	3	20	20	5
Quadracel (Sanofi Pasteur.,Ltd.)	Diphtheria, Tetanus, Pertussis, Polio	Primary immunisation and primary booster series USA	3	20	20	5
Vaxelis (Merck and Sanofi Pasteur Vaccine Company)	Diphtheria, Tetanus, Pertussis, Polio, *H. influenzae* type B, *N. meningitidis* serogroup B	Primary immunisation and primary booster series USA	3	20	20	5
Infranix hexa 6-in-1 (GlaxoSmithKline Biologicals,. plc)	Diphtheria, Tetanus, Pertussis, Polio, *H. influenzae* type B	Primary immunisation UK	8	25	25	NA
Vaxelis 6-in-1 (Merck and Sanofi Pasteur Vaccine Company)	Diphtheria, Tetanus, Pertussis, Polio, *H. influenzae* type B	Primary immunisation UK	3	20	20	5
REPEVAX (Sanofi Pasteur.,Ltd.)	Diphtheria, Tetanus, Pertussis, Polio	Primary booster series	3	5	2.5	5

1.2.5-Epidemiology of *B. pertussis* in the pre and post vaccine era-

Pertussis is classically a disease of young children, with whooping cough being a prevalent respiratory pathogen in the early 1900s, causing significant morbidity and mortality in infants in the pre-vaccine era. This is depicted by around 1.7 million cases reported in the USA between 1922 and 1931 resulting in 73,000 deaths (Cherry, 1999).

Since the 1940s, vaccines have dramatically reduced the number of cases and mortality of pertussis (Figure 1.6) (Cherry et al., 1988). The WCV introduced in the 1940s resulted in around a 150-fold reduction in pertussis incidence (Welsby, 1985, Madsen, 1933).

However, due to reputational damage the WCV was replaced by ACVs in the 1990s in many countries. Despite showing effective initial protection in countries who participated in the switch from WCV to ACV, a resurgence in pertussis is now being observed. Cases peak every 2-5 years characteristic of *B. pertussis* spread in the pre-vaccine era (Figure 1.6) (Cherry, 2015). In part due to this resurgence there has been increased research into *B. pertussis* to develop our understanding of the fundamental biology of *B. pertussis*.

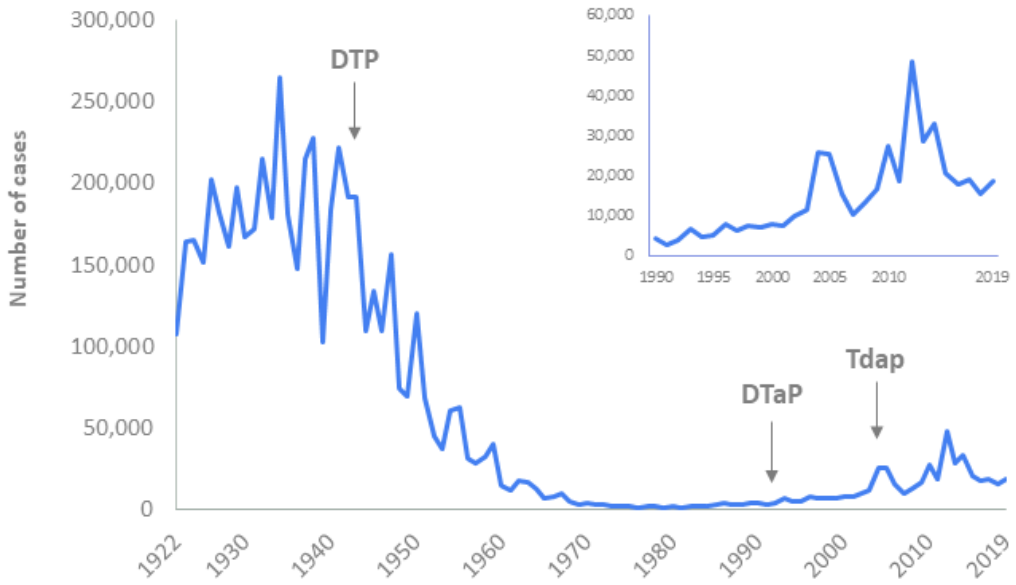

Figure 1.6 - *B. pertussis* cases reported to the CDC between 1922-2019. DTP- Whole cell vaccine introduced. DTaP- Acellular vaccine introduced. Tdap- Booster immunisation introduced. Figure from CDC, 2019 (CDC, 2019)

1.2.6- Resurgence of *B. pertussis*-

Increased research into the resurgence of *B. pertussis* has suggested that it is a multifactorial phenomenon. Factors such as waning immunity in the population, adults acting as reservoirs

of *B. pertussis*, vaccine escape mutants, and sub-optimal vaccine induced immunity have all been highlighted for their contribution.

Waning Immunity post-vaccination –

The waning of anti-*B. pertussis* immunity in vaccinated populations is thought to be of key importance in disease resurgence. Immunity induced by vaccination is noticeably shorter than that post natural infection. WCV induces immunity for 4-12 years, whereas natural infections induce immunity for 7-20 years, with the ACV only inducing immunity for 5-7 years after 3 doses (Wendelboe et al., 2005, Gustafsson et al., 2006). This waning means there is an increased reliance on boosters to maintain protective immunity within populations, increasing the burden on health care systems. Therefore, there is a requirement for improvement of the current vaccine regimen to facilitate a more durable and protective immune response if we wish to halt the spread of *B. pertussis* through the population.

Adult reservoirs for *B. pertussis*-

In recent years, research into pertussis epidemiology has displayed a shift in infected populations. Pertussis is classically thought of as a disease of the young with most of the disease burden occurring in children too young to be vaccinated, or children who have not completed the full booster regimen. However, it has recently become apparent that pertussis is not limited to infections in naïve populations and can occur in vaccinated adolescent and adults. These older populations may be important in the recent resurgence of disease due to waning immunity allowing the asymptomatic spread of *B. pertussis*. This is supported by data from China, where 5% of 897 serum samples taken randomly from 20-39-year olds, were found to have high levels of antiPtx IgG antibodies displaying recent infection(Chen et al., 2016).

This is worrying due to the fact that *B. pertussis* is highly transmittable during the early stages of infection, where one infected individual can cause up to 17 cases in naïve populations (Kilgore et al., 2016). Control of disease spread in these populations is therefore essential in decreasing pertussis cases. One strategy for protecting these populations is cocooning immunisation, which aims to protect naïve individuals by immunising adults in close contact with children, such as health care givers and parents. Therefore, reducing the risk of contact with asymptomatic carriers of pertussis (Rowe et al., 2018). However, it has been realised that the scale of vaccination required to have adequate protection of infants is unrealistic out with family units. Therefore, a more promising approach that has been

implemented in several countries is maternal vaccination. This strategy relies on the transplacental transfer of anti-*B. pertussis* maternal antibodies from mother to infant upon vaccination of the mother during pregnancy with Tdap. This approach has displayed promise, with studies showing high titres of protective maternal antibodies in infants born from maternally vaccinated mothers, reducing the risk of infection prior to primary vaccination of the child (Switzer et al., 2019).

However, one potential drawback of this approach is an observed blunting of the child's anti-*B. pertussis* immune response upon primary vaccination in childhood. The effect of this on potency and longevity of vaccine induced protection against *B. pertussis* is yet to be determined (Hardy-Fairbanks et al., 2013, Kent et al., 2016). Another potential issue is that studied cohorts of mothers have been primarily WCV primed in their childhood. WCV priming is known to induce a broader immune response upon ACV boosters than ACV primed individuals. Due to the swap to ACV in many countries, studies into the effectiveness of maternal vaccination in ACV primed mothers are essential to validate the maternal vaccination strategies effectiveness for the coming generations.

Vaccine escape mutants-

Another factor that may be important in disease resurgence is the development of vaccine escape mutants strains through the loss of the expression of proteins contained in the ACV (Jadhav and Gairola, 1999). One key vaccine antigen, PRN, appears to not be essential for bacterial survival inside the human host as strains deficient in PRN have been in circulation since the introduction of the ACV.

In Australia, during a prolonged pertussis epidemic between 2008-2012, PRN deficient strain numbers increased dramatically (Safarchi et al., 2016). Recent *in vivo* work utilising BALB/c mouse models, displayed that PRN negative strains were more effective at colonising mice vaccinated with the ACV than PRN positive strains in a mixed infection models (Safarchi et al., 2015). This is further supported by analysis of US clinical isolates taken from individuals with at least one vaccine dose, where 85% of isolates were PRN negative (Martin et al., 2015). Therefore, vaccines reliant on PRN as a key antigen may not be suitable for the next generation of *B. pertussis* vaccination strategies. However, the absence of PRN comes with a fitness cost, with infection efficiency of naïve mice found to be reduced (Safarchi et al., 2015). This suggests that strains infecting naïve and vaccinated populations may be different due to the fitness cost of PRN loss limiting it to infecting vaccinated populations. Therefore,

novel vaccines may have to be effective at inducing immunity against both PRN positive and negative strains to protect all susceptible populations.

Interpretation of the antibody profiles induced upon ACV vaccination provides insight into why PRN deficient strains have evolved through selection pressure. Upon comparative analysis of convalescent and post-ACV vaccination serum, the vast majority of bactericidal antibodies generated upon ACV vaccination target PRN (Lesne et al., 2020). Conversely, convalescent serum displayed a broader range antigenic targets for bactericidal antibodies. This displays that populations vaccinated with the ACV display robust humoral response targeting PRN which may have been the key driver for PRN deficient strains to evolve.

PRN is not the only ACV protein found to be deficient in *B. pertussis* clinical isolates. A small number of strains have been observed to be deficient in the expression of FHA. One isolate was detected during the 2013-2017 Australian pertussis outbreak which was both PRN and FHA deficient, with two other strains being isolated in Iran which were solely FHA deficient (Xu et al., 2019, Saedi et al., 2021). In both studies absence of FHA was determined by immunoblotting of whole cell lysates for FhaB protein, with initial findings further elucidated by Illumina sequencing. The Australian isolate was further analysed by liquid chromatography tandem mass spectroscopy (LC-MS). Sequencing displayed an alteration in the *fhaB* coding sequence of all three mutants. The Iranian strains, named IR34 and IR178, displayed a large 330bp deletion and a single base deletion in *fhaB* respectively (Saedi et al., 2021). Interestingly the Australian clinical isolate displayed the addition of a guanine residue, resulting in a premature stop codon in the *fhaB* coding sequence in a proportion of its bacterial population with some displaying the wildtype sequence (Xu et al., 2019). LC-MC analysis of the Australian isolate verified FhaB expression was indeed altered, with 2.3% expressed as peptides in the FHA- isolate compared to 30.7% in an FHA+ isolate. Interestingly, this displays that the Australian FHA- isolate is not totally deficient in FHA expression, a phenotype attributed to the mixed population of mutated and unmutated *fhaB* in the clinical isolate upon *in vitro* culturing.

These findings suggest that there may be further potential for vaccine escape by circulating *B. pertussis* strains reinforcing the need for new vaccine strategies. However, the relevance of FHA- strains to clinical infections needs to be further elucidated. This is due to the low numbers of FHA deficient strains isolated, suggesting a high fitness cost despite high selection pressure for FHA loss. It is also noteworthy that it has not been verified that these

strains are not a result of spontaneous FHA mutations arising during sampling and culturing from patients.

Sub-optimal vaccines induced immunity-

Due to *B. pertussis* resurgence, there has been an increased interest in what immune responses confers protection during infection to elaborate how vaccine induced immunity may not be optimal for protection. During infection bacterial antigens presented on dendritic cells activate a CD4+ T helper cell mediated response, which has been characterised to be important in immune protection.

T helper 1 cell response to bacterial pathogens-

CD4+ T helper 1 cell (Th1) responses are characterised by the release of cytokines that stimulate a strong phagocytic response during infection, such as interferon-γ (IFNγ) (Romagnani, 2000). IFNγ signalling is thought to be key in the development of antimicrobial immunity during infections, and has been shown to induce the recruitment and activation of macrophages and natural killer cells to the site of infection, inducing increased levels of antigen presentation by myeloid cells (Tau and Rothman, 1999, den Hartog et al., 2022). Recruitment and activation of these cells results in a bactericidal environment at the site of infection. The importance of this is highlighted by the significance of IFNγ in the immune response against *B. pertussis* infection in murine models. Using a lethal dose challenge model it was observed that the lethal dose of *B. pertussis* is reduced in IFNγ receptor null mice (Mahon et al., 1997). The role of Th1 T cells in immunity against *B. pertussis* was further displayed in immunosuppressed mice models, where adoptive transfer of CD4+ T cells from convalescent mice facilitated clearance upon *B, pertussis* challenge (Mills et al., 1993).

T helper 17 cell response to bacterial pathogens-

CD4+T helper 17 cells (Th17) are a subset of CD4 positive T cells that secrete IL-17 upon activation. These cells have been identified as being important in the protective immune response against extracellular pathogens, especially at mucosal sites (Peck and Mellins, 2010). The Th17 response occurs early during infection, with IL-17 detected within the first 24 hours (Chung et al., 2003). This suggests that Th17 cells are involved in immune surveillance at mucosal sites and therefore will be important in detection and clearance of mucosal pathogens such as *B. pertussis*. Th17 cell activation results in the induction of antimicrobial peptide expression from epithelial cells at the site of infections, such as B-

defensin-2, as well as stimulation of the recruitment of immune cells via the induction of the expression of chemotactic factors, such as macrophage inflammatory proteins (Kao et al., 2004, Miyamoto et al., 2003). The importance of the Th17 response during *B. pertussis* infection has been highlighted in mouse infection models, where the addition of anti-IL17 antibodies to mice vaccinated with the WCV resulted in failure to clear infection (Higgins et al., 2006).

The importance of the Th17 response appears to be due to the populations ability to readily recruit neutrophils to the site of nasal colonisation, through the production of the cytokine IL-17. This is highlighted by the fact that *Il17A−/−* mice displayed defects in their ability to clear *B. pertussis* infection from their nasal cavity. A particular subset of neutrophils has been characterised as important in this clearance process (Borkner et al., 2021). Neutrophil anti-bacterial functions are well characterised in the literature with the secretion of antimicrobial peptides (AMPs), opsonisation of bacteria in an antibody-dependent manner, and extracellular trap formation being key in the management of bacterial infections. In *B. pertussis* infections phagocytosis of bacteria by antibody and complement does not appear to be the primary mechanism of neutrophil mediated killing. Alternatively, there seems to be a clear importance in the neutrophil extracellular trap (NET) mediated killing of bacteria. This is displayed by the enrichment of Siglec-F+ neutrophils in *B. pertussis* infected airways (Borkner et al., 2021). Siglec-F+ neutrophils have greatly increased NET activity compared to other neutrophil populations.

Tissue resident memory cells-

Protective immunity to *B. pertussis* induced by primary infection appears to not solely be reliant on recruitment of peripheral T cells upon infection, with tissue resident memory T cells (TRM) being observed to be enriched at mucosal sites and activated upon *B. pertussis* colonisation (Wilk et al., 2017, Misiak et al., 2017). TRM are a subset of memory T-cells which can reside in a broad range of barrier tissues (Mueller and Mackay, 2016). They play a key role in the protection of these sites from infection, due to their ability to induce rapid effector functions, facilitating the TRMs to sense infection and alarm the immune system, recruiting other immune cells, and proliferate at the site of activation (Iijima and Iwasaki, 2014, Turner and Farber, 2014). These findings display that TRMs can play a key protective role upon reinfection with bacterial pathogens.

Unsurprisingly this is the case in *B. pertussis* where TRMs are found to accumulate in the respiratory tract of mice upon primary infection where they persist (Misiak et al., 2017, Wilk et al., 2017, Borkner et al., 2021). Upon reinfection these populations proliferate, secreting IFNγ and IL-17. The importance of TRMs has been highlighted experimentally, where treatment with a receptor agonist which prevents T and B cell migration from the lymph nodes resulted in a exacerbated primary infection, but had no effect during secondary infection in murine models (Wilk et al., 2017). This study further displayed the critical role of TRMs in protection against *B. pertussis* infection through adoptive transfer of TRM populations from convalescent mice to naïve mice. This displayed naïve mice were as protected against *B. pertussis* infection as convalescent mice upon the presence of TRM populations.

WCV and ACV induced immune responses-

The immune response induced by the current vaccines has been of increased interest due to the recent resurgence of disease. Understanding the response stimulated by vaccination and how they correlate to protective immunity allows a greater insight into vaccine failure, and how future vaccines can be improved. Studies have displayed that immune responses induced upon *B. pertussis* challenge in vaccinated individuals vary dependent on vaccine type used for primary immunisation (Ryan et al., 1998). The importance of this primary immunisation inducing a robust, protective response is highlighted by the fact that boosting immunisations are unable to alter the initial skewing of the immune response (Van der Lee et al., 2018a, van der Lee et al., 2018b).

WCV immunisation induces immunity like that induced during wildtype infection in baboon models with a robust TRM and Th1/Th17 cellular response observed upon pertussis challenge (Warfel et al., 2016).

Cellular immune response induced upon ACV vaccination vary between animal models, with a Th2/Th17 response induced in murine models and a predominantly Th2 with low Th1 response in non-human primates (Ross et al., 2013, Brummelman et al., 2015, Warfel et al., 2014). Analysis of cytokine profiles of children post ACV priming and booster vaccinations reinforced the finding that ACV immunisation induced a primarily Th2 cellular immune response, with high levels of IL5 (Th2) and low levels of IFNγ (Th1) cytokines (Mascart et al., 2007).

A robust Th2 response directs the immune system towards humoral immunity, a response not optimal for protection against *B. pertussis* infection where cellular immune responses have been characterised to be critical (Wilk et al., 2019). This is further highlighted by vaccination with ACV failing to induce TRM accumulation at mucosal sites (Wilk et al., 2019). The suboptimal immune response induced by the ACV is emphasised by the fact that vaccination with the ACV failed to prevent colonisation or transmission of *B. pertussis* in baboon infection models (Warfel et al., 2014).

In summary these results display ACV primary immunisations direct the anti-*B. pertussis* immune response in a sub-optimal direction, contrasting to the protective responses induced upon WCV immunisation. Therefore, adaption of the current vaccine regimens to induce a WCV-like response is an area of increasing research.

1.2.7-Bacterial outer membrane vesicles (OMVs) as vaccine antigens-

Bacterial OMVs-

A characteristic of gram-negative bacteria is the release of vesicles composed of bacterial OM proteins and lipids via blebbing from the bacterial surface. It was initially believed this was a spontaneously occurring process during bacterial cell growth and replication. However recent findings have begun to suggest that OMV release is a highly regulated process controlled by genetic factors (Volgers et al., 2018).

Improved understanding of genetic factors in OMV release has resulted in an increased interest into utilising vesicles as vaccines against bacterial pathogens. This is a promising strategy as it will allow the presentation of bacterial OM antigens to the host immune cells in the same orientation as seen on whole bacterium. It also has the added advantage that these OM proteins are expressed alongside highly immunogenic compounds, such as LPS, which may boost epitope antigenicity. For this to be a feasible strategy for vaccine development, the mechanisms for OMV biogenesis will have to be elucidated, allowing the genetic modification of bacteria to produce high numbers of OMVs *in vitro*.

Promise of OMVs as vaccine antigens-

Bacterial OMVs have been utilised successfully in a vaccine against Meningococcal group B pathogens: a group of gram-negative bacterial pathogens which cause bacterial meningitis (Petousis-Harris, 2018). OMV vaccines were utilised due to difficulties in the development of an effective acellular vaccine: the classical strategy of combining bacterial polysaccharide

with an antigenic carrier displayed poor antigenicity and had potential of stimulating autoimmune reactions against foetal neural tissues (Finne et al., 1983). Two OMV-based vaccines have had high uptake in Cuba, Norway and New Zealand, Bexsero (GlaxoSmithKline Biologicals,. plc) and VA-MENGOC-BC (Novartis, AG), which have effectively protected adolescents from disease by inducing bactericidal activities upon challenge (Petousis-Harris, 2018). These findings suggest that OMV based vaccines are a feasible strategy for the control of diseases caused by gram negative bacterial pathogens such as *B. pertussis*.

B. pertussis OMVs have been analysed as vaccine candidates in murine models, effectively protecting against colonisation by PRN positive and negative strains, inhibiting infection 2 weeks post vaccination and inducing populations of CD4+ TRMs against *B. pertussis* (Zurita et al., 2019). These findings suggest that an OMV vaccine could tackle the challenges currently seen in *B. pertussis* control, as immune responses induced upon OMV vaccination effectively inhibit infection with vaccine escape mutants, displays efficient induction of immune memory and successfully clears *B. pertussis* infections in murine models.

Proposed mechanisms for OMV biogenesis-

Recent studies have hypothesised three main mechanisms for OMV biogenesis: changes in envelope stability via depletion of protein crosslinks, as a response to stress, and finally due to an increased membrane fluidity.

Envelope stability-

It is thought that a reduction in envelope stability may be important in the release of OMVs from the bacterial OM. Envelope stability occurs due to protein cross linking between the PG layer and the OM. As previously discussed, multiple proteins have been found to form crosslinks with the PG layer, the most common being Braun's lipoprotein (Lpp) (Braun, 1975). Covalent interactions have also been found to contribute to membrane stability, such as interactions between the PG and the OM protein OmpA as well as the membrane spanning Tol-pal complex (Wang, 2002, Cascales et al., 2002).

It is thought that these crosslinks are depleted during OMV release, allowing a region of membrane instability. This decreased stability would aid OMV release as it would allow the membrane to contort to form vesicles more easily.

The role of envelope crosslinking interactions in OMV release has been analysed in gram-negative bacterial systems. In *E. coli* systems the absence of OmpA expression results in an increase in OMV production when compared to wildtype (Sonntag et al., 1978). This trend was further supported in another gram negative bacteria, *Pseudomonas aeruginosa*, where knock out of the OmpA homologue OprF resulted a marked increase in vesicle production (Wessel et al., 2013). Studies looking at the importance of the Tol/Pal system in OMV biogenesis displayed similar results, where gene knock out dramatically increased OMV yields (Bernadac et al., 1998).

The role of Lpp in OMV release has been more difficult to elucidate using mutational techniques. This is due to the absence of Lpp-PG crosslinks causing membrane stability issues, resulting in membrane leakage and bacterial death (Sonntag et al., 1978). However, correlations have been found between Lpp-PG bonds and OMV synthesis. In Δ*nlpI E. coli*, a hyper vesiculating mutant, it has been found that Lpp-PG interactions occur at a much lower level than in wildtype *E. coli* (Schwechheimer et al., 2015).

Extra cytoplasmic stress response-

The bacterial envelope is important in protecting the bacterium from environmental stress, allowing the bacteria to survive in challenging conditions. However, cellular stress can also occur due to malfunctions in cellular processes. Bacterial envelope stress is sensed by a system called the extra-cytoplasmic stress response, of which three mechanisms have been linked to OMV biogenesis (Ruiz et al., 2006)

Two of these mechanisms, the sigma factor E response and the two-component regulator Cpx response, become active when they sense the presence of misfolded proteins at the bacterial outer membrane (Rowley et al., 2006). These systems, control genes important in peptide degradation and folding as well as LPS biosynthesis. Investigation into the role of this system in *E. coli* OMV biogenesis by mutation of the sensory protease of the sigma factor E response (DegS), displayed significantly increased OMV production (McBroom et al., 2006). This suggests that extra cytoplasmic stress responses have an inhibitory role in OMV biogenesis through the sensing and management of periplasmic protein accumulation.

Another stress response linked to OMV synthesis is the phage shock response, which is responsible for sensing and protecting the bacterium from external noxious stimuli, such as phage infections and temperature fluctuations. This response has been displayed to promote

OMV release in *E. coli* where treatment with stimuli, such as increased temperature, resulted in greater OMV release (McBroom and Kuehn, 2007, Rowley et al., 2006).

Membrane fluidity and curvature-

Membrane fluidity and curvature is believed to be an important factor in OMV release, with increased fluidity allowing the bacterial membrane to bulge, promoting vesicle formation. Outer membrane lipid composition and characteristics are thought to be key determinants of membrane fluidity.

The LPS outer layer of the OM is stabilised by salt bridge interactions between cations in the core region of the polysaccharide molecules (Alexander and Rietschel, 2001). Disruption of these salt bridges can increase repulsion between LPS, inducing membrane bending and bulging (Mashburn-Warren et al., 2008). The role of these interactions in OMV release has been studied using the Pseudomonas quinolone signal (PQS), a quorum sensing molecule produced by *P. aerginosa*, which is observed to induce OMV production in gram-negative bacteria. PQS is thought to entrap cations important in salt bridge formation. This entrapment would explain PQS stimulation of OMV release due to increased repulsion between LPS (Mashburn-Warren and Whiteley, 2006).

Creating a *B. pertussis* hypervesiculating bacteria-

If OMVs were to be utilised in a vaccine, optimising of OMV production would be beneficial to therapeutic development. One strategy of doing this is to develop hypervesiculating mutants of *B. pertussis,* which produce much greater yields of OMVs. To do this the processes controlling OMV secretion must be elucidated. As discussed earlier mutational studies have identified factors involved in OMV release in other gram-negative bacterial species. These findings can be translated into *B. pertussis* and provide targets for mutagenesis to increase OMV production.

Current hypervesiculating mutants-

To date two hypervesiculating *B. pertussis* mutants have been identified (de Jonge et al., 2022a, de Jonge et al., 2022b). As discussed previously OM stability is a key factor in OMV biogenesis, with mutation of Braun's lipoprotein (Lpp), an envelope stabilising protein in *E. coli,* being observed to induce hypervesiculation (Suzuki et al., 1978b, Weigand et al., 1976). However, with no Lpp homolog observed in *B. pertussis,* research into hypervesiculation

phenotypes has targeted another well characterised OM stabilising protein complex, the Tol-pal system (de Jonge et al., 2022a, Bernadac et al., 1998).

Mutagenesis of the Pal component of the Tol-Pal system was restricted in this study due to essentiality in *B. pertussis,* with mutation causing a lethal effect (de Jonge et al., 2022a). Conditional *Δpal* strains were successfully generated by deletion of the target genes in strains harbouring the wildtype gene on an inducible plasmid, allowing titration of *pal* expression to maintain strain viability. Quantification of OMVs from this studies was carried out indirectly by quantification of protein concentrations of purified OMVs from broth culture. *Δpal* strain displayed approximately six-fold increase in protein levels in purified OMVs compared to wildtype.

The second hypervesiculating mutant identified in *B. pertussis* is a double mutant of genes involved in the maintenance of OM lipid asymmetry (de Jonge et al., 2022b). Lipid asymmetry is a key factor in the OM barrier function of bacteria, maintaining the balance between the inner PL layer and the outer LPS layers of the bacterial OM. Disruption of this balance by PL enrichment of the inner leaf of the OM results in increased OMV biogenesis in gram-negative bacteria (Roier et al., 2016a). The PL LPS balance is maintained by a PL transport system (Mla) in *E. coli,* which transports PL across the IM into the periplasmic space (Malinverni and Silhavy, 2009). In this study they targeted, *mlaF,* encoding the ATPase which fuels the IM complex of the Mla system, and *pldA,* encoding the OM phospholipase A to induce PL accumulation in the periplasmic space (de Jonge et al., 2022b). Indirect quantification of purified OMVs by protein quantification displayed an approximately 5-fold increase in protein concentration eluding to a hypervesiculating phenotype.

These two mutant strains display that hypervesiculating phenotypes can be induced in *B. pertussis.* However, the indirect quantification method of OMVs utilised means the extent of hypervesiculation is uncertain. Protein composition of purified fractions could be skewed by proteins secreted by bacteria as well as cellular debris. This is especially relevant to this study where inactivation of bacteria was carried out by heat treatment of cultures at 56˚C before OMV purification. Direct quantification by nanoparticle tracking analysis (NTA) would be beneficial to verify the hypervesiculating phenotypes identified by this body of work.

PG biosynthesis as a target for manipulation to produce hyper vesiculating mutants-

Recent work has identified genes involved in PG synthesis as potential targets for genetic manipulation in the hope of increased OMV production by *B. pertussis*. Interestingly in a recent study *mre/mrd* operon was found to be conditionally essential dependent on the activation state of the BVG two component system (Belcher et al., 2020). Transposon directed insertion site sequencing (TraDIS) of *B. pertussis* transposon mutant libraries plated on BVG+ or BVG- modulating conditions, displayed that the *mre/mrd* operon was essential for bacterial viability during BVG- plate growth, but non-essential during BVG+ plate growth (Figure 1.7). Therefore, these genes are promising targets for genetic manipulation in the hope of increasing OMV production as knockout would effect PG synthesis influencing OM stability.

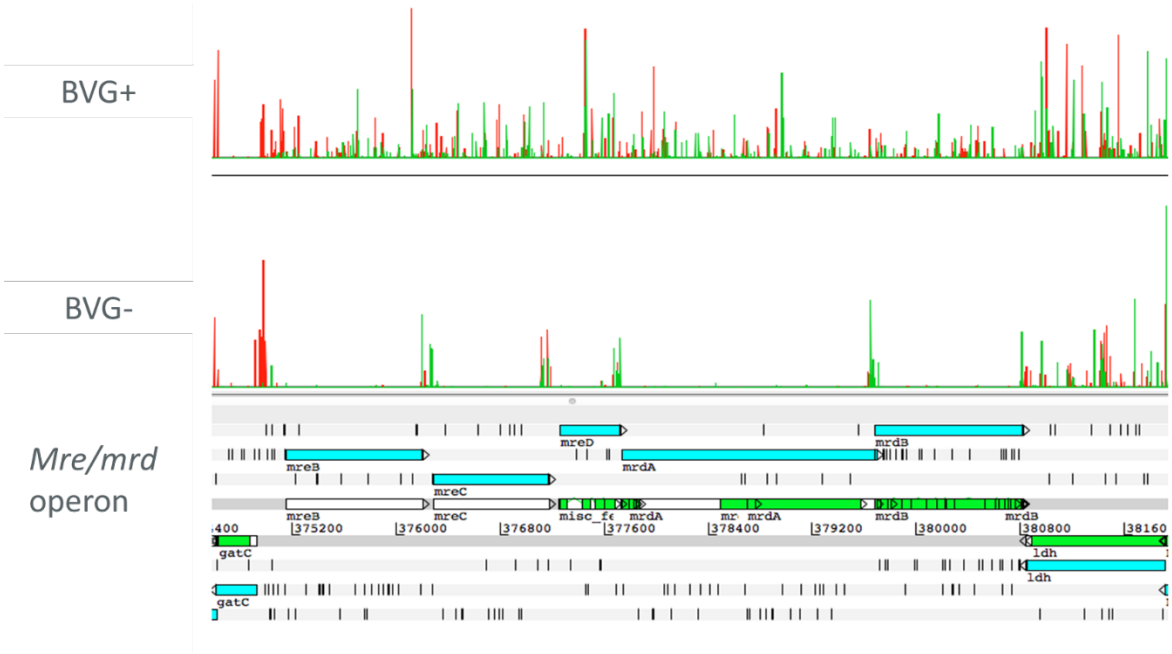

Figure 1.7 - Transposon insertion site frequency aligned to the *Mre/mrd* operon during BVG+ or BVG- plate growth conditions. Orientation of insertion depicted by red and green and height of peak displays frequency at the specific site. Figure from Belcher et al., 2020 (Belcher et al., 2020).

High throughput screening for hypervesiculating mutants-

With increased interest in inducing hypervesiculating phenotypes into gram-negative bacteria along with the development of high throughput mutagenesis studies, broad screening approaches have been utilised in the attempt to identify novel hypervesiculating mutants. High throughput screening techniques have been revolutionised with the development of transposon directed mutagenesis screens allowing for high throughput mutant library generation, which can then be screened for phenotypes of interest downstream

(Mazurkiewicz et al., 2006, Mei et al., 1997, Chiang and Mekalanos, 1998, Roier et al., 2016b). Our collaborators at GSK have utilised these approaches to develop a high throughput assay to screen for increased secretion of lipid structures into the culture supernatant. This assay identified previously uncharacterised hypervesiculating mutants in *B. pertussis* with three of the strains with the highest lipid secretion displaying mutation in the same gene, *rpsA* (Unpublished Data). The protein encoded by *rpsA* is ribosomal associated involved in translation with no obvious link to OM stability and therefore OMV biogenesis (Aliprandi et al., 2008). This work highlights the key insight that high throughput screens can provide regarding the identification of novel OMV biogenesis mechanisms.

1.3-Aims and Objectives of PhD-

The identification of the *mre/mrd* operon to be conditionally essential during *in vitro* growth on charcoal agar plates, suggested a fundamental difference in the essentiality of the elongasome in *B. pertussis* when compared to other gram-negative bacteria. The fact that *B. pertussis,* a highly fastidious bacteria in *in vitro* culture, could tolerate the loss of these genes where other more robustly growing bacteria could not posed some interesting questions requiring further interrogation. My thesis will be divided into three parts in which I have addressed these questions.

Question 1- Does mutation of *mre/mrd* alter *B. pertussis in vitro* growth, morphology, and OM stability?

In *E. coli* mutation of *mre/mrd* greatly alters the bacteria's growth, morphology, and OM stability where rescue of viability was only achieved upon growth in nutrient limited conditions. As the *mre/mrd* operon was identified to be tractable in *B. pertussis* I aimed to determine whether comparable phenotypic changes were induced in *B. pertussis mre/mrd* mutants as in *E. coli.* Therefore, I aimed to:

1. Generate *mre/mrd* deletion strains of *B. pertussis* and *mre/mrd* complementation constructs
2. Analyse that ability of *mre/mrd* mutant strains ability to grow during plate and broth *in vitro* culture.
3. Observe morphological changes to external and internal architecture of *mre/mrd* mutant strains.
4. Assess whether *mre/mrd* mutant strains have a reduced ability to tolerate OM stress due to altered stability of the bacterial cell envelope.

Question 2- What are the mechanism by which *B. pertussis* tolerates the loss of *mre/mrd* expression?

Mutation of *mreB* causes detrimental effects on gram-negative bacteria, where deletion is lethal in *B. subtilis*, *C. crescentus* and conditionally lethal in *E. coli* dependent on growth conditions. In *B. pertussis* this is not the case with mutants displaying comparable viability to wildtype during BVG+ and BVG- broth culture, and BVG+ plate culture. Therefore, *B. pertussis* displays conditional tolerance to *mre/mrd* mutation dependent on both BVG activation state and growth medium. To investigate this, I aimed to:

1. Characterise the transcriptome of *B. pertussis* wildtype during broth and plate *in vitro* culture upon BVG+ and BVG- modulation.
2. Identify and analyse genes differentially expressed between conditions where BP_{536}*ΔmreB* is conditionally essential to identify hypothetical mechanism of tolerance to loss of elongasome PG biosynthesis.
3. Validate identified mechanisms of tolerance by experimental investigation.

Question 3- Do *mre/mrd* mutants hypervesiculate at a level comparable to other putative hypervesiculating mutant strain?

OMVs are promising vaccine antigens to bolster the current vaccine regimen against *B. pertussis,* displaying improved breadth and longevity of protection when compared to ACV in murine models. The characterisation of mutant *B. pertussis* strains that hypervesiculate would greatly aid vaccine production if OMVs were to be utilised as additional vaccine antigens. OMV biogenesis is strongly linked to OM stability, with hypervesiculating strains in gram-negative bacteria being produced by mutagenesis of genes encode OM stabilising proteins. As the PG sacculus plays a key role in OM stability I hypothesised that *mre/mrd mutant* strains would display a hypervesiculating phenotype when grown *in vitro*. To verify this hypothesis and analyse OMVs produced for feasibility as vaccine antigens I aimed to:

1. Quantify OMV production from *mre/mrd* mutant strains.
2. Analyse key factors in the OMVs feasibility as vaccine antigens

From high throughput screening of a *B. pertussis* transposon mutant libraries for increased lipid structure secretion, GSK identified putative hypervesiculating strains. In these strains the ribosomal protein RpsA is truncated. This poses the question whether the increased lipid

secretion from these strains is indeed a vesiculating phenotype and if so how does RpsA truncation result in a hypervesiculating phenotype? To answer these questions, I aimed to:

1. Quantify and characterise OMVs produced by *rpsA* truncation strains
2. Investigate transcriptomic alterations in *rpsA* truncation strains to try an elucidate alterations in gene expression induced by the mutation.

As the *mre/mrd* mutants were generated in the BP536 strain background, with GSK mutants being in the detoxified pertussis toxin *B. pertussis* strain PTg, to directly compare vesiculation phenotypes I aimed to:

1. Mutate *mreB* in PTg strain background.
2. Quantify OMV production and characterise antigen profile of *mreB* and *rpsA* mutants in parallel.

Chapter 2 Materials and methods

2.1-Bacteria, plasmids, and growth conditions-

B. pertussis strains utilised in this work are BP536, a streptomycin resistant clone of Tohama I and PTg, a clone of Tohama I where PT is detoxified by substitution of Arginine^{9} with Lysine and Glutamic acid^{129} with Glycine (ArgPT-9K/129G) (Pizza et al., 1989). Wildtype and mutant strains were grown on charcoal agar for 3 days at 37˚C. For liquid culture, Stainer-Scholte (SS) broth was utilised. SS medium was supplemented with heptakis (1g/l) (SSH), casamino acids (10g/l) (SSC), or both (SSCH). Media was supplemented with 50mM $MgSO_4$ for induction of BVG- phase conditions. Conjugation strain ST18 *E. coli* was utilised to transfer plasmid carrying the mutant gene (pSS4940GG) and complementation constructs (pBBRTetGG) into BP536 (Table 2.1). ST18 was grown in Luria Bertani broth at 37˚C supplemented with 50mM aminolaevulinic acid for which ST18 is auxotrophic. For molecular cloning and amplification of plasmid constructs NEB 5-α *E. coli* were utilised. Carriage of plasmids was selected by supplementation of media with gentamycin (30ug/ml) and tetracycline (15ug/ml) for pSS4940GG and pBBRTetGG respectively (Table 2.1).

Table 2.1- Plasmid information

Plasmid	Selection	Purpose	Source

pSS4940GG	Gentamycin	Suicide vector for allelic exchange adapted for Golden Gate cloning	Preston Lab stock
pBBRTetGG	Tetracycline	Shuttle/expression vector used for complementation adapted for Golden Gate cloning	Preston Lab stock
pMMB208	Chloramphenicol 20ug/ml	Inducible expression vector	(Morales et al., 1991)

2.2-Mutant generation-

Regions flanking the genes targeted for mutagenesis were amplified by PCR using Q5 high fidelity 2x master mix (NEB) following the manufacturers guidelines, with the only alteration being the addition of DMSO to 10% reaction volume (Table 2.2). For *mreB,* these regions were cloned either side of a kanamycin resistance cassette. For all other mutants these regions were joined together and introduced into the pSS4940GG suicide vector by golden gate cloning to allow for the in-frame deletion of target genes (Table 2.1) (Figure 2.1) (Engler et al., 2008).

Table 2.2- Primer information

Primer	Sequence	Purpose
*ΔmreB*LeftFragF	aaaaggtctctcgagattcgggggcgttgg	*mreB* deletion/insertion mutant generation
*ΔmreB*LeftFraR	aaaaggtctccatgtgcatgggagctcagctagattc	*mreB* deletion/insertion mutant generation
*ΔmreB*RightFragF	aaaaggtctcaggtctgagcctgtctcgcg	*mreB* deletion/insertion mutant generation
*ΔmreB*RightFragR	aaaaggtctcgaactgggcggctcgtacagc	*mreB* deletion/insertion mutant generation
KanF	aaaaaaggtctccacatgacgtcttgtgtctcaaaatctc	*mreB* deletion/insertion mutant generation
KanR	aaaaaaggtctcagaccttagaaaaattcatccagcatc	*mreB* deletion/insertion mutant generation
*ΔmreC*LeftF	aaaaggtctctcgagacgccgaactcatcaagaagg	*mreC* deletion mutant generation
*ΔmreC*LeftR	aaaaggtctcgatgtgcgcttgtcgttgcatggat	*mreC* deletion mutant generation
*ΔmreC*RightF	aaaaggtctctacatagatgtcgatggagcggacta	*mreC* deletion mutant generation
*ΔmreC*RightR	aaaaggtctcgaactagatcagacggcggaagattc	*mreC* deletion mutant generation
*ΔmreD*LeftF	aaaaggtctctcgagatttcaacaagggcgccaaa	*mreD* deletion mutant generation
*ΔmreD*LeftR	aaaaggtctcgatgtgcgacagcagccagaccag	*mreD* deletion mutant generation
*ΔmreD*RightF	aaaaggtctctacatagaatcttccgccgtctgatc	*mreD* deletion mutant generation
*ΔmreD*RightR	aaaaggtctcgaactaggatattcgcgcacccag	*mreD* deletion mutant generation
*ΔmrdA*LeftF	aaaaggtctctcgagaatgcgctgtcctacacctt	*mrdA* deletion mutant generation
*ΔmrdA*LeftR	aaaaggtctcgatgtggttgcggtccaggatctcg	*mrdA* deletion mutant generation
*ΔmrdA*RightF	aaaaggtctctacatagccttgttcatggggttcg	*mrdA* deletion mutant generation
*ΔmrdA*RightR	aaaaggtctcgaactaaagaactccactcccagcag	*mrdA* deletion mutant generation
*ΔmrdB*LeftF	aaaaggtctctcgagagcgcaccctgttcgataattg	*mrdB* deletion mutant generation
*ΔmrdB*LeftR	aaaaggtctcgatgtggaagtaccaggccagcatcat	*mrdB* deletion mutant generation
*ΔmrdB*RightF	aaaaggtctctacatacagacacacctggacttcatc	*mrdB* deletion mutant generation
*ΔmrdB*RightR	aaaaggtctcgaactagaatacgaggcgatgaaccg	*mrdB* deletion mutant generation
*ΔmreB*Fval	gaatctagctgagctcc	Validation of *mreB* mutants coding sequence
*ΔmreB*Rval	gggcggctcgta	Validation of *mreB* mutants coding sequence
KanRval	ttagaaaaattcatccagcatc	Validation of *mreB* mutant kanamycin cassette
PromoterF	aaaaggtctctcgagccacgtcttgttcgttgagc	Generation of *mre/mrd* promoter for complementation constructs
PromoterR	aaaaggtctcagggagctcagctagattcaggag	Amplification of *mre/mrd* promoter for complementation constructs generation
*mreB*F	aaaaggtctcatcccatgttcggattcctgcgcag	Amplification of *mreB* coding sequence for complementation constructs generation
*mreB*R	aaaaggtctcgaacttcagtcgttgatgaagatgg	Amplification of *mreB* coding sequence for complementation constructs generation
*mreC*F	aaaaggtctcatcccatgcaacgacaagcgacccc	Amplification of *mreC* coding sequence for complementation constructs generation
*mreC*R	aaaaggtctcgaactttagtccgctccatcgacatcgg	Amplification of *mreC* coding sequence for complementation constructs generation
*mreD*F	aaaaggtctcatcccatgtcgatggagcggactaag	Amplification of *mreD* coding sequence for complementation constructs generation
*mreD*R	aaaaggtctcgaacttcagacggcggaagattcgac	Amplification of *mreD* coding sequence for complementation constructs generation
*mrdA*F	aaaaggtctcatcccatgttcgaattcaagaaaacc	Amplification of *mrdA* coding sequence for complementation constructs generation
*mrdA*R	aaaaggtctcgaacttcattggcggcgctcctgcatg	Amplification of *mrdA* coding sequence for complementation constructs generation
*mrdB*F	aaaaggtctcatcccatgaaacgcctgggcctgatc	Amplification of *mrdB* coding sequence for complementation constructs generation
*mrdB*R	aaaaggtctcgaacttcaggccggcgcggggcgg	Amplification of *mrdB* coding sequence for complementation constructs generation
*ΔBP2057*RightF	aaaaggtctctcgaggctgggcgtgctgatg	BP2057 mutagenesis
*ΔBP2057*RightR	aaaaggtctcatcaacgctggcctcccgt	BP2057 mutagenesis
*ΔBP2057*LeftF	aaaaggtctcattgagccggccgccc	BP2057 mutagenesis
*ΔBP2057*LeftR	aaaaggtctcgaactaccgccgctcgcc	BP2057 mutagenesis
BP2057PromF	aaaaggtctctcgaggaccccggcgcca	Amplification of promoter for BP2057 complementation construct generation
BP2057PromR	aaaaggtctcagggaaaacgcattggcttttgcctcc	Amplification of promoter for BP2057 complementation construct generation
BP2057F	aaaaggtctcatcccatgagcaaaatcgaagtcaag	Amplification of BP2057 coding sequence for BP2057 complementation construct generation
BP2057R	aaaaggtctcgaacttcaggccgcgtc	Amplification of BP2057 coding sequence for BP2057 complementation construct generation
BP2057ValF	aatccgcgccagcag	Validation of BP2057 mutagenesis
BP2057ValR	ctttctgctcgtcggtgc	Validation of BP2057 mutagenesis
BetGlyF	aagcttcctgacctatggaggcaaaagcc	Generation of coding sequences for pMMB208 expression vector
BetGlyR	gaattcggctcaggccgcgtc	Generation of coding sequences for pMMB208 expression vector

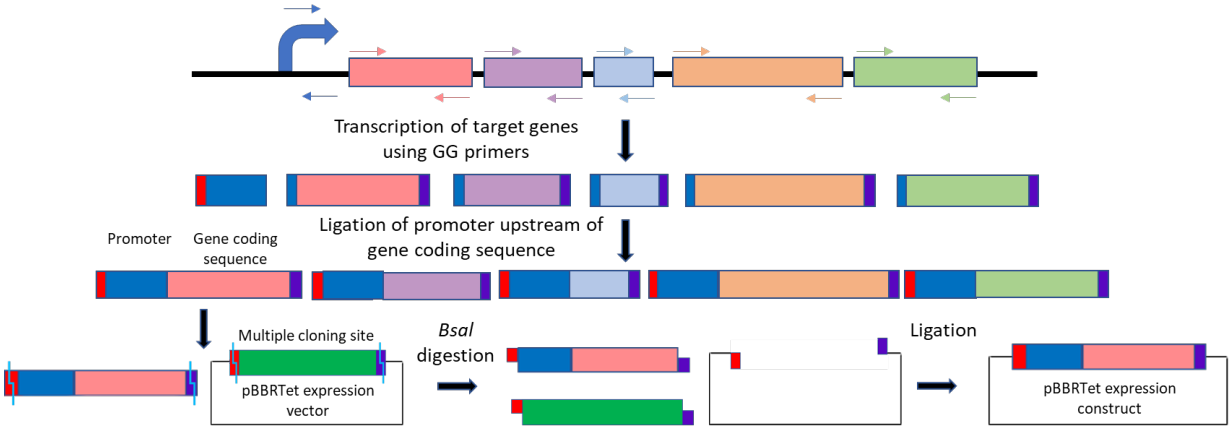

Figure 2.1- Synthesis of truncated genes for gene deletion by allelic exchange. Gene fragments synthesised by PCR utilising primers engineered to add on golden gate complementary ends (orange, yellow and purple). Gene fragments are ligated together and inserted by digestion with Bsal restriction enzyme into pSS4940 suicide vector during golden gate cloning reaction.

ST18 donor *E. coli* was transformed with these constructs and introduced into *B. pertussis* by conjugation. Conjugations were done as described in the literature (Allen and Maskell, 1996). Conjugants were initially selected by growth on charcoal agar supplemented with gentamycin (30ug/ml) and 50mM $MgSO_4$. As the pSS4940 plasmid does not replicate in *B. pertussis* plating on gentamycin selects for recombination events where the plasmid has integrated into the *B. pertussis* chromosome (Table 2.1). The pSS4940 plasmid contains a I-*Sce*I gene controlled by a *ptx* promoter. As *ptx* is a BVG+ induced gene this promoter is inactive during BVG- conditions and active under BVG+ modulating conditions. Initial selection was carried out in BVG- modulating conditions due to the presence of 50mM $MgSO_4$.

Individual colonies were then secondary selected by passaging on charcoal agar. In the absence of 50mM $MgSO_4$ the *B. pertussis* grows in the BVG+ growth phase. Therefore, the *ptx* promoter is activated expressing the I-*Sce*I gene causing a lethal event if the clones contain the integrated plasmid. This selects for clones that do not contain the integrated plasmid and have undergone a secondary recombination event. In these clones the wildtype or mutant gene have been looped out, resulting in either mutation of the target allele or reversion back to wildtype respectively (Figure 2.2). PCR amplification of coding regions to verify truncation was carried out using LeftF and RightR primers used for mutagenesis (Table 2.2).

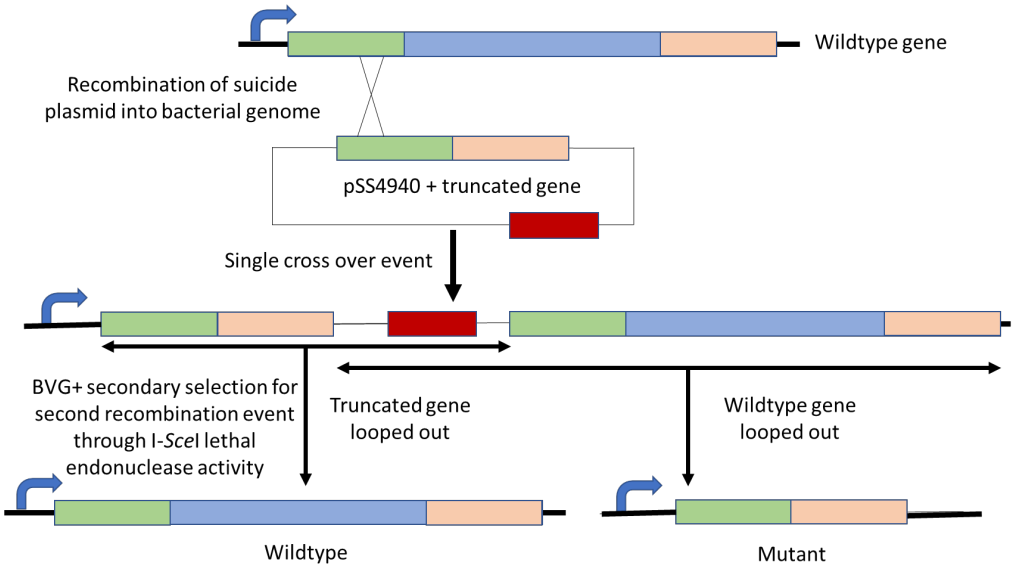

Figure 2.2- Allelic exchange by homologous recombination. Suicide vector recombined with bacterial genome inserting truncated gene alongside wildtype allele. Counter selection against single crossover mutants results in either truncated or wildtype gene being removed. Mutants selected by antibiotic resistance gene (red).

2.3-Complementation-

Complementation constructs were cloned by the amplification of the endogenous promoter of the genes and the wildtype coding sequence of the gene (Table 2.2). These products were ligated together and inserted into the pBBRTetGG vector by Golden Gate cloning (Table 2.1 & Figure 2.3). These constructs were cloned in to pBBRTetGG vector and introduced into mutant strains by conjugation as previously described.

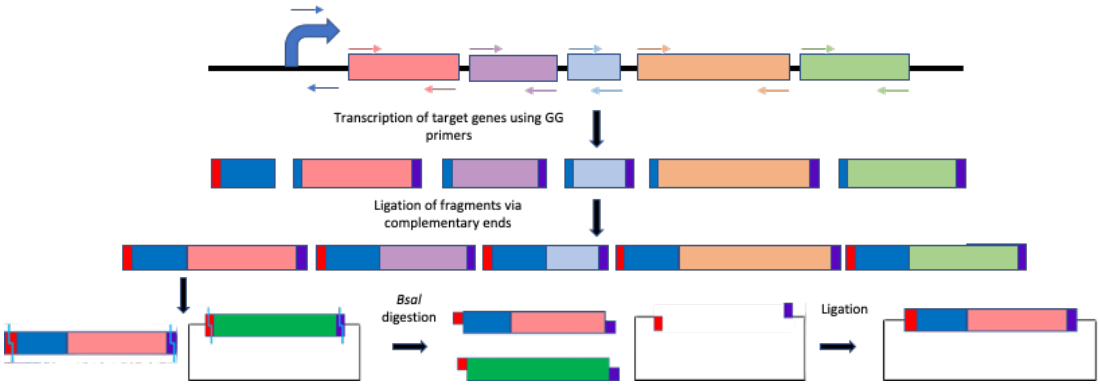

Figure 2.3– Complementation construct generation by golden gate cloning. Target genes synthesised with golden gate primers producing fragments with complementary ends. Fragments are ligated, digested and inserted into expression plasmid by golden gate cloning.

2.4-Colony count for viability on plates-

Plate grown *B. pertussis* strains were resuspended in sterile PBS. Suspensions were standardised to an OD_{600} of 1 and diluted to $1x10^{-6}$-$1x10^{-9}$, and 100µl plated on charcoal agar plates. Modulation for BVG- growth conditions was done by the addition of 50mM $MgSO_4$ to the charcoal agar.

2.5-Liquid culture growth analysis-

Analysis of growth was carried out by measurement of OD_{600} values over the time course of bacterial growth. *B. pertussis* strains were grown in 96 well deep well plates (1ml culture volume), baffled flasks (50ml culture volume) and 96 well plates (200µl culture volume). Cultures were seeded at an OD_{600} of 0.1 and OD readings were taken across the growth curve from 0-72 hours.

2.6-Detergent susceptibility assay-

B. pertussis BP536 wildtype and mutant strains were grown in deep well culture plates in SSCH medium with and without $MgSO_4$ modulation for BVG- and BVG+ growth respectively. SDS was added at a range of concentrations from 0.1mM-1mM to growth medium and the ability of the bacteria to grow under these conditions was analysed by measuring OD_{600} after 24 hours of growth.

2.7- Scanning Electron Microscopy (SEM) of bacteria and Electron Microscopy of OMVs-

2.7.1 SEM imaging of bacteria

B. pertussis plate grown bacteria were resuspended in PBS to an OD_{600} of 1. 50µl of this suspension was placed onto a Silicon wafer and left to settle for 30mins at room temperature. 2.5% glutaraldehyde (GDA) in PBS was then added to cover the Silicon wafer and the fixed bacteria were stored at 4˚C overnight. Wafers were rinsed gently in PBS 3 times for five minutes each time. Samples were postfixed in aqueous 1% Osmium Tetroxide for 1hour in fume hood at room temp. Samples were then washed in distilled water 2 times for five minutes each time, then serially dehydrate in Acetone in glass vials: 50, 70, 90, 100% dry Acetone 3 times per concentration for five minutes each time. Sample was then placed in 1:1 dry Acetone: HMDS (Hexamethyldisilane) for 15 mins. Samples were then washed with

100% HMDS 3 times for five minutes. HMDS was removed after which the samples were mounted by for SEM analysis.

Analysis of images was carried out using Image-J software (Rasband, 2011). Cells for measurement were determined by division of images into 10 by 10 grid and a random number generator was utilised to produce coordinates for squares in which bacterial cells were to be measured. Number of bacterial cells measured for morphology analysis n=60.

2.7.2 EM imaging of OMVS

5µl of purified OMV samples was applied to a glow discharged copper 200-square mesh grids (Quorum Gloqube Plus). Grid was blotted to remove excess solution and negatively stained for 30 seconds using NanoW (Nanoprobes). The grid was airdried and then imaged.

2.8-Transmission electron microscopy (TEM)-

B. pertussis strains were grown for three days on charcoal agar plates. A 10µl inoculation loop was utilised to take biomass from the secondary streak which was placed in 2.5% GDA in PBS. Sample preparation was carried out following the same protocol as SEM up to HMDS treatment but with cells in suspension not attached to a Silicon wafer. After sequential dehydration cells were moulded using Spurrs epoxy resin and oven treatment (70˚C for 8 hours). Moulds were then sectioned for TEM imaging.

Analysis of images was carried out using Image-J software (Rasband, 2011). Cells for measurement were determined by division of images into 10 by 10 grid and random number generator was utilised to produce coordinates for squares in which bacterial cells were to be measured. Number of bacterial cells measured for internal architecture analysis n=27

2.9-RNA extraction for BP536 BVG+ and BVG- plate growth analysis-

BP536 wildtype was grown on charcoal agar plates in triplicate for 72 hours. Biomass from each plate was resuspended at an OD_{600} of 1 in PBS before being pelleted by centrifugation at 10 000xg for 10 minutes at room temperature. RNA was extracted using TRI Reagent® (Invitrogen) following the manufacturers protocol. RNA was treated using the TURBO DNA-free Kit (Invitrogen) following the manufacturers protocol.

2.10-Quality check of BVG+ and BVG- modulation by qPCR-

Using Protoscript taq RT-PCR kit (NEB) along with NEB random primer mix, cDNA was synthesised from RNA samples. cDNA was utilised for qPCR analysis of the amount of the transcript of the classical BVG+ gene *ptxA* when compared to the housekeeping gene *recA*

(Table 2.3). qPCR reaction utilised 1x SYBR Green Universal Master Mix (Applied Biosystems) to which 0.4µM primer pairs and 1.25ng of cDNA was added. qPCR reactions were carried out using the StepOnePlus Real-Time PCR system with an annealing temp of 60℃.

Table 2.3- qPCR primers

Primer	Sequence
*ptxA*F	GACCACGACCACGGAGTATT
*ptxA*R	CGCGATGCTTTCGTAGTACA
*recA*F	AACCAGATCCGCATGAAGAT
*recA*R	ACCTTGTTCTTGACCACCTT

2.11-RNA extraction from BP536, BP_{536}*ΔmreC*, PTg, BP_{PTg}50D6 and BP_{PTg}C7 during BVG+ broth culture -

B. pertussis strains were grown in SSCH liquid medium at 37℃ at 180rpm in a standing shaking incubator. Culture volume was 50ml in a 250ml conical flask. Strains were grown to mid-log determined by reaching an OD_{600} of 1.5-2. 5ml of culture was then pipetted onto 5ml of frozen SSCH medium to halt transcription and stored at -80℃. Volume for an OD_{600} of 1 was removed and pelleted by centrifugation. Pellets were treated with 0.1 mg/ml of lysozyme after which RNA was extracted using the RNeasy micro kit (Qiagen) following the manufacturers protocol. Extracted RNA was treated with DNase turbo kit (Invitrogen) to remove gDNA contamination and quality of RNA extracted was analysed using Agilent bioanalyzer with the Agilent RNA 6000 kit (Agilent).

Library preparation was then carried out using Illumina Stranded Total RNA Prep with Ribo-Zero Plus (Illumina). For rRNA depletion *B. pertussis* specific rRNA depletion probes were utilised. Library quality was assessed by Agilent Tape (Agilent) deck before sequencing by MiSeq (Illumina).

2.12-RNA sequencing-

Extracted RNA was utilised for strand specific RNAseq. Sequencing was performed by Novogene UK for BP536 plate growth analysis. RNAseq for *B. pertussis* broth growth analysis was carried out using MiSeq.

2.13-RNA-seq pseudoalignment-

The fastQ files generated were then pseudo aligned using kallisto allowing quantification of the abundance of transcripts in the extracted RNA (Bray et al., 2016). Samples were aligned to the annotated Tohama I reference genome which contains 3,816 *B. pertussis* genes (Parkhill et al., 2003).

2.14-Differential expression analysis of RNA-seq data-

Using the output files generated by Kallisto pseudoalignment, gene expression was then analysed using DESeq2 to identify differentially expressed genes (Love et al., 2014). Gene differential expression was determined by log2 fold change of gene expression between conditions. Genes were characterised as differentially expressed if they displayed a log2 fold change of >2 or <-2 with a p value of <0.05. P values generated by the Wald test.

2.15-Cluster of Orthologous Genes (COG) analysis-

Genes were grouped by functional groups by COG analysis. The reference COG file was generated from the Tohama I reference genome using the eggNOG (evolutionary genealogy of genes: Non-supervised Orthologous Groups) database (Parkhill et al., 2003, Huerta-Cepas et al., 2019). Genes annotated NA or S to illustrate unknown functions in COG database where further investigated by manual searching of annotated Tohama I genome using Artemis, a genome browser and annotation tool (Carver et al., 2012). If gene function was identified by this analysis, they were added to the associated COG categories. Genes with unknown function (S) and transposase for highly conserved IS481 elements (L) were removed from the analysis.

2.16-Betaine and Proline supplementation-

BP536 wildtype and BP_{536}*ΔmreB* plate grown strains were resuspended in PBS to an OD_{600} of 1 and serially dilution to $1x10^{-6}$ OD. This dilution was plated on charcoal agar plates modulated to the BVG- growth phases with and without betaine/proline supplementation (1-100mM).

2.17-Betaine glycine uptake inducible expression system generation and analysis-

The three gene betaine glycine uptake system was amplified by PCR using Q5 high fidelity polymerase (NEB) which was then cloned into pMMB208 expression vector by restriction digestion (Table 2.1 & 2.2). The effect of betaine uptake system expression was analysed by

colony count analysis of BP536 wildtype and BP_{536}*ΔmreB* strains with and without IPTG induction of expression and with and without betaine supplementation.

2.18-Quantification of lipid content of culture supernatant and purified OMVs using lipophilic dye FM4-64-

B. pertussis cultures was spun down at 10,000g for 20 minutes to pellet bacteria. 45µl of bacterial free supernatant was aliquoted into black Greiner 96 well flat bottom plates. FM4-64 dye (Invitrogen) was resuspended to 10ug/ml final concentration in culture medium and 5µl was added to each well. Fluorescence units were quantified by measuring emission at 640nm upon excitation at 515nm. Quantification of purified OMVs lipid content was carried out following the protocol above but with 1µl of purified OMVs diluted in 44µl of PBS.

2.19-OMV purification-

50ml cultures were grown in 250ml conical flasks. At 72 hours of growth cultures were spun down to pellet bacteria with the supernatant then double filtered using 0.22um stericup vacuum filter units (Millipore). Filtered supernatant was centrifuged by ultracentrifugation using a SW-32 Beckman ultracentrifuge rotor in 38.5ml sterile Ultra-clear thin wall tubes (Beckman) spinning at 32,000rpm for 2 hours to pellet OMVs. The culture supernatant was poured off and replaced by PBS to wash the OMV pellet and re-spun for 2 hours at 32,000rpm. OMV pellet was resuspended in 200µl PBS by shaking at 4C overnight and treated with 100 units of benzonase enzyme (Abcam) for 1 hour at room temperature.

2.20-Protein quantification of purified OMVs by *DC* Assay-

Purified OMVs protein content was quantified using the *DC* assay (BioRad) following the manufacturers protocol. Bovine serum albumin was used for standard curve production.

2.21-SDS page analysis of OMV protein content-

OMV purified samples were run in NuPAGE 4-12% Bis-Tris gels (Invitrogen) after denaturation by boiling. Sample volumes were standardised to either protein concentration or lipid concentration of OMVs. Gels were stained using Coomassie blue protein stain.

2.22-Dynamic light scattering (DLS) measurement of OMV samples-

60µl of purified OMVs in PBS was measured using Malvern high performance DLS with a He-Ne laser as an angle of 173˚ at 25˚C. Three biological replicates per strain were analysed.

2.23-Nanoparticle tracking analysis (NTA) of purified OMVs-

Using NanoSight NS500 OMV particle size and concentration was measured for wildtype and mutant strains. Samples were diluted 1:100-1:1000 in PBS and loaded into the sample chamber. Four videos were recorded for 60s and the size of individual OMVs and total number of OMV particles were measured using the Nanoparticle Tracking Analysis software (NanoSight Ltd.). All measurements were taken at room temperature at a flow rate of 20 units. Three biological replicates were analysed per strain.

2.24-Statistical analysis-

Students T-test and One way ANOVA using Tukey post hoc analysis was utilised to analyse pairwise and multiple comparisons respectively using SigmaPlot Version 14.5. Statistical significance was defined as a p value of <0.05.

2.25-Data handling and plotting-

Data handling and analysis was carried out using Microsoft Excel Version 2302. Data visualisation and plotting was carried out using RStudio Version 4.2+ and ggplot2 (Wickham, 2016, RStudio, 2020)

Chapter 3 Characterisation of the effect of *mre/mrd* mutation on *B. pertussis* growth and morphology-

Mutagenesis of the *mre/mrd* operon reduces bacterial viability due to the induction of a lytic phenotype coupled with an alteration in bacterial morphology in other gram-negative bacteria. The identification of the *mre/mrd* operon as conditionally essential in *B. pertussis* suggests that *mre/mrd* mutation may not have the same phenotypic effects as observed in other bacteria. Therefore, I aimed to characterise the effect of *mre/mrd* mutation on *B. pertussis* growth, morphology, and OM stability.

3.1-Generation of *mre/mrd* mutants and complemented strains-

3.1.1- Generation of *mre/mrd* mutants-

Mutagenesis of *mre/mrd* genes, where the wildtype allele is swapped with a truncated form of the gene, was carried out prior to the start of my PhD. Mutagenesis strategy was designed to maintain downstream reading frames as to only affect targeted gene's expression (Table 3.1). The flanking regions of the coding sequence were amplified, and these fragments were assembled and inserted into the pSS4940GG suicide vector by golden gate cloning. Constructs were then verified by Sanger sequencing. Constructs were utilised for allelic exchange mutagenesis and mutant strains produced were validated by colony PCR screening. Mutagenesis was successful for all 5 *mre/mrd* genes displaying that they can be deleted in *B. pertussis.*

Table 3.1- Location of mutation for *mre/mrd* deletion

Gene	Gene size (bp)	Genome position (bp)	Internal deletion genome position (bp)	Deletion size (bp)	Presence of Kanamycin cassette
mreB	1,043	375155-376198	375157-376210	1,053	Y (810bp)
mreC	884	376287-377171	376301-377151	850	N
mreD	464	377257-377721	377292-377704	412	N
mrdA	1,952	377735-379687	377953-379288	1,335	N
mrdB	1,146	379684-380830	380064-380968	904	N

3.1.2-Complementation of *mre/mrd* knockouts-

To assess whether phenotypic changes observed in mutant strains were a direct result of the single gene deleted, I reintroduced endogenous gene expression of wildtype *mre/mrd* into

mutant strains by complementation. The coding sequence of the wildtype allele was cloned downstream of the *mre/mrd* operons endogenous promoter and introduced into pBBRTetGG expression vector. The coding sequence of the promoter and wildtype *mre/mrd* genes were amplified by PCR and verified by gel electrophoresis (Figure 3.1 & Table 3.2). The promoter and gene fragments were assembled and inserted into pBBRTetGG by golden gate sequencing. Restriction digest of these expression constructs displayed bands of the predicted insertion sizes during gel electrophoresis, suggesting that cloning had been successful (Figure 3.2 & Table 3.2). Successful cloning into expression constructs were then verified by Sanger sequencing. *mreB* complementation constructs were generated and verified prior to the start of my PhD.

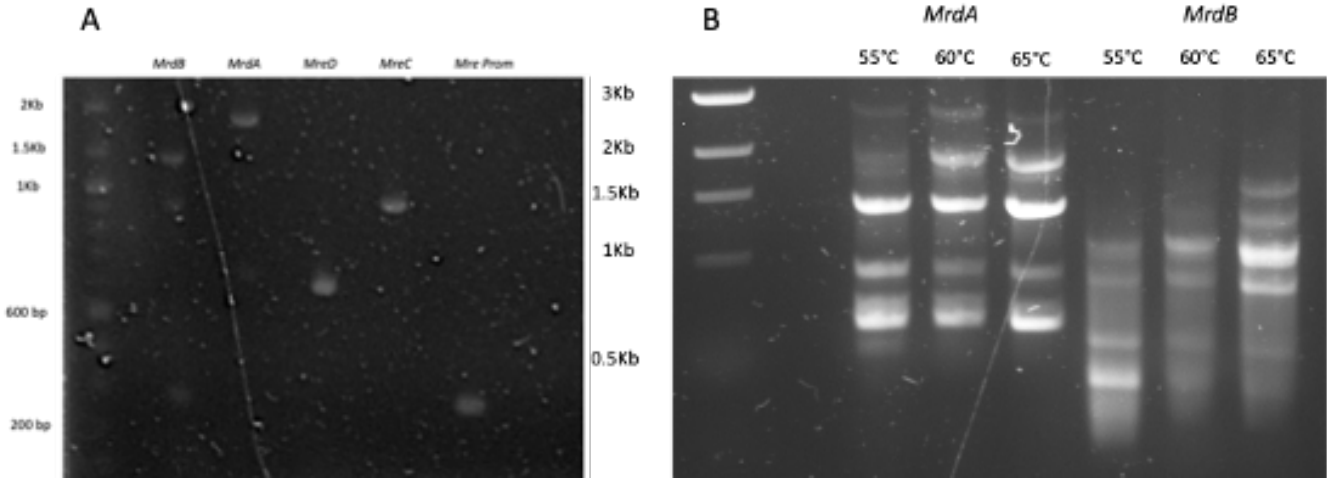

Figure 3.1– PCR amplification of complementation construct fragments for golden gate cloning. A) Q5 polymerase amplification of fragments, B) Gradient PCR of *mrdA* and *mrdB* fragments. Due to the presence of unspecific PCR products fragments for *mrdA* and *mrdB* PCR products of correct size were purified by gel extraction of specific product (1952bp and 1136bp respectively)

Table 3.2- Expected fragment size *mre/mrd* constructs

Construct	Gene size (bp)	Promoter size (bp)	Expected band size (bp)
MrdA	1952	254	2206
MrdB	1136	254	1390
MreC	884	254	1138
MreD	569	254	823

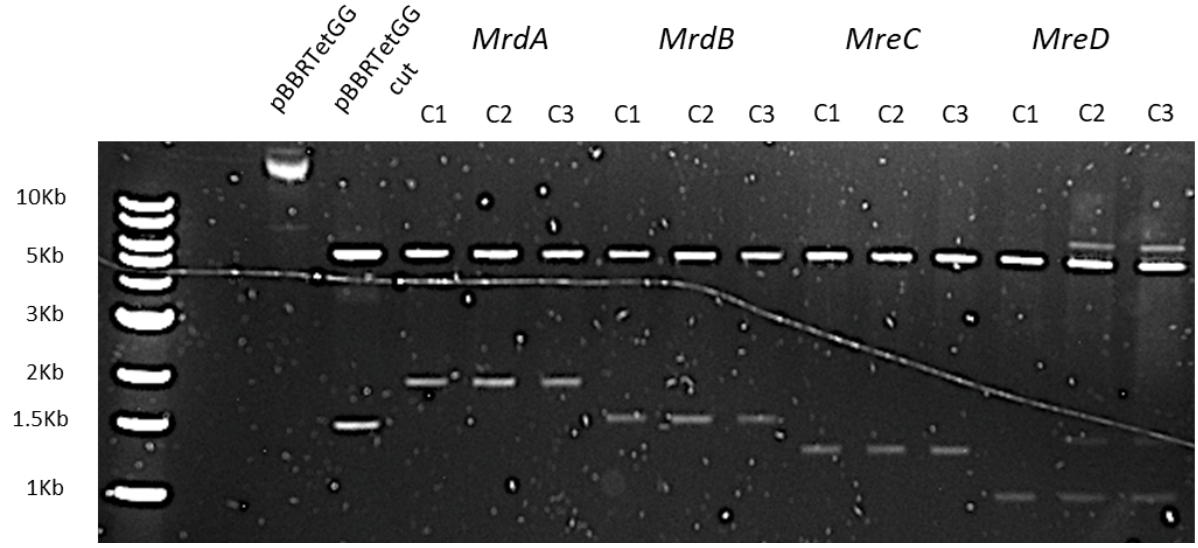

Figure 3.2 - Restriction digest analysis of *mre/mrd* complementation constructs to evaluate size of inserted PCR product.

3.2-Characterisation of the effects of *mre/mrd* KO on bacterial physiology

3.2.1-Do *mre/mrd* mutations alter the ability of *B. pertussis* to grow in plate conditions?

To verify that the conditional essentiality observed during the TraDIS screen was maintained when the *mre/mrd* operon was directly mutated by deletion of the coding sequence, the colony forming units (CFU) produced upon plating a $1x10^{-9}$ dilution of a 1 OD_{600} suspension on BVG+ and BVG- modulating plates was analysed (Figure 3.3) (Belcher et al., 2020). In BVG+ growth conditions, mutant CFUs were reduced but displayed no significant change when compared to BP536. Interestingly this was not the case during BVG- growth, with mutants displaying a significant change in CFU produced. Mutants were not viable under these modulating conditions, with no growth observed until *mre/mrd* expression was re-introduced by complementation. It is worth noting that complementation of gene expression did not significantly change CFU produced by either BP536 wildtype or mutant strains in the BVG+ conditions. This displays that complementation of *mre/mrd* expression does not increase BP536 wildtype or *mre/mrd* mutant strain growth during BVG+ conditions .

Overall, this analysis displays that the conditional essentiality observed during the TraDIS screen remains upon direct mutagenesis of the *mre/mrd* operon. These finding also validates that the complementation constructs successfully reintroduce gene expression as they successfully rescue mutant viability during BVG- growth.

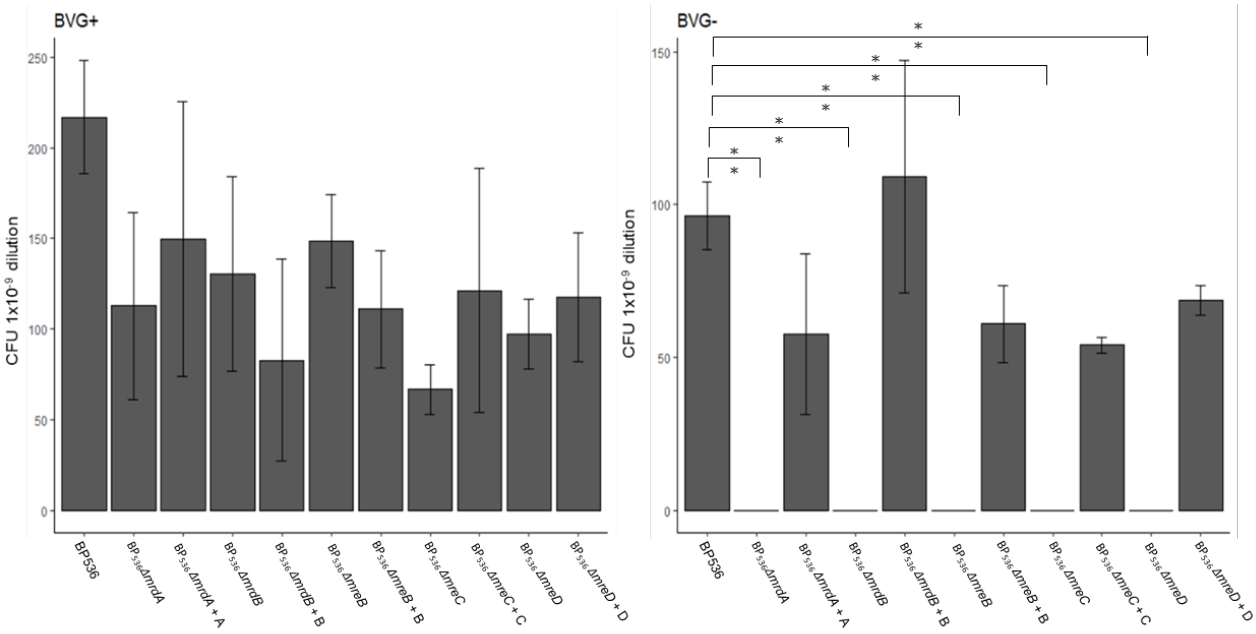

Figure 3.3- Conditional essentiality of *mre/mrd* mutants during plate growth dependent on BVG activation state. Colony forming units (CFU) produced upon plating a $1x10^{-9}$ dilution of a 1 OD_{600} suspension of BP536 wildtype, *mre/mrd* mutant and complemented strains on BVG+ or BVG- modulated charcoal agar plates were counted. Conditional essentiality of the *mre/mrd* operon was observed with mutants displaying viability during BVG+ growth but not BVG- growth. Results are representative of three biological replicates. **=$p \leq 0.01$, Students T-test. Error bars = Standard error of the mean.

3.2.2-Do *mre/mrd* mutations alter the ability of *B. pertussis* to grow in broth conditions?

With such a stark difference in bacterial viability during plate growth, dependent on BVG activation phase, it was investigated if the same phenotype was observed during broth growth of the mutant strains. This analysis was carried out using change in OD_{600} values of broth cultures as a proxy for bacterial growth and viability. All cultures were seeded at an OD_{600} of 0.1 and OD values were taken at 48 hours of growth. Quite strikingly the conditional essentiality displayed during plate growth was not observed in broth culture (Figure 3.4). In both BVG+ and BVG- conditions mutant strains grew comparably to BP536 wildtype, suggesting that the conditional essentiality previously described is a plate growth specific phenomenon. It is also worthy to note that mutants grew comparably to BP536 wildtype independent of culture volume, culturing method or air: volume ratio, with 50ml, 96 well and 96 deep well culturing techniques displaying consistent mutant growth to wildtype levels.

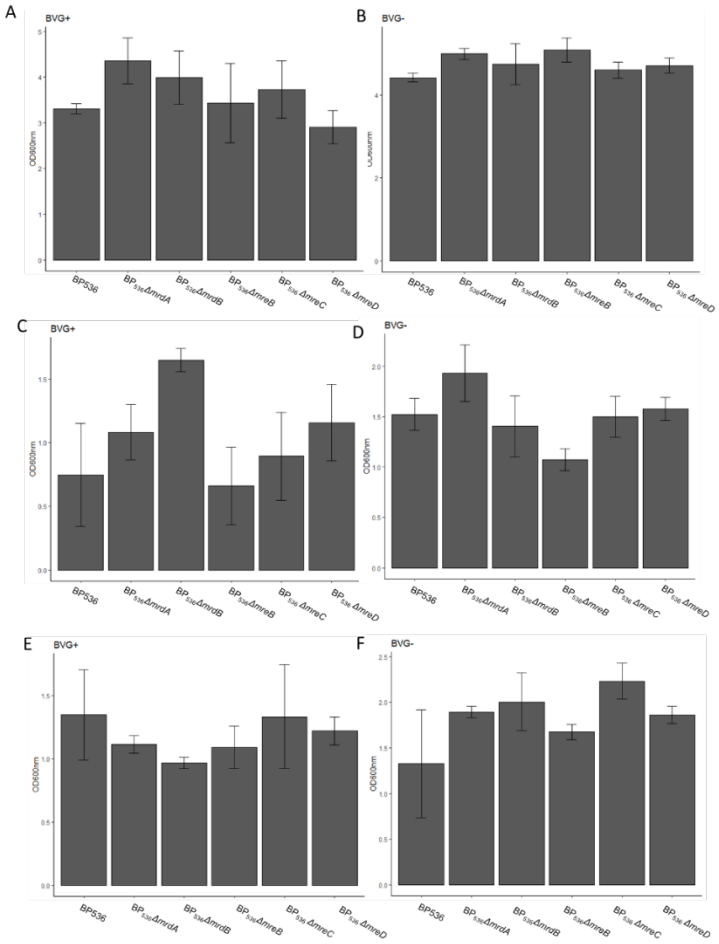

Figure 3.4- Growth of *mre/mrd* mutant strains in Stainer-Scholte broth conditions. OD_{600} reading at 48 hours of growth in A&B) Deep well plate, C&D) 50ml baffled flask or E&F) 96 well plate. Data representative of three biological replicates. No statistical difference between OD_{600} values were observed when compared to BP536 wildtype (Students T-test). Mutants grew comparably to wildtype independent of culture method or BVG activation state displaying *mre/mrd* mutations do not negatively effect growth in broth conditions. Error bars = Standard error of the mean.

To assess how different media compositions alter mutants ability to grow during liquid culture, BP_{536}*ΔmreB* growth was assessed in plain SS, SSC, SSH and SSCH medium in deepwell plate cultures in parallel with BP536 wildtype (Figure 3.5). Casamino acids is a media supplement containing predominantly casein with small amounts of cystine and tryptophan, which can be utilised as a nitrogen source by bacteria. In *B. pertussis* culturing, this supplement facilitates high levels of bacterial growth and metabolism. Heptakis is a cyclodextrin that sequesters hydrophobic molecules inhibitory to *B. pertussis* growth released during *in vitro* culturing and enabling *B. pertussis* to reach higher culture density.

BP_{536}*ΔmreB* did not display a significant alteration in growth upon media supplementation when compared to BP536. The highest OD_{600} value was observed in SSCH media for both

BP536 and BP$_{536}$*ΔmreB*, suggesting the mutants are comparably viable at high growth rates (Figure 3.5). SSC media was found to significantly increase BP536 and BP$_{536}$*ΔmreB* growth at the 24-hour timepoint, but comparable OD_{600} to SS and SSH was observed after 48-hours of growth. Addition of heptakis did not significantly increase BP536 or BP$_{536}$*ΔmreB* growth rates, with comparable OD_{600} values to SS at 24- and 48-hours of growth. Heptakis supplementation aided growth only when supplemented alongside casamino acids, with SSCH reaching significantly higher OD_{600} values at 24-hour and 48-hour timepoints than SSH and SSC. These findings display that deletion of *mreB* does not alter *B. pertussis's* ability to grow under differing media conditions.

The fact that BP$_{536}$*ΔmreB* viability is not altered at high rates of biomass production is particularly interesting because tolerance of *mreB* mutation in *E. coli* was found to be induced by reducing bacterial growth rate by nutrient limitation (Bendezú and de Boer, 2008). I hypothesised that this may be what facilitates tolerance of *mreB* mutation in *B. pertussis* due to the modest growth rate observed in *in vitro* culture . However, this analysis suggests this is not the case.

.

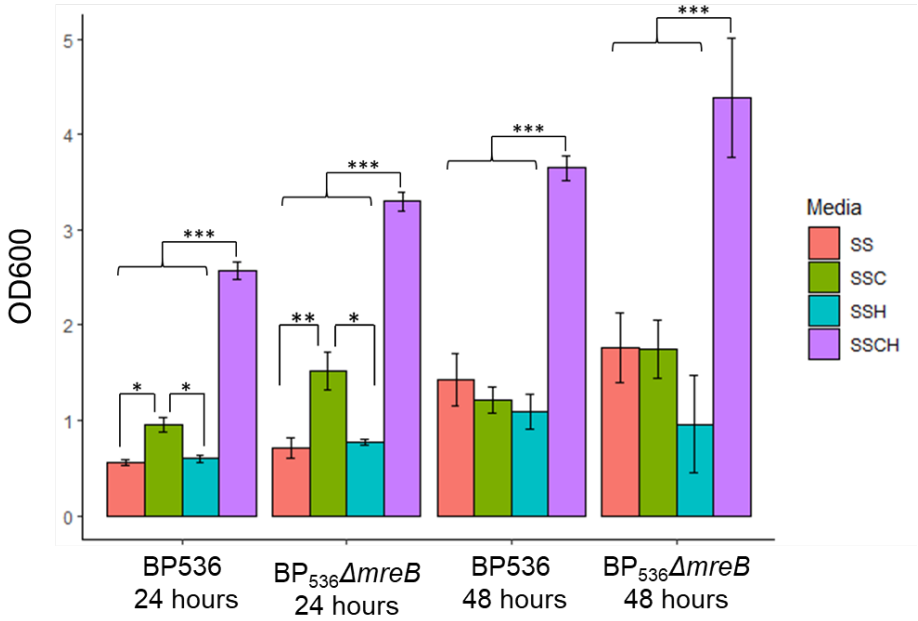

Figure 3.5 – Analysis of the effect of media supplementation on BP$_{536}$*ΔmreB* growth in Stainer-Scholte medium. Stainer-Scholte (SS) media was supplemented with casamino acids (C) and/or heptakis (H) and utilised for deep well culture growth. OD_{600} readings were taken at 48-hours for growth as a proxy for mutant viability. Data representative of three biological replicates. *=p<0.05, **=p<0.01, ***=p<0.001 One way ANOVA, Tukeys post-hoc. Error bars = Standard error of the mean.

3.2.3-Does *mreB* mutation affect the cell walls ability to tolerate detergent induced stress?

To assess the structural integrity of the *mre/mrd* mutant strains, I analysed their ability to tolerate OM stress induced by introduction of the detergent SDS to the growth medium. SDS inhibition of growth was calculated as a percentage of strain growth in the absence of SDS. There was no significant change in SDS inhibition of growth in BP536, BP_{536}*ΔmreB,* and complemented (BP_{536}*ΔmreB+B*) strains in BVG+ or BVG- growth conditions regardless of SDS concentration (Figure 3.6). This suggests that despite mutation of *mreB* there is no alteration in *B. pertussis's* ability to tolerate OM stress induced by SDS.

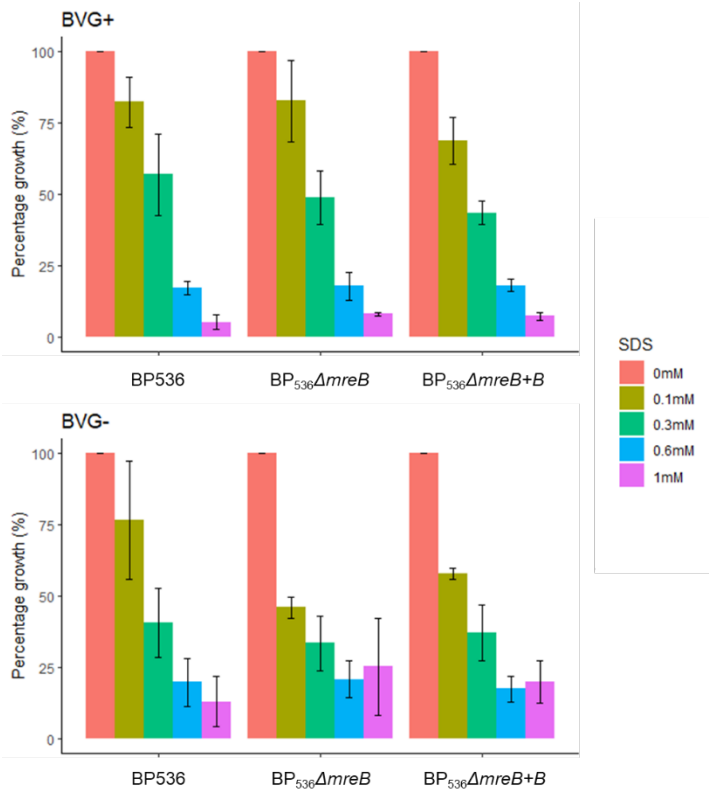

Figure 3.6- SDS susceptibility assay. To assess outer membrane stability of mutants their ability to tolerate a range of detergent concentrations during deep well broth growth was analysed. OD_{600} readings were taken after 24-hour as a proxy for bacterial viability. Data representative of three biological replicates. Error bars = Standard error of the mean.

3.2.4-Do *mre/mrd* mutations affect bacterial morphologies?

To assess the effect of *mre/mrd* mutations on *B. pertussis* morphology, SEM images of BP536 wildtype, mutant and complemented strains were analysed. These images display clear morphological change upon *mre/mrd* mutation compared to *B. pertussis* wildtype. The classical rod shape of *B. pertussis* was not observed in mutant strains, with their morphology

resembling that of cocci shaped bacteria, with associated decrease in bacterial length and increase in bacterial width (Figure 3.7). Upon complementation these changes were reversed, with mutants displaying rod morphology. However, the significant increase in bacterial width was maintained in complemented strains with an increase in bacterial length being the cause of the reversion back to rod shape. Calculation of bacterial volume displayed that all mutants had increased average volume, however, the significant increase was only observed in BP$_{536}$*ΔmreB* and BP$_{536}$*ΔmreC* mutant strains. Interestingly, a significant increase in bacterial volume was also observed in all complemented strains apart from BP$_{536}$*ΔmreD+D,* however this is most likely due to the increased length observed.

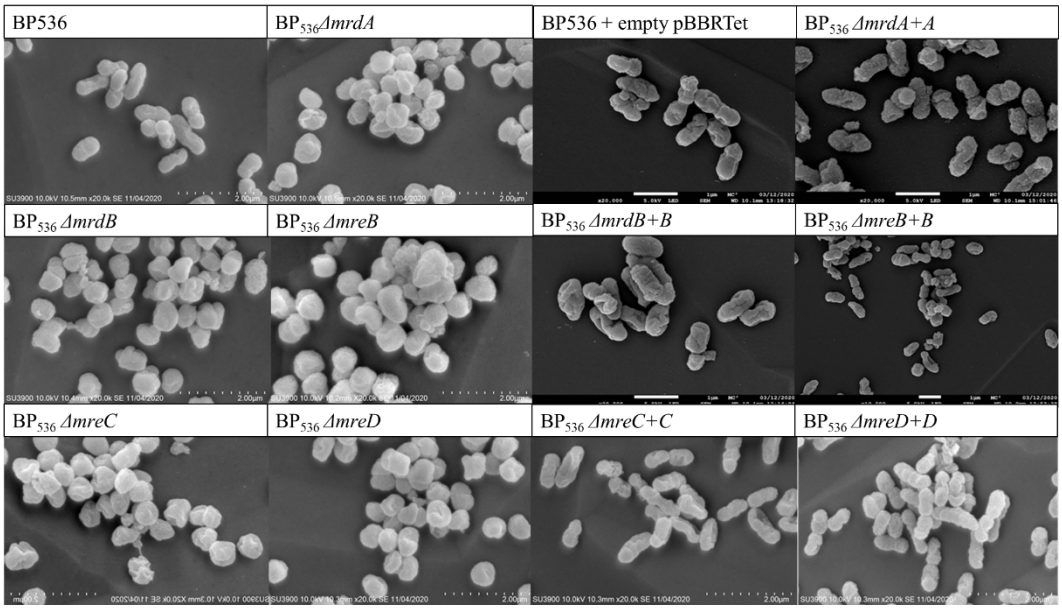

Strain	Length (µm)	Width (µm)	Volume (µm^3)
BP536	0.875 ±0.162	0.374 ±0.036	0.083 ±0.026
BP$_{536}$*ΔmrdA*	0.649 ±0.097 (***)	0.495 ±0.075 (***)	0.102 ±0.036 (NS)
BP$_{536}$*ΔmrdB*	0.629 ±0.071 (***)	0.519 ±0.077 (***)	0.102 ±0.028 (NS)
BP$_{536}$*ΔmreB*	0.684 ±0.107 (***)	0.584 ±0.049 (***)	0.137 ±0.041 (***)
BP$_{536}$*ΔmreC*	0.673 ±0.071 (***)	0.545 ±0.056 (***)	0.12 ±0.029 (***)
BP$_{536}$*ΔmreD*	0.594 ±0.077 (***)	0.495 ±0.055 (***)	0.087 ±0.025 (NS)
BP$_{536}$*ΔmrdA+A*	0.911 ±0.161 (NS)	0.504 ±0.09 (***)	0.153 ±0.076 (***)
BP$_{536}$*ΔmrdB+B*	0.965 ±0.174 (NS)	0.512 ±0.067 (***)	0.167 ±0.061 (***)
BP$_{536}$*ΔmreB+B*	0.902 ±0.13 (NS)	0.470 ±0.049 (***)	0.132 ±0.038 (***)
BP$_{536}$*ΔmreC+C*	1.034 ±0.355 (NS)	0.391 ±0.157 (**)	0.114 ±0.079 (**)
BP$_{536}$*ΔmreD+D*	0.809 ±0.179 (NS)	0.345 ±0.056 (NS)	0.066 ±0.028 (NS)

Figure 3.7- SEM analysis of *mre/mrd* mutants morphology. Morphology was characterised by measurement of strain average length width and volume ± standard deviation of the mean. One way ANOVA and Tukeys Post-Hoc. ***=p≤0.001.], **=p≤0.01 n=60

To analyse whether internal structures were altered in BP_{536}*ΔmreB* strains compared to BP536, transmission electron microscopy (TEM) was utilised to analyse bacterial cross-sections. Mutant bacteria had altered internal morphology with a decrease in uniformity of the bacterial cytoplasm and periplasm when compared to wildtype (Figure 3.8). This change in uniformity appeared to be as a result of IM invagination into the cytoplasmic space, coupled with decreased association with IM and OM membranes resulting in increased space between the two membranes of the bacterial cell wall. This altered morphology was characterised by measurement of periplasmic area which displayed a significant increase in BP_{536}*ΔmreB*.

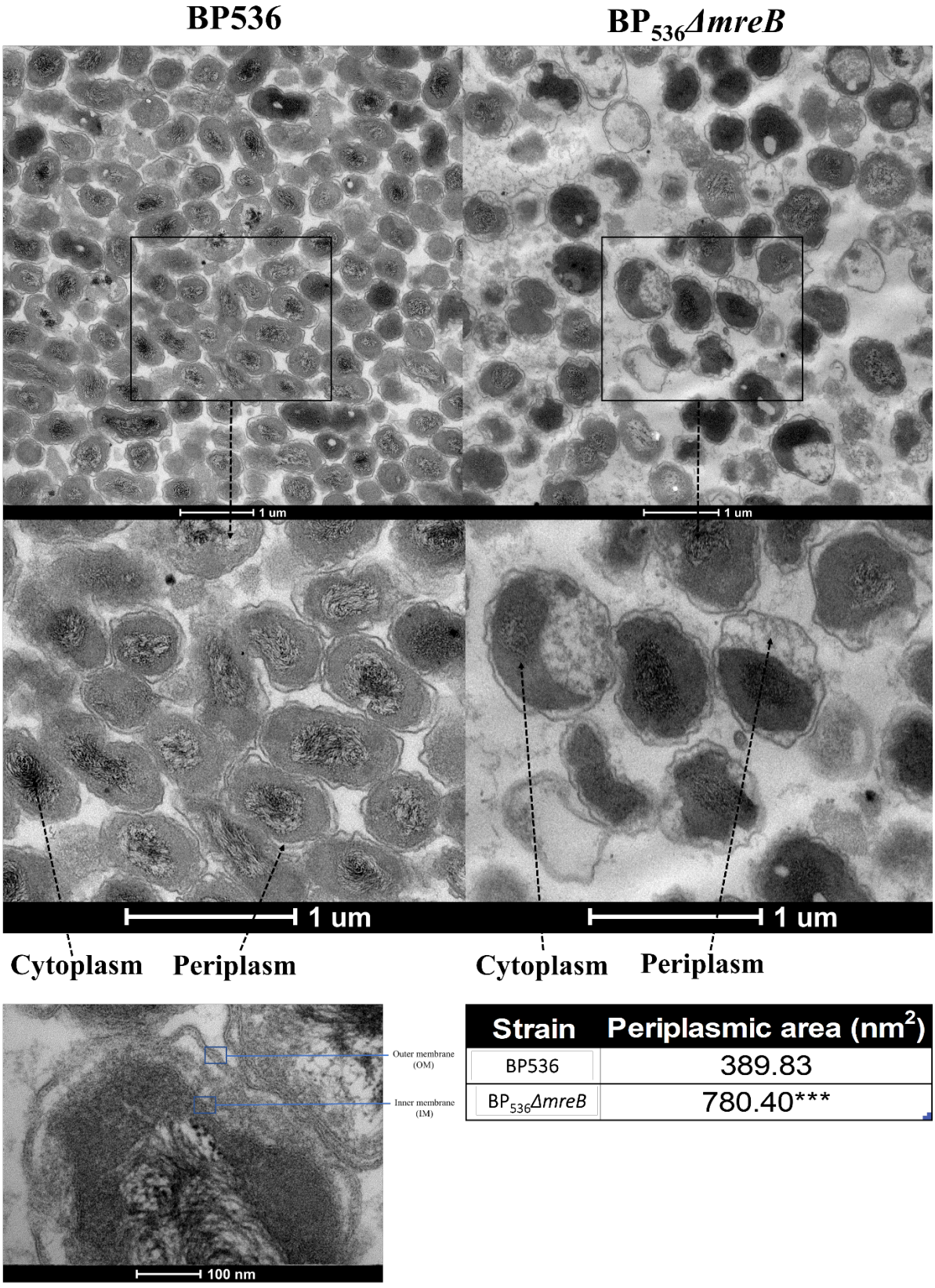

Strain	Periplasmic area (nm^2)
BP536	389.83
$BP_{536}\Delta mreB$	780.40***

Figure 3.8 – TEM analysis of changes in bacterial architecture upon *mreB* mutation. Changes in structure of strains periplasmic was characterised by measurement of area (nm^2). One way ANOVA and Tukeys Post-Hoc. ***=p≤0.001 n=27

3.3-Discussion

3.3.1-Do *mre/mrd* mutations result in decreased bacterial viability as seen in other gram-negative bacteria?-

One of the novel findings of this research is that *B. pertussis* displays no significant perturbation to its growth or viability during BVG+ plate and broth and BVG- broth growth conditions upon *mre/mrd* mutations. Mutants were observed to only be non-viable during BVG- plate culture growth (Figure 3.3 & 3.4). This phenotype has not been observed in other gram-negative bacteria, where growth in nutrient limited conditions or the induction of overexpression of alternate PG biosynthesis mechanisms was required to tolerate the loss of the *mre/mrd* operon.

Mutation of *mreB* in *E. coli* displayed that growth in minimal media, with low biomass doubling rates, facilitated tolerance the loss of elongasome PG biosynthesis. This mechanism of tolerance is thought to be due to the low level of bacterial growth allowing the alternate PG biosynthesis pathway, the divisome, to produce and incorporate PG at a rate high enough to maintain cell wall integrity.

The identification of a growth rate dependent mechanism of tolerance to loss of the *mre/mrd* in *E. coli* could relate to *B. pertussis's* ability to tolerate *mre/mrd* knockout. I hypothesised that due to the low growth rate of *B. pertussis* when compared to *E. coli* during *in vitro* culturing, that *B. pertussis* may be inherently more tolerant to loss of elongasome expression than other gram-negative bacteria.

However, analysis of the growth of BP_{536}*ΔmreB* and BP536 *B. pertussis* strains in different supplemented growth mediums displayed that mutant strains had a directly comparable growth phenotype to BP536. Growth in SSCH media facilitated significantly increased growth after 24- and 48-hours in both BP536 and BP_{536}*ΔmreB.* This suggests that tolerance of *mreB* mutation in *B. pertussis* is not dependent on low biomass doubling rates, with high doubling rates tolerated comparably to BP536 (Figure 3.5). However, I cannot conclusively say growth rate doesn't play a role in tolerance of *mre/mrd* mutations in *B. pertussis* as the growth rate in SSCH is still modest in comparison to *E. coli.*

3.3.2-Does the mutation of *mreB* result in altered cell wall permeability and integrity as seen in other cell wall biosynthesis mutants?-

In previous studies of mutation of *mre/mrd*, mainly in *E. coli*, alterations in the elongasome resulted in highly osmotically unstable mutants which were prone to lysis. This displayed that elongasome PG biosynthesis in *E. coli* was key to maintenance of cell wall structural integrity, with manipulation resulting in osmotic instability. In *B. pertussis* these trends do not appear to be as severe as observed in *E. coli.* This is highlighted by the ability of *B. pertussis mre/mrd* mutants to grow comparably to wildtype in broth conditions, where osmotic pressures on the bacterial cell wall are at its highest (Figure 3.4&3.5).

Direct analysis of BP_{536}*ΔmreB* strain membrane integrity was carried out by quantifying their ability to tolerate SDS during culture growth (Figure 3.6). SDS sensitivity analysis displayed no significant decrease in the ability of BP_{536}*ΔmreB* to tolerate detergent concentrations compared to wildtype in broth in both the BVG- and BVG+ growth phases, suggesting little to no compromise of cell wall integrity upon *mreB* mutation. (Figure 3.6).

Overall, this analysis displays that despite removal of elongasome PG biosynthesis in *B. pertussis* we do not see the classical lytic-prone phenotype observed in other gram-negative bacteria.

3.3.3-Do *mre/mrd* mutations result in altered bacterial morphology?-

Unsurprisingly in previous mutagenesis studies of the *mre/mrd* operon in gram negative bacteria displayed altered cellular morphology, with a switch from the classical rod shape to cocci shaped bacterium. Due to the lack of effects of *mre/mrd* mutagenesis on bacterial viability and cell wall characteristics, verification of this change in morphology validated that the elongasome was indeed non-functional in the mutant strains (Figure 3.7). The characteristic change in morphology was observed with mutagenesis of each gene in the operon. This suggests that *B. pertussis* requires all these genes for functional bacterial elongation. Therefore, this displays that the *mre/mrd* operon encodes the sole mechanism of PG biosynthesis for bacterial elongation. This supports previous findings in other gram-negative bacteria where all 5 genes have been observed to be essential for elongasome function and bacterial viability.

TEM analysis of *mreB* mutant strain further supported the observation that mutagenesis does alter cell wall morphology (Figure 3.8). BP_{536}*ΔmreB* displayed an obvious alteration in

periplasm and cytoplasm uniformity. This morphological change appeared to be a result of both IM invagination into the cytoplasmic space, and OM separation from the IM resulting in an increased periplasmic area. These findings suggest that cell wall cross linking and stability are altered in mutant strains.

3.4- Conclusions and Future Directions

Loss of elongasome expression induces a lethal, lytic phenotype in other gram-negative bacteria meaning the *mre/mrd* operon has been thought of as essential. As *mre/mrd* essentiality was observed to be conditional dependent on BVG activation state I aimed to determine whether the disruption of bacterial morphology growth and OM stability observed in other bacteria were induced upon *mre/mrd* mutations in *B. pertussis.*

Overall, this body of work has displayed that *B. pertussis*'s viability is not as greatly effected by the loss of *mre/mrd* PG biosynthesis as other gram-negative bacteria. *Mre/mrd* expression was essential during BVG- plate growth with mutant growth not significantly altered in all other *in vitro* growth conditions analysed.

This tolerance to loss of elongasome PG biosynthesis shown by *B. pertussis* was furthered by the fact that unlike previously characterised *mre/mrd* mutants in other gram-negative bacteria, mutant *B. pertussis* did not display an osmotically unstable phenotype during broth culture growth, despite clear alterations in bacterial morphology and architecture.

In this body of work, I characterised the effect of deletion of each gene of the *mre/mrd* operon. It would be relevant to also characterise whole operon deletion strains to determine whether the phenotypes observed vary in the absence of the whole *mre/mrd* PG biosynthesis machinery.

From these findings I pose the question how does *B. pertussis* tolerate to loss of these classically essential genes without any obvious detrimental effect on bacterial viability?

Chapter 4- How does *B. pertussis* tolerate mutation of the *mre/mrd* operon?

4.1-Results

It was identified by mutant growth profiling that *mre/mrd* mutant strains viability was dependent on both BVG activation phase, and culture medium. This led me to hypothesise that alterations in gene expression, between viable and nonviable growth conditions, facilitated tolerance of the loss of elongasome PG biosynthesis.

To investigate this, I carried out transcriptomic profiling of BP536 during growth in culturing conditions where *mre/mrd* mutants are viable and non-viable. RNA was extracted from plate grown BP536 *B. pertussis* under BVG+ or BVG- modulated conditions and directly compared to existing RNAseq data of broth grown BP536 grown under BVG+ and BVG- modulation. Transcriptomic profiles of *B. pertussis* grown under these conditions were then compared to identify differentially expressed genes between conditions where *mre/mrd* mutants are viable (BVG+ broth, BVG+ plate and BVG- broth) and non-viable (BVG- plate). Through this analysis I aimed to identify specific genes or pathways that could facilitate tolerance of *mre/mrd* knockout which could be investigated further experimentally.

4.1.1-Quality check of RNAseq data-

To determine correct BVG modulation of samples, expression of the *ptxA* a classical BVG+ induced gene was analysed by qPCR (Figure 4.1). cDNA was generated from extracted RNA and utilised for qPCR analysis. The average CT of *ptxA* was standardised to the CT value for the housekeeping gene *recA* to calculate -ΔCT to display relative abundance of target mRNA (Figure 4.1A). This analysis displayed BVG+ modulated samples had higher ΔCT values than BVG- when compared to the housekeeping gene *recA*.

The change in *ptxA* expression between BVG+ and BVG- modulated samples was displayed further by quantification of the fold change of gene expression by $2^{-\Delta\Delta CT}$ analysis using the average BVG- CT value as untreated (Figure 4.1B). This displayed a significantly higher fold change in *ptxA* gene expression in all BVG+ modulated samples when compared to BVG- modulated sample. Overall, this analysis displays BVG+ and BVG- modulation of the plate growth medium was successful.

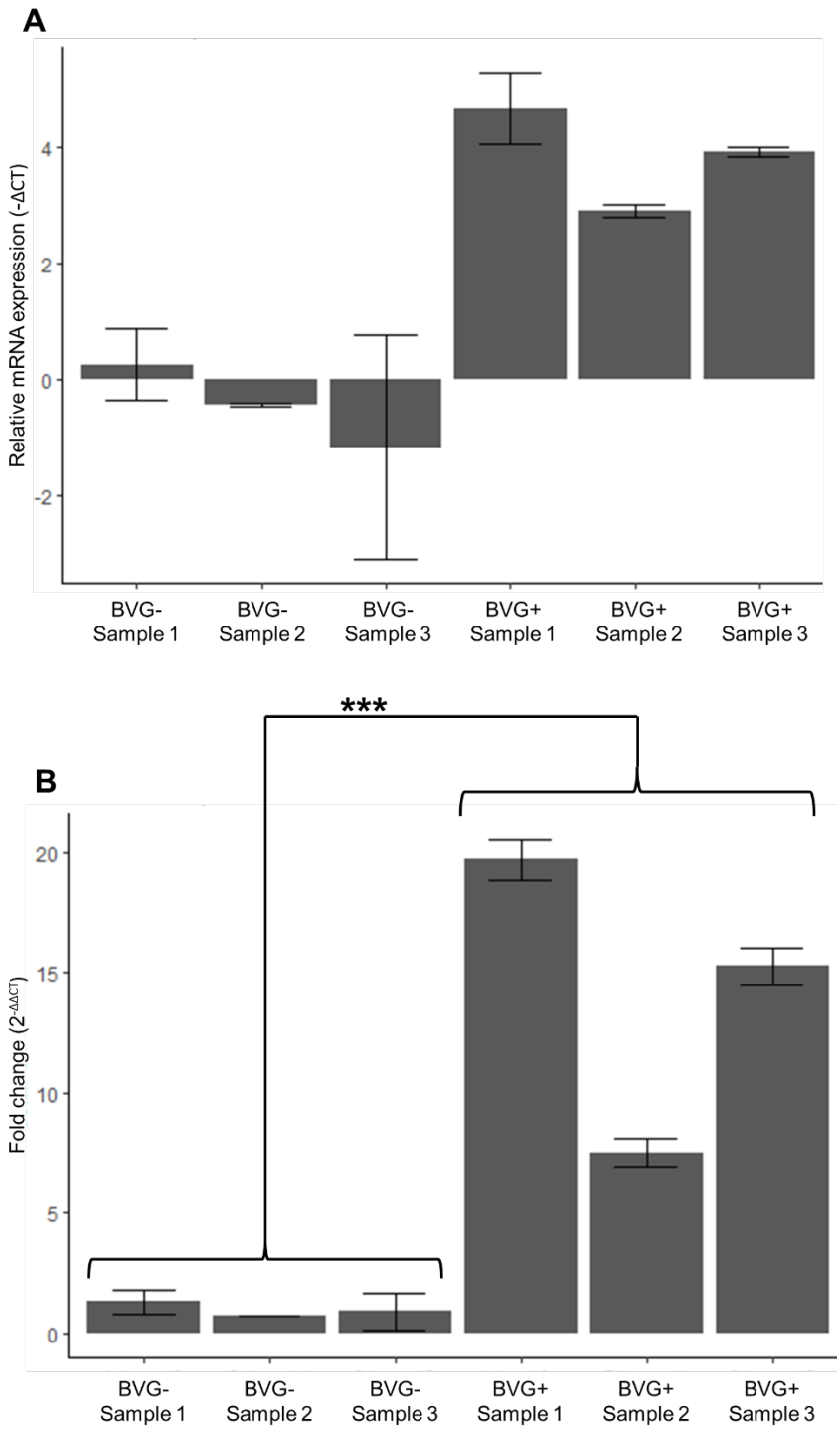

Figure 4.1- qPCR analysis of *ptxA* expression across BVG+ and BVG- RNA samples. A) Relative abundance of *ptxA* mRNA versus *recA* housekeeping gene. B) Fold change of *ptxA* against average expression across BVG- samples. One way ANOVA and Tukeys Post-Hoc. ***=p≤0.001.

4.1.2-Does the upregulation of alternate PG biosynthesis mechanisms facilitate *B. pertussis* to tolerate *mre/mrd* mutations?-

Initial analysis of RNAseq data was formed from a hypothesis driven screen looking at previously characterised tolerance mechanisms. Tolerance of the loss of elongasome PG biosynthesis is a novel phenotype with mutation in other bacteria greatly reducing bacterial viability. In previous studies the ability to tolerate the loss of this fundamental pathway was introduced by the upregulation of the alternate PG biosynthesis pathway, the divisome. Therefore, I hypothesised that upregulation of this alternate PG biosynthesis pathway may be what facilitates *B. pertussis* to tolerate the loss of *mre/mrd* expression. If this was the case, we would expect to see significantly increased level of divisome PG biosynthesis in growth conditions where *mre/mrd* mutants are viable (BVG+ plate, BVG+ broth and BVG-broth) when compared to nonviable conditions (BVG- plate).

I analysed this by looking at the level of expression of divisome genes comparing conditions where the mutants are viable or non-viable (BVG+ vs BVG- plate and BVG- broth vs plate) (Figure 4.2). This analysis displayed that in BP536 there was no large-scale upregulation of the expression of divisome genes during BVG+ plate or BVG- broth growth conditions when compared to BVG- plate growth. This analysis displays that despite upregulation of divisome PG biosynthesis being a previously characterised mechanism of tolerance to *mre/mrd* knockout, it does not appear to be the mechanism that maintains *mre/mrd* mutant *B. pertussis* strains viability. However, as this screen is carried out in BP536 wildtype I cannot discount that divisome gene expression is upregulated in the mutant strains.

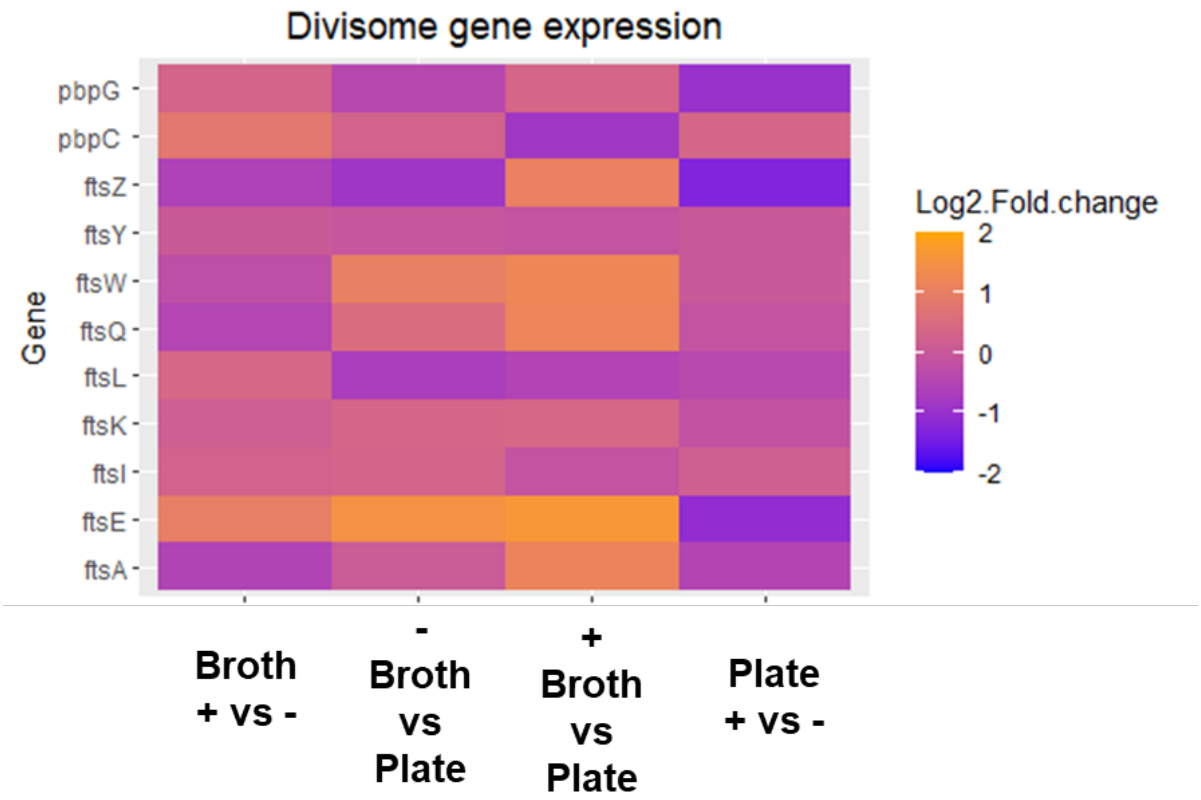

Figure 4.2- Heatmap of BP536 wildtype divisome PG synthesis gene expression. Rows= Genes of interest. Columns= Growth conditions. Colour density displays Log2 fold change.

4.1.3-Does analysis of BVG+ vs BVG- plate conditions generate gene targets for further experimental investigation?-

Firstly, I looked at genes differentially expressed between BVG+ and BVG- plate conditions, as this was the initial conditional essentiality observed during TraDIS screening. We hypothesised that this mechanism of tolerance would be BVG regulated as this is the variable on which *mre/mrd* essentiality has been observed to be dependent upon.

From this screen 96 genes were upregulated during BVG+ plate conditions with 61 genes being down regulated (Figure 4.3). When these differentially expressed genes were grouped by function utilising COG analysis it was observed that unsurprisingly many genes upregulated during BVG+ or BVG- plate conditions were classical BVG regulated genes.

I concentrated my analysis on BVG+ upregulated genes. This is due to the fact that *mre/mrd* mutagenesis has been observed to induce uncontrollable OM instability, therefore, it is most likely the upregulation of a proteins expression that would facilitate tolerance to membrane instability. I further concentrated my analysis on genes that are membrane located as these are the most likely candidates for stabilising the OM. COG analysis categories M, N and U

were selected as they correspond to cell wall biosynthesis, cell motility and secretion respectively which all are membrane localised processes (Figure 4.4, Table 4.1).

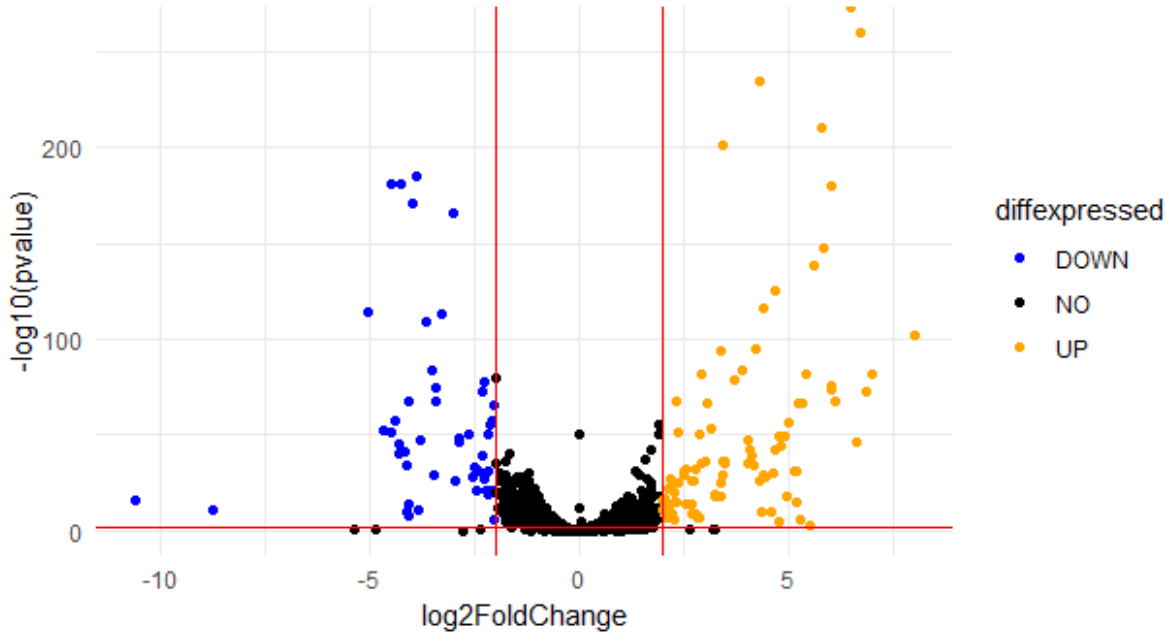

Figure 4.3 – Distribution of differentially expressed genes in BVG+ plate when compared to BVG- plate growth. Red lines depict values of selection for differential expression Log_2 Fold change > 2 or <-2, p <0.05 the Wald Test.

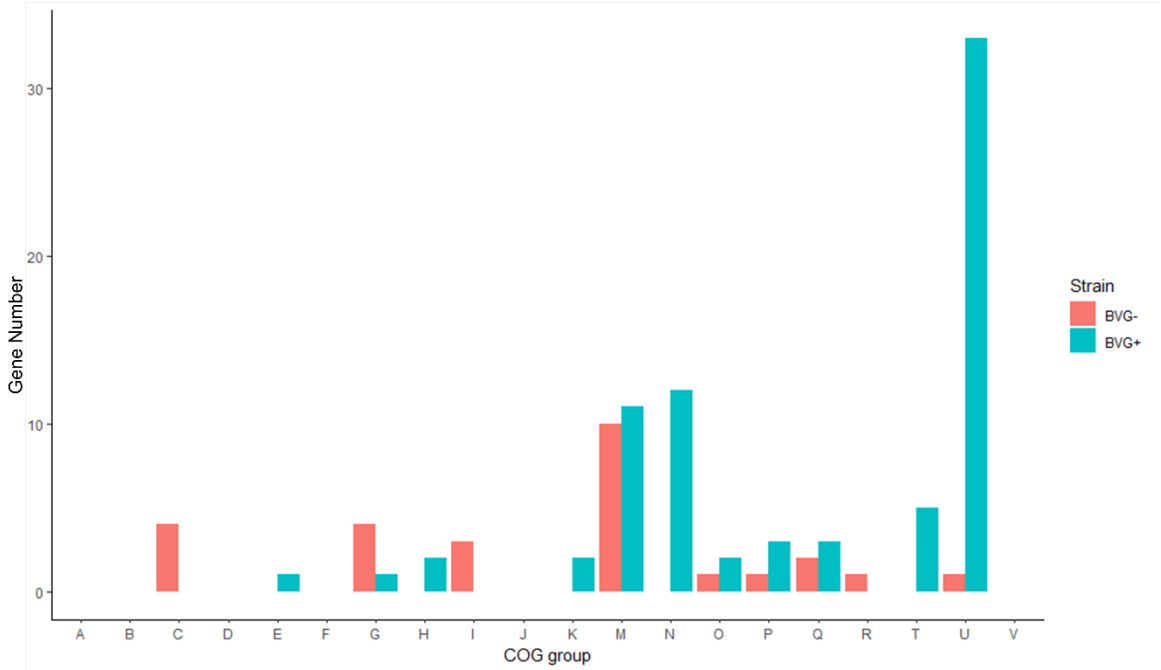

COG category	Function	COG category	Function
A	RNA processing and modification	L	Replication and repair
B	Chromatin structure and dynamics	M	Cell wall/membrane/envelope biogenesis
C	Energy production and conversion	N	Cell motility
D	Cell cycle control and mitosis	O	PTM, protein turnover and chaperones
E	Amino acid metabolism and transport	P	Inorganic ion transport and metabolism
F	Nucleotide metabolism and transport	Q	Secondary structure
G	Carbohydrate metabolism and transport	R	General function prediction only
H	Coenzyme metabolism	S	Unknown
I	Lipid metabolism	T	Signal transduction
J	Translation	U	Intracellular trafficking and secretion
K	Transcription	V	Defence mechanisms

Figure 4.4- Grouping of differentially expressed genes in BVG- vs BVG+ plate growth conditions by COG category.

Table 4.1- Table of BVG+ plate differentially expressed genes in COG categories M (Cell envelope biogenesis), N (Cell motility), and U (Intracellular trafficking and secretion).

Gene	COG category	log2FoldChange	p value	Description	Gene name
BP3783	M	5.838501	3.35E-148	NAD+ ADP-ribosyl transferase activity	*ptxA*
BP0762	M	2.694812	4.20E-27	type I secretion membrane fusion protein	*cyaD*
BP0399	M	2.184208	3.60E-15	Glycosyltransferases involved in Lipid A modification	*gtrB*
BP3405	M	3.059509	9.87E-68	outer membrane protein	*ompQ*
BP3494	MU	6.72707	4.41E-261	Serum resistance protein BrkA	*brkA*
BP1054	MU	6.504897	0	Pertactin may have a role in bacterial adhesion.	*Prn*
BP1201	MU	5.348689	4.62E-67	Autotransporter beta-domain	*tcfA*
BP2667	MU	4.317725	6.93E-236	haemagglutination activity domain	*fhaS*
BP1879	MU	4.136186	2.09E-40	haemagglutination activity domain	*fhaB*
BP2907	MU	3.456104	1.06E-201	haemagglutination activity domain	*fhaL*
BP0763	MU	2.200949	4.88E-28	Transport of cyclolysin	*cyaE*
BP1406	N	2.656435	0.09662	Flagellar biosynthesis protein	*flhB_1*
BP1880	N	2.927832	9.32E-83	Fimbrial protein	*fimA*
BP1883	NU	4.919371	2.54E-50	cell adhesion	*fimD*
BP2241	NU	4.811063	9.57E-45	Flagellar motor switch type III secretory pathway	*bscQ*
BP1881	NU	4.419962	1.43E-116	Chaperone	*fimB*
BP3796	NU	4.371349	1.01E-10	IV secretion system protein	*ptlH*
BP1882	NU	4.242636	5.93E-96	Usher protein	*fimC*
BP1119	NU	4.063258	8.58E-48	Type-1 fimbrial protein, A	*fim2*
BP2246	NU	2.839926	9.95E-08	Type III	*bscL*
BP1112	NU	2.284845	2.01E-25	Inverse autotransporter, beta-domain	*bipA*
BP2235	NU	2.268528	7.73E-16	Type III secretion protein	*bscC*
BP2674	NU	2.139937	1.05E-22	Type-1 fimbrial protein, A	*fimX*
BP3787	U	6.049186	1.28E-74	pertussis toxin subunit 3 precursor	*ptxC*
BP3785	U	6.046539	6.02E-77	pertussis toxin subunit 4 precursor	*ptxD*
BP1251	U	6.022812	1.35E-180	pertussis toxin subunit 2 precursor	*ptxB*
BP3786	U	5.445782	1.40E-82	pertussis toxin subunit 5 precursor	*ptxE*
BP3792	U	5.284419	2.37E-06	type IV secretion system	*ptlI*
BP3784	U	5.260023	7.63E-67	pertussis toxin subunit 2 precursor	*ptxB*
BP2264	U	4.317632	1.31E-26	type III secretion protein	*bscF*
BP2738	U	3.737984	7.38E-80	Autotransporter	*bapC*
BP3794	U	5.196534	8.43E-16	type IV secretion	*ptlF*
BP2239	U	4.766062	6.87E-06	Type III secretion protein	*bscS*
BP3789	U	4.672245	1.97E-43	Type IV secretion system protein PtlB	*ptlB*
BP3793	U	4.413921	6.49E-30	Type IV secretion system protein PtlE	*ptlE*
BP3790	U	3.433389	1.46E-29	Type IV secretory pathway VirB4 components	*ptlC*
BP2238	U	3.380832	6.50E-19	Type III secretion	*bscT*
BP1884	U	3.168134	4.39E-54	POTRA domain	*fhaC*
BP3795	U	2.578837	3.25E-14	type IV secretion	*ptlG*

This analysis displayed many genes being upregulated during BVG+ plate growth were involved in OM antigen production and toxin secretions with Ptx, FHA, BrkA and FIM secretion systems making up the majority of genes differentially expressed. These systems are envelope associated and made up of multiple protein components forming complexes that span the bacterial inner and outer membranes. These complexes facilitate the secretion of bacterial toxins and OM antigens across the bacterial envelope to the outer surface of the bacterium where they are presented or secreted. These systems could theoretically contribute to tolerance of *mre/mrd* mutation through the stabilisation of the bacterial envelope. However, as there are multiple systems upregulated during BVG+ plate growth, selection of genes or systems to investigate by mutagenesis techniques was hindered.

4.1.4-Does transcriptomic analysis of BVG- plate vs broth conditions generate gene targets for further experimental investigation?-

Due to BVG+ vs BVG- plate analysis not yielding any obvious candidates for investigation, I redirected my analysis to investigate the BVG- broth vs plate growth, which is hypothesised to be a culture medium induced mechanism of *mre/mrd* mutation tolerance. 270 genes were upregulated during broth growth and 261 genes upregulated during plate growth conditions (Figure 4.5). COG analysis displayed there was a wide range of mechanisms upregulated in both broth and plate growth conditions (Figure 4.6). In broth conditions genes involved in translation made up a larger proportion of differentially expressed genes than during plate growth. In plate growth conditions, an increased number of differentially expressed genes were involved in the metabolism of amino acid and inorganic compounds.

For the identification of hypothetical tolerance mechanisms, I concentrated my analysis on genes which may stabilise the bacterial outer membrane or regulate cell wall integrity (Table 4.2). This analysis identified a hypothetical mechanism of tolerance to *mre/mrd* mutations.

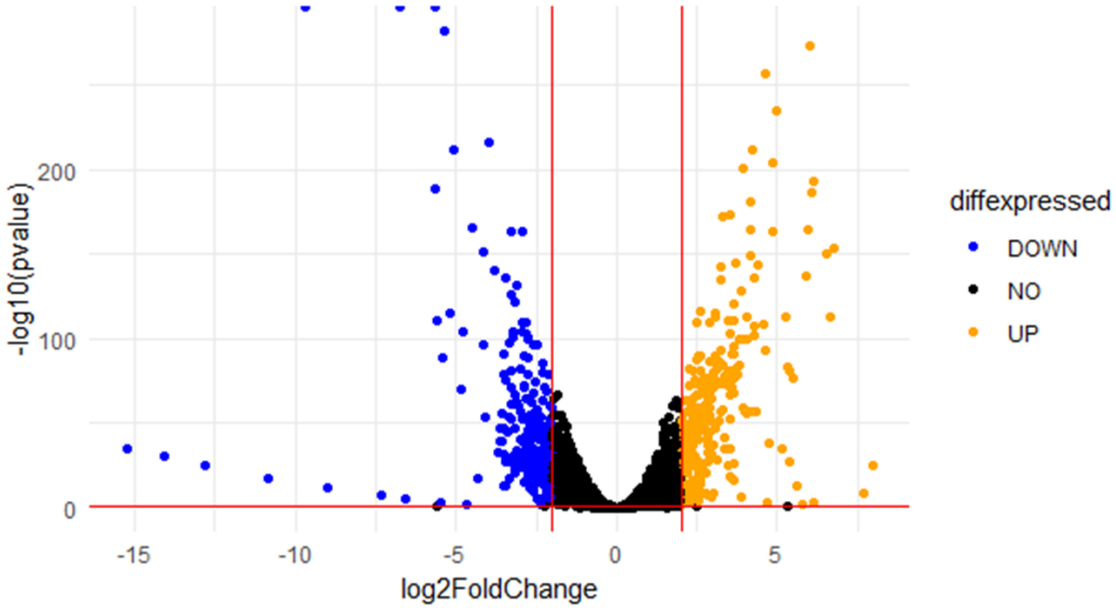

Figure 4.5 – Distribution of differentially expressed genes in BVG- broth when compared to BVG- plate growth. Red lines depict values of selection for differential expression Log_2 Fold change > 2 or <-2, p <0.05 the Wald Tes

t.

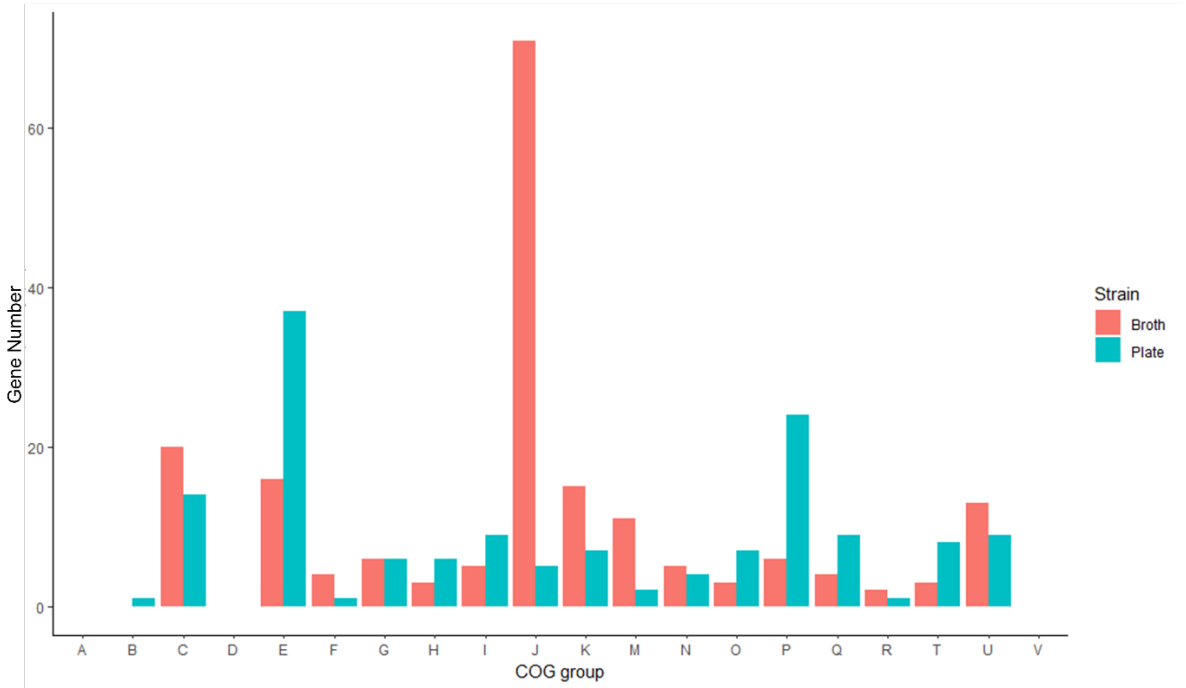

COG category	Function	COG category	Function
A	RNA processing and modification	L	Replication and repair
B	Chromatin structure and dynamics	M	Cell wall/membrane/envelope biogenesis
C	Energy production and conversion	N	Cell motility
D	Cell cycle control and mitosis	O	PTM, protein turnover and chaperones
E	Amino acid metabolism and transport	P	Inorganic ion transport and metabolism
F	Nucleotide metabolism and transport	Q	Secondary structure
G	Carbohydrate metabolism and transport	R	General function prediction only
H	Coenzyme metabolism	S	Unknown
I	Lipid metabolism	T	Signal transduction
J	Translation	U	Intracellular trafficking and secretion
K	Transcription	V	Defence mechanisms

Figure 4.6 – Grouping of differentially expressed genes in BVG- broth vs plate growth conditions by COG category.

Table 4.2- Table of BVG- broth differentially expressed genes of interest in COG categories M (Cell envelope biogenesis), N (Cell motility), and U (Intracellular trafficking and secretion) and the glycine betaine uptake system.

Gene	COG category	log2FoldChange	p value	Description	Gene name
BP2055	E	-4.64115	1.82E-257	Glycine betaine ABC transporter substrate-binding	*proX*
BP2056	E	-3.72284	6.83E-146	Glycine betaine/proline transport system permease protein	NA
BP2057	E	-4.22008	3.40E-212	Glycine betaine/proline transport ATP-binding protein	NA
BP1624	GM	-3.11623	3.34E-29	Capsule export ABC transporter	*kpsT*
BP0085	M	-2.89808	1.16E-45	lipopolysaccharide biosynthesis	*bplI*
BP0666	M	-2.48325	9.88E-68	hexosamine metabolism	*glmS*
BP0878	M	-2.70062	4.88E-61	Outer membrane phospholipase A	-
BP1107	M	-2.42972	9.99E-77	ABC-type transport system involved in lipoprotein release permease component	*lolC*
BP1625	M	-2.55746	3.58E-20	Capsule polysaccharide export protein	*kpsE*
BP1629	M	-2.05889	1.94E-13	UDP-glucose GDP-mannose dehydrogenase family	*wbpO*
BP1630	M	-2.04116	3.40E-10	Vi polysaccharide biosynthesis protein vipB tviC	*wbpP*
BP2988	M	-2.84649	7.85E-34	membrane protein involved in D-alanine export	*dltB*
BP0939	N	-3.01931	3.39E-38	HicA toxin of bacterial toxin-antitoxin,	-
BP1119	NU	-2.08787	2.24E-31	Type-1 fimbrial protein, A	*fim2*
BP1568	NU	-2.92426	1.01E-70	Fimbrial	*fimA*
BP1881	NU	-3.05068	3.43E-48	chaperone	*fimB*
BP2245	NU	-2.64361	5.56E-23	Type III	*hrcN*
BP1623	U	-2.71196	6.35E-47	Capsule export ABC transporter	*kpsM*
BP2239	U	-2.46415	0.07284257	Type III secretion protein	*bscS*
BP2432	U	-2.75148	6.81E-21	Belongs to the peptidase S26 family	*lepB*
BP3081	U	-6.76214	3.51E-154	ABC-type Mn2 Zn2 transport systems permease components	*mntB*
BP3636	U	-3.94234	3.73E-60	Protein translocation channel SecYEG.	*secY*
BP3789	U	-2.84101	3.38E-33	Type IV secretion system protein PtlB	*ptlB*
BP3790	U	-2.16406	1.17E-64	Type IV secretory pathway	*ptlC*
BP3794	U	-2.41872	2.37E-11	type IV secretion	*ptlF*

It was observed that a three gene system important in the uptake of the well characterised osmoprotectant glycine betaine was upregulated during broth growth. This poses the question whether the ability to uptake betaine glycine to regulate bacterial osmotic pressure could facilitate tolerance to *mre/mrd* mutations*?*

4.1.5-Does betaine glycine uptake facilitate *B. pertussis* to tolerate *mre/mrd* knockout?-

Differential expression analysis of known outer membrane porins and osmo-protectant uptake systems, important in maintaining the osmotic balance in bacteria, was carried out across growth conditions. This displayed that the betaine glycine uptake system (BP2055-BP2057) was highly upregulated during broth growth when compared to plate in both BVG- and BVG+ growth phases (Figure 4.7). This suggests that betaine glycine uptake plays an important role in broth culturing of *B. pertussis.*

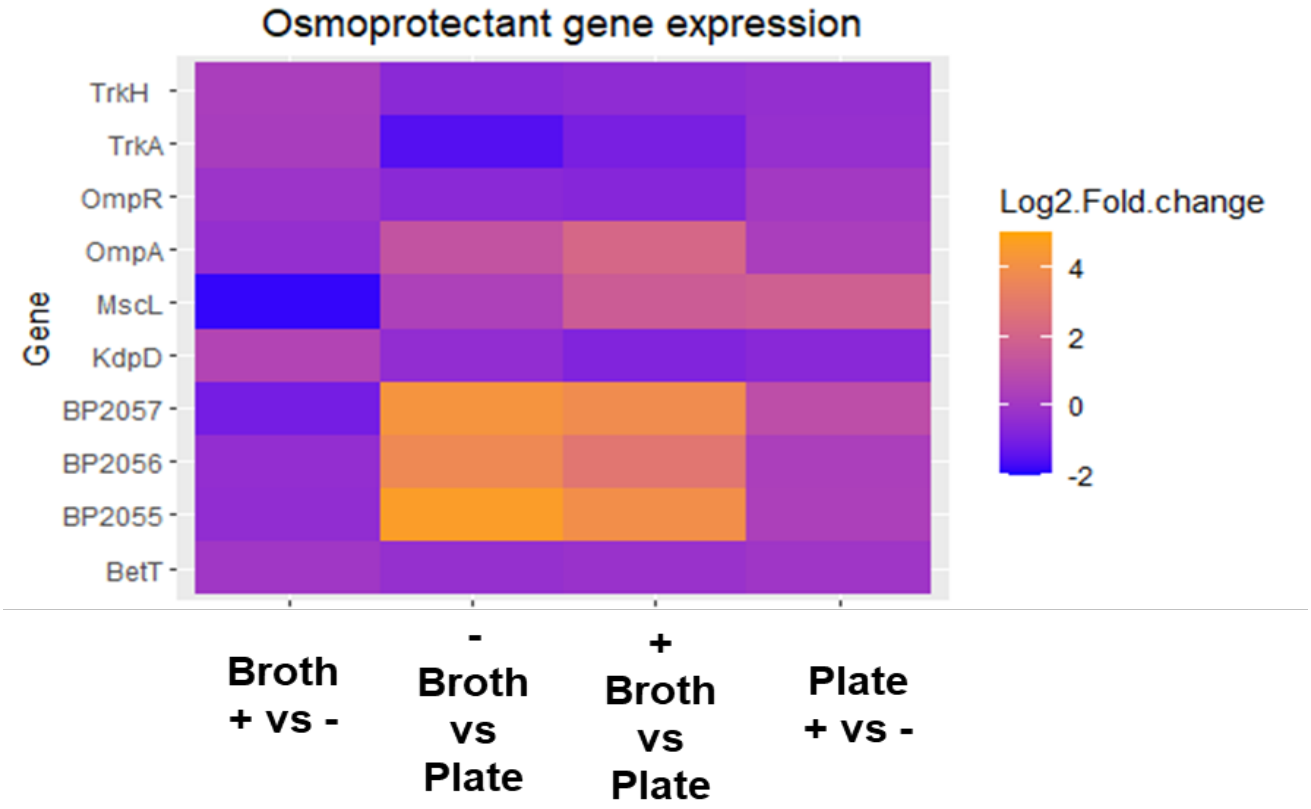

Figure 4.7- Heatmap of BP536 wildtype osmo-protectant gene expression. Genes of interest along Y-axis. Growth conditions comparisons along X-axis. B=broth, P=Plate. Colour density displays Log2 fold change.

To analyse whether betaine glycine uptake played a role in the tolerance of *mre/mrd* mutations, I analysed the effect of betaine supplementation on CFU produced during BVG+ and BVG- plate growth of BP536 wildtype and BP_{536}*ΔmreB*. Upon supplementation of BVG-

modulated plates with 10mM betaine, we see a significant restoration of viability in the BP_{536}*ΔmreB* strain (Figure 4.8). However, growth is not restored to the level observed during BP_{536}*ΔmreB* BVG+ plate growth suggesting there may be alternate unidentified mechanisms which also play a role in tolerance of *mreB* loss in the BVG+ growth phase.

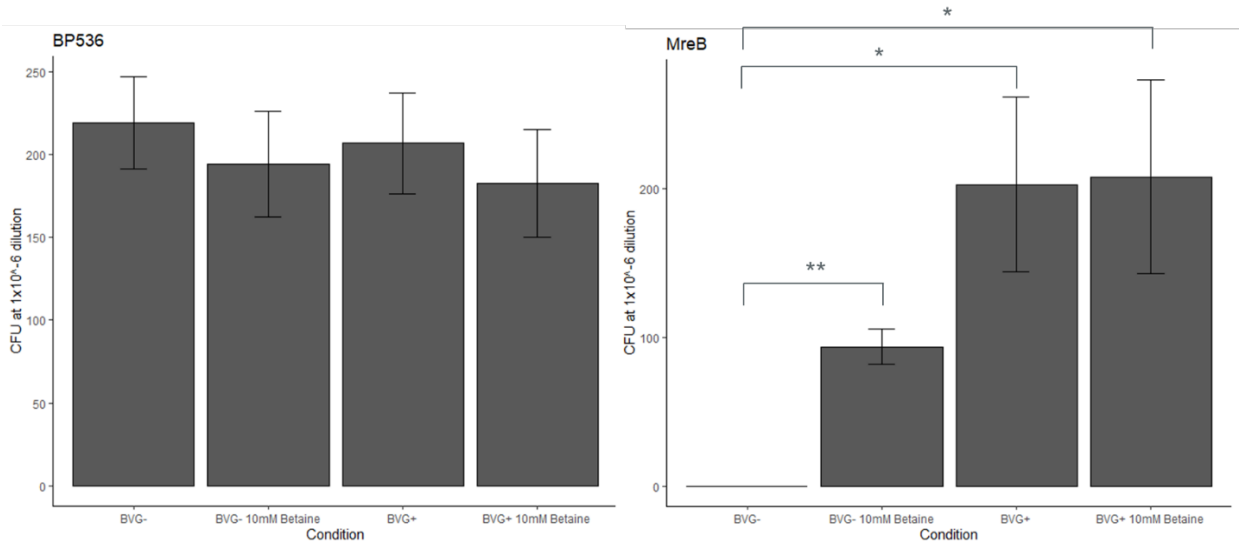

Figure 4.8- Betaine supplementation during BVG- plate growth rescues mutant viability. Colony forming units (CFU) produced upon plating a $1x10^{-6}$ dilution of a 1 OD_{600} suspension of BP536 wildtype or BP_{536}*ΔmreB* on BVG+ or BVG- modulated charcoal agar plates. Supplementation with betaine significantly restored BP_{536}*ΔmreB* viability during BVG- growth. Results are representative of three biological replicates. *=p≤0.05, Students T-test. Error bars = Standard error of the mean.

To analyse whether restoration of *mreB* mutant viability was dependent on betaine concentration, I analysed the effect of various betaine concentrations on *B. pertussis* plate viability. I did this by quantifying CFU produced on BVG- modulated plates supplemented with betaine concentrations ranging from 1-100mM. We see that BP536 grows comparably across all conditions, suggesting no effect of supplementation on the wildtype strains viability (Figure 4.9). In the BP_{536}*ΔmreB* strain we see restoration of viability from 1mM supplementation in a concentration dependent manner up to 10mM of betaine. Between 10-100mM betaine we see a plateau in CFU produced suggesting this is the point of betaine saturation.

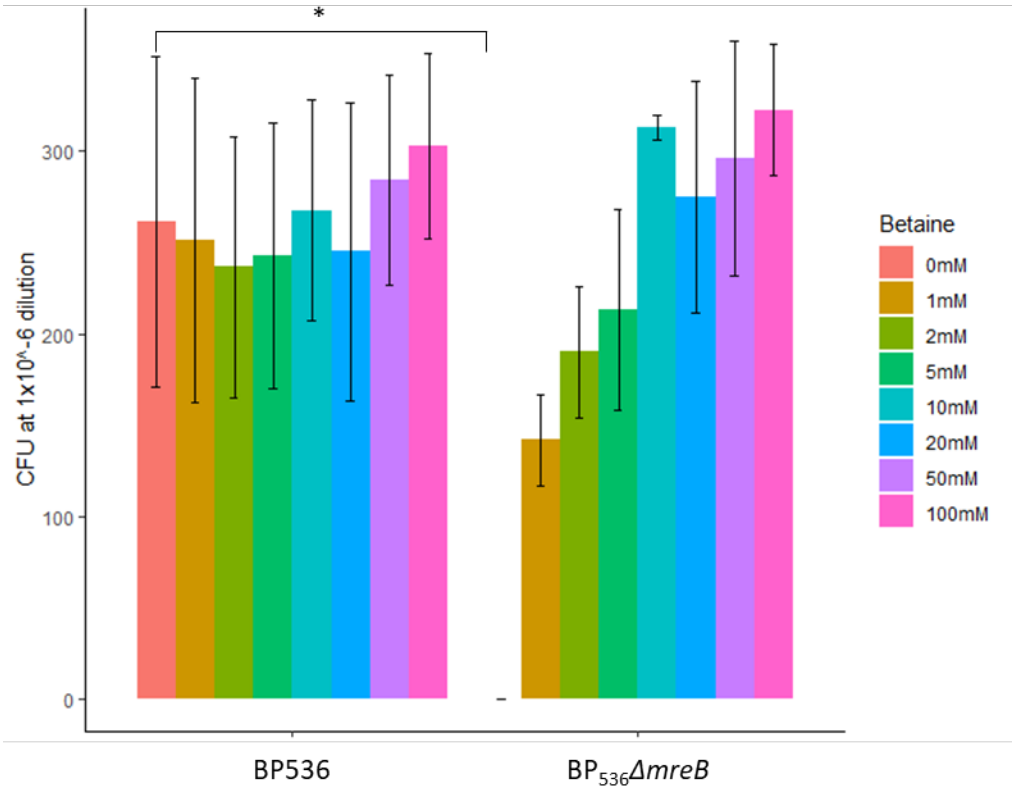

Figure 4.9- Analysis of the effect of varying betaine concentrations on BP_{536}*ΔmreB* viability restoration. BVG- plates were supplemented with varying concentrations of betaine. CFU produced upon plating a $1x10^{-6}$ dilution of a 1 OD_{600} suspension were quantified. Betaine significantly restored BP_{536}*ΔmreB* viability during BVG- growth even at the lowest concentrations. Results are representative of three biological replicates. *=p≤0.05, Students T-test. Error bars = Standard error of the mean.

To analyse whether this phenomenon was betaine specific, or could be induced upon supplementation with alternate osmoprotectants, I supplemented BVG- plate medium with proline. Viability was not restored in BP_{536}*ΔmreB* when proline was supplemented between 1-100mM suggesting that this mechanism of tolerance may be betaine specific (Figure 4.10). Whether this is due to proline transport being not as efficient as betaine uptake or the fact that proline is a key metabolite in *B. pertussis* meaning it may be metabolised before reaching protective intracellular concentrations has not been determined.

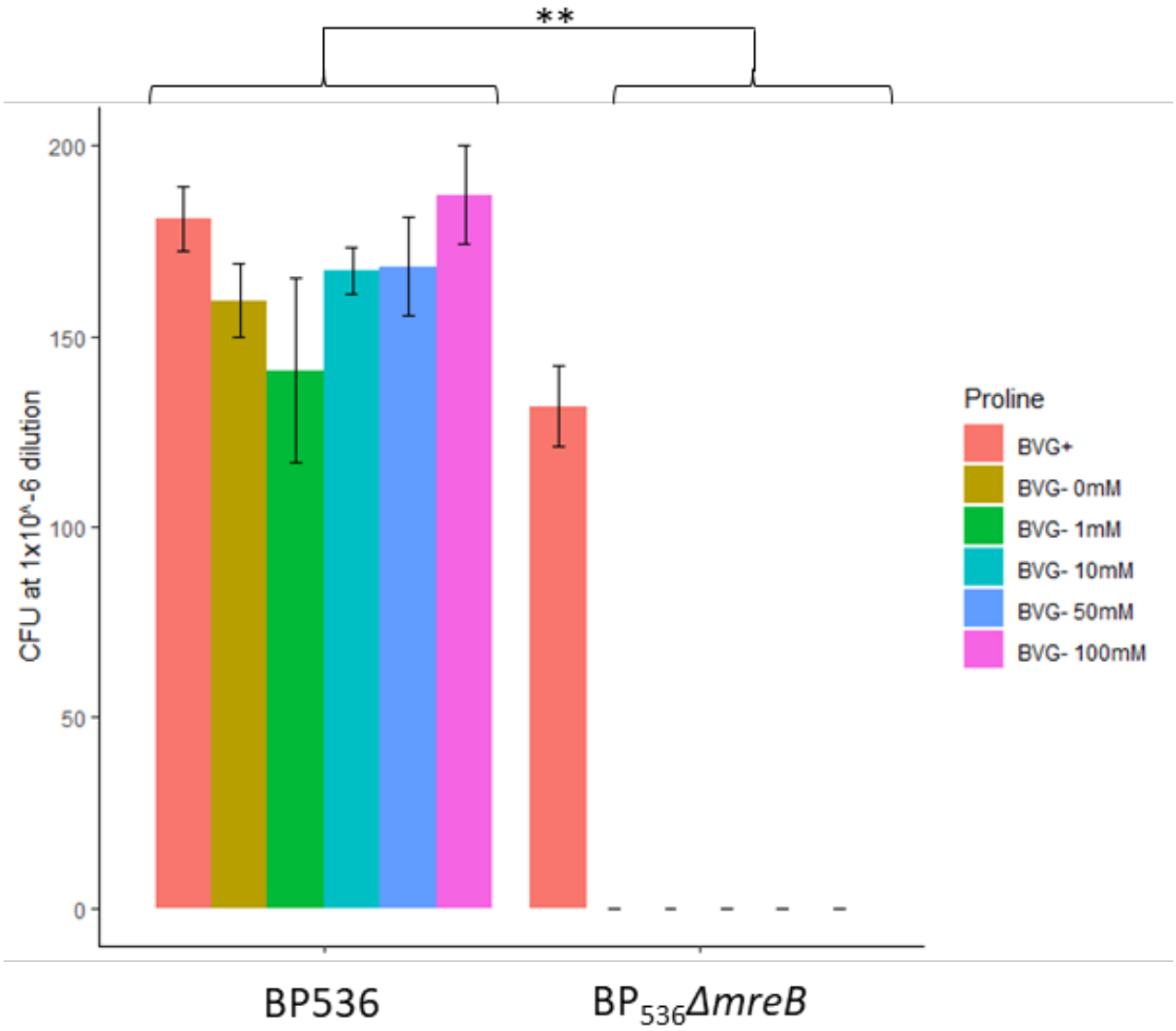

Figure 4.10- Proline supplementation during BVG- plate growth does not rescue mutant viability. CFU produced upon plating a $1x10^{-6}$ dilution of a 1 OD_{600} suspension of BP536 wildtype or BP_{536}*ΔmreB* on BVG+ or BVG- modulated charcoal agar plates, with and without proline supplementation were counted. Proline supplementation failed to restore BP_{536}*ΔmreB* viability during BVG- growth. Results are representative of three biological replicates **=p≤0.001, Students T-test. Error bars = Standard error of the mean.

4.1.6-Does increased expression of the betaine glycine uptake system (B/G) facilitate tolerance of *mreB* mutation during BVG- plate growth without supplementation with betaine-

To determine whether the induction of expression of B/G aided bacterial viability in the same manner as betaine supplementation, I cloned the three genes of B/G (BP2055-2057) into pMMB208, a broad-host range expression vector, generating a transcriptional fusion of B/G and the *lacZ* promoter. Induction of expression of these genes by activating the *lacZ* promoter

was via the addition of IPTG. This allows the induction of expression of B/G during BVG-plate growth through the supplementation of the growth medium with IPTG. B/G was amplified by PCR and inserted into pMMB208 expression vector (Figure 4.11).

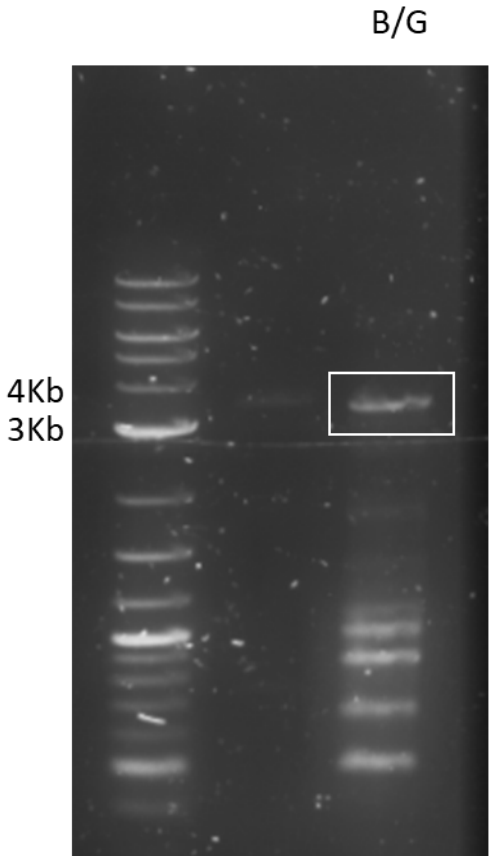

Figure 4.11- Gel of PCR amplified Betaine glycine uptake system (B/G). Expected size = 3.475Kb. Fragments of interested selected by band excision and gel purification.

Analysis of the effect of induction of betaine glycine uptake was analysed by quantifying CFU produced upon induction of the pMMB208B/G constructs expression by addition of IPTG, with and without the presence of 10mM betaine. An empty vector control was utilised (pMMB208EV). The presence of the pMMB208B/G construct produced comparably greater CFUs to the pMMB208EV control regardless of supplementation of IPTG or betaine (Figure 4.12). This suggests that, firstly, the inducible plasmid may be leaky meaning expression is not limited by the availability of IPTG. Secondly, it suggests that induction of betaine glycine uptake in BP536 wildtype facilitates increased plate viability. This same finding is mirrored in the BP_{536}*ΔmreB+B* strain. In the BP_{536}*ΔmreB* strain we see that betaine supplementation rescues viability of pMMB208EV strain, with and without IPTG induction. In the BP_{536}*ΔmreB*+pMMB208B/G strain we see comparable rescuing of viability upon supplementation with Bet, IPTG or Bet and IPTG, suggesting viability restoration is not

solely dependent on betaine supplementation, and that the availability of the uptake system apparatus also restores bacterial viability during BVG- plate growth.

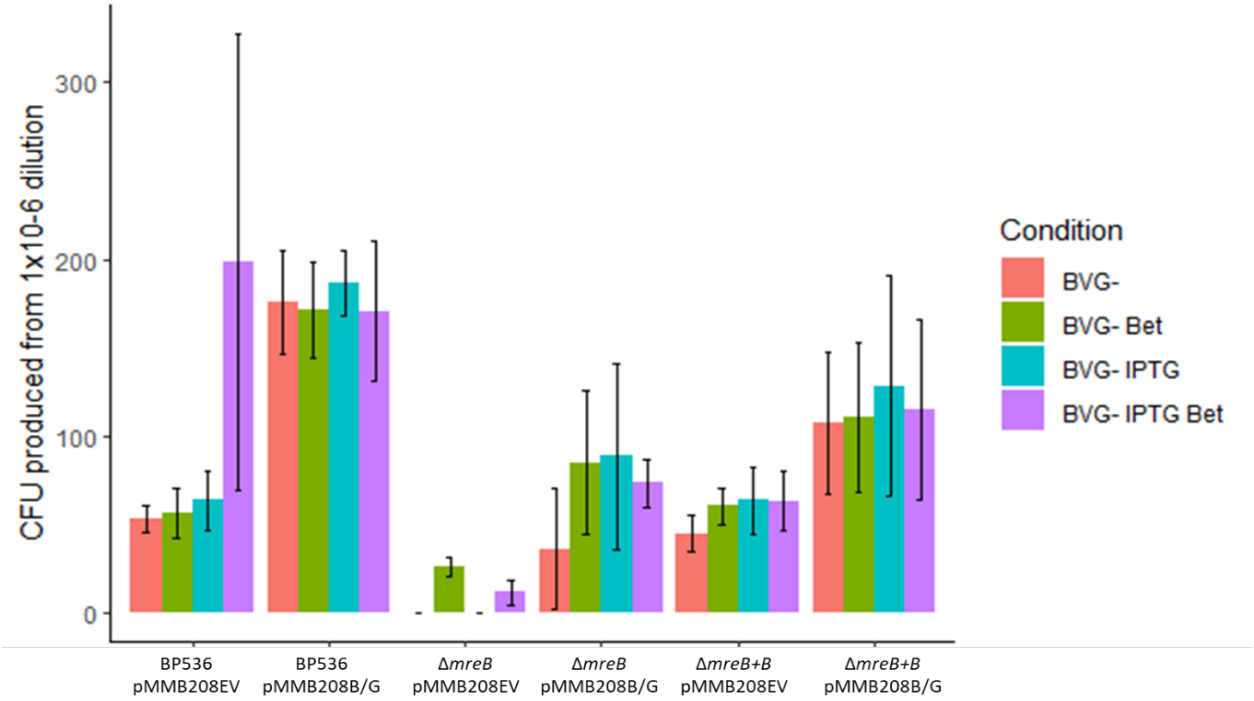

Figure 4.12-Analysis of the effect of induction of B/G expression on BP$_{536}$*ΔmreB* BVG- plate viability. Graph displays CFU produced upon plating of BP536, BP$_{536}$*ΔmreB* and BP$_{536}$*ΔmreB+B* strains containing pMMB208B/G or pMMB208EV expression vectors at 1x10-6 dilution of a 1 OD$_{600}$ suspension. B/G- betaine glycine uptake system expression construct, EV- empty expression vector. Error bars= Standard error of the mean. Data representative of three biological replicates.

4.1.7-Does the knockout of the ATPase of B/G, *BP2057*, ablate the ability of BP536 and BP$_{536}$*ΔmreB* to grow in broth culture conditions?-

As B/G is highly upregulated during *B. pertussis* broth growth I aimed to investigate its role in broth viability in the BP536 wildtype and BP$_{536}$*ΔmreB* strains. I decided to target the *BP2057* gene of the B/G as this is the associated ATPase and is required to fuel transport of betaine into the bacteria. An allelic exchange construct was generated by amplification of flanking regions of *BP2057* with complementary ends, facilitating ligation by golden gate reaction, effectively deleting the *BP2057* coding sequence (Figure 4.13).

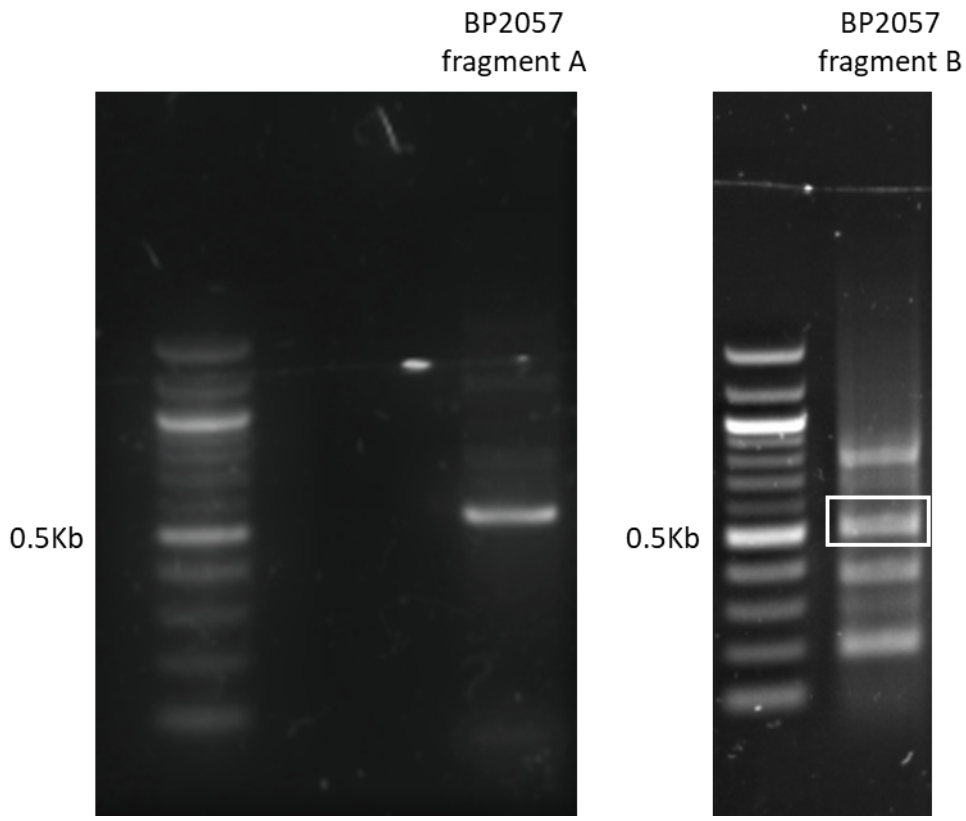

Figure 4.13- Gel of PCR amplified *BP2057* flanking fragments. Fragment A expected size = 0.516Kb, fragment B expected size = 0.498Kb. Fragments of interested selected by band excision and gel purification.

These constructs were utilised for allelic exchange, to introduce the internally deleted *BP2057* allele into BP536 wildtype, producing a BP_{536}*ΔBP2057* strain. The successful deletion of *BP2057* was verified by colony PCR (Figure 4.14).

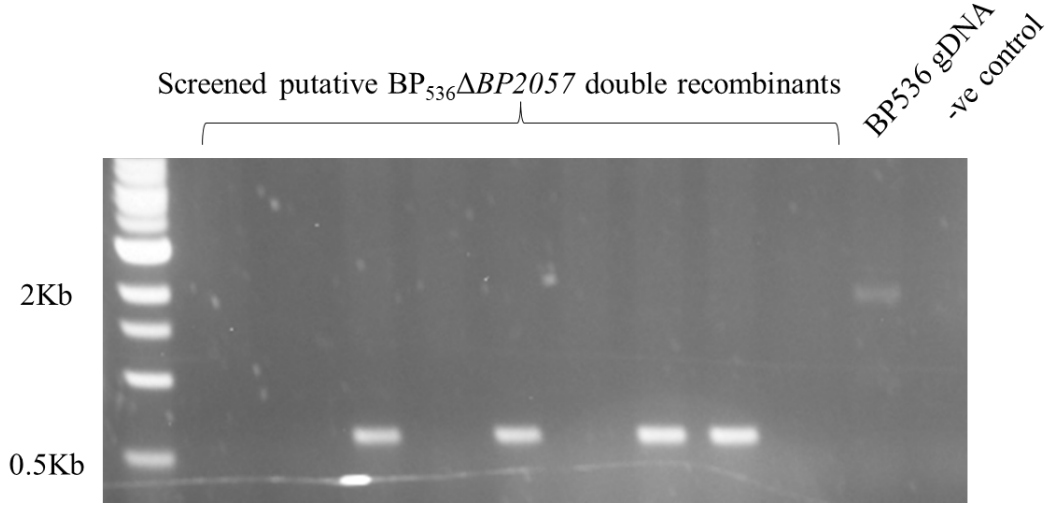

Figure 4.14 – Verification of BP_{536}*ΔBP2057* double recombinants by colony PCR. As clones upon secondary selection can be either wildtype or mutant successful deletion of *BP2057* was verified by PCR. Expected product size = wildtype- 1857bp, Mutant- 604bp.

To analyse the effect of *mreB* mutation on BP_{536}*ΔBP2057* growth during broth culture, double mutant strains needed to be generated. I utilised the pSS4940*BPΔmreB* construct to delete the *mreB* gene in the BP_{536}*ΔBP2057* strain. Successful deletion was verified by colony PCR using primers to amplify the *mreB* coding region and the inserted kanamycin cassette (Figure 4.15). Gel electrophoresis analysis of PCR products displayed that *mreB* had been successfully deleted in the BP_{536}*ΔBP2057* strain.

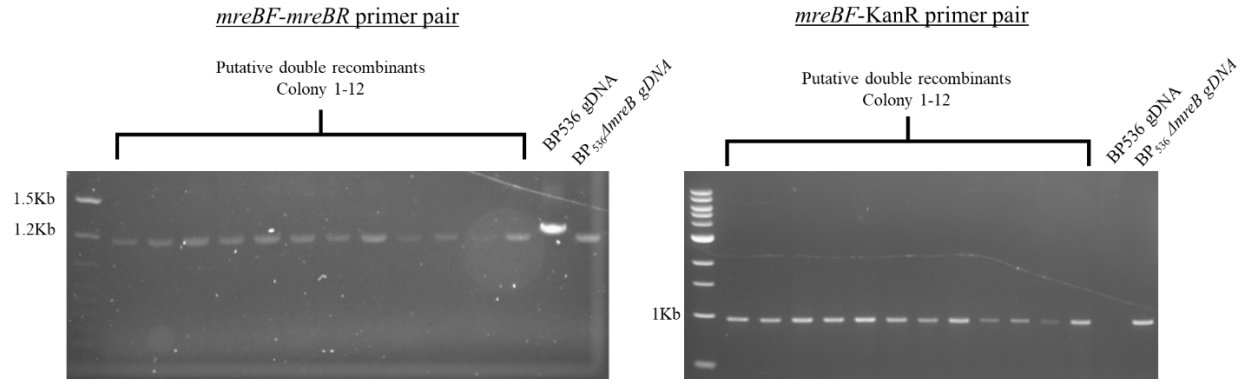

Figure 4.15 -Colony PCR of verification of successful truncation of *mreB* in BP_{536}*ΔBP2057* strains. Verification of *mreB* mutant allele insertion into BP_{536}*ΔBP2057* strain by colony PCR. Colonies 1-20 (C1-12) *mreBF-mreBR* primer pair coding region amplification wildtype= 1548bp, Mutant= 1305bp. *mreBF*- KanR primer pair kanamycin cassette amplification wildtype=0bp Mutant=830bp

To assess the effect of *BP2057* deletion on BP536 and BP_{536}*ΔmreB* growth phenotypes, mutant strains were grown in deepwell culture plates under BVG+ and BVG- modulating conditions. This analysis displayed no significant alteration in growth phenotypes of mutant strains compared to BP536 wildtype (Figure 4.16). This suggest that tolerance of *mre/mrd* mutations are not solely dependent on betaine uptake.

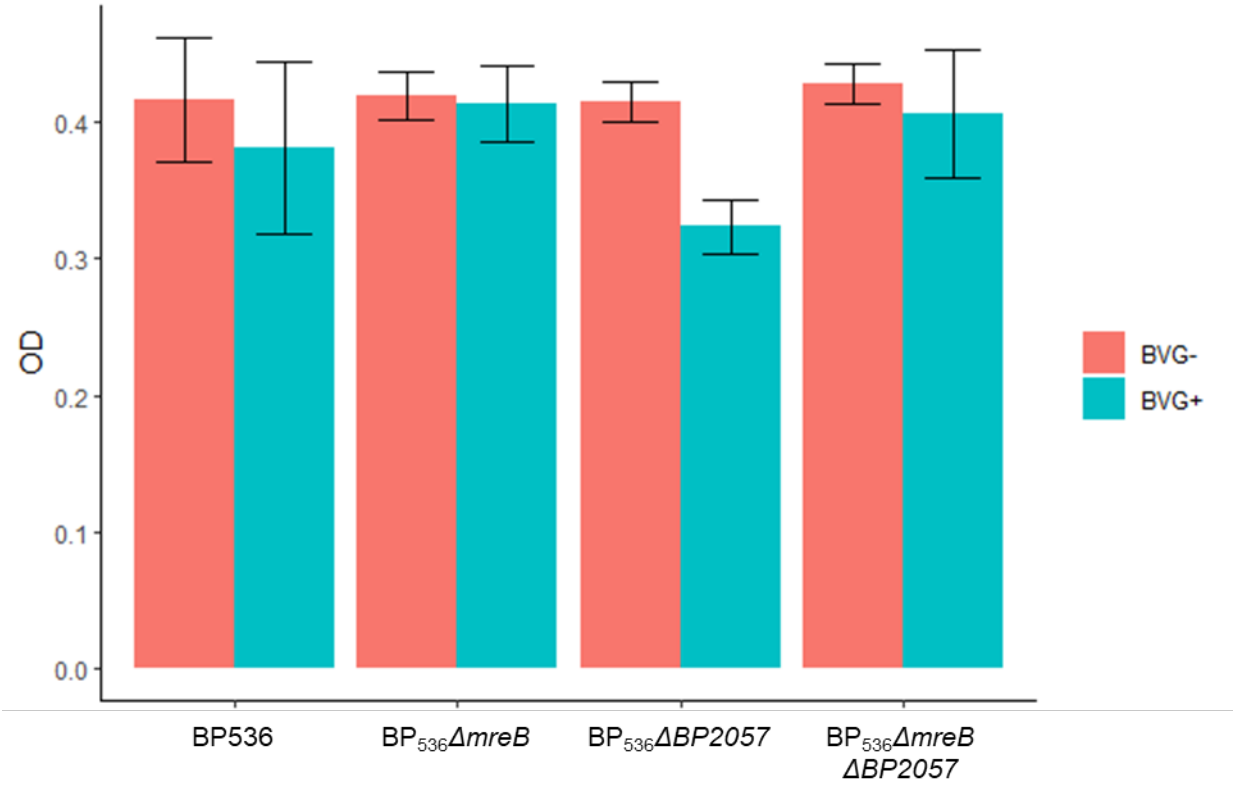

Figure 4.16- Comparative analysis of BP_{536}*ΔmreB*, BP_{536}*ΔBP2057* and BP_{536}*ΔmreBΔBP2057* strains deepwell growth. Culture OD_{600} at 16-hours of growth under BVG- and BVG+ modulated conditions in SS growth medium. Data representative of two biological replicates. Error bars= Standard error of the mean.

4.1.8-Could transcriptomic analysis of BVG+ Broth growth of BP536 and *mreC* mutant provide insight into hypothetical tolerance mechanisms?-

To assess whether *mre/mrd* mutations resulted in alterations in *B. pertussis* gene expression which facilitates the tolerance of the loss of these fundamental cell wall biosynthesis genes, I carried out transcriptomic analysis of BP536 wildtype and BP_{536}*ΔmreC* gene expression during mid-logarithmic growth phase in SSCH BVG+ broth growth conditions. Interestingly, only one gene was identified to be differentially expressed between the two strains at this timepoint, the *mreC* gene which I have knocked out (Figure 4.17). This displays rather remarkably that the knockout of *mreC* is highly tolerated in *B. pertussis* with mutants displaying a transcriptome almost identical to wildtype.

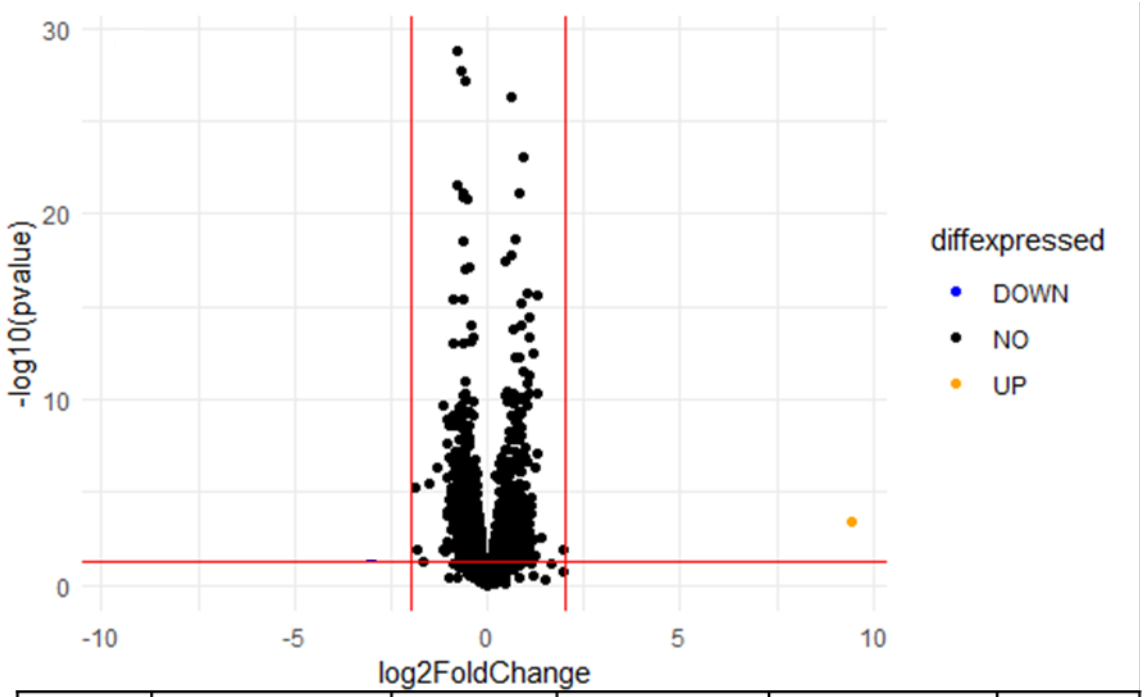

Gene	log2FoldChange	p value	COG category	Description	Preferred name
BP0375	-9.52378	2.13E-26	M	Involved in formation and maintenance of cell shape	mreC

Figure 4.17- Volcano plot and table of differentially expressed genes between BP536 wildtype and BP_{536}*ΔmreC* strain during SSCH broth culture. RNA extracted at mid-Log growth phase. Red lines depict values of selection for differential expression Log_2 Fold change > 2 or <-2, p <0.05 the Wald Test.

4.2- Discussion

4.2.1-Do alternate PG biosynthesis mechanisms step in to facilitate tolerance to *mre/mrd* mutations?-

In *E. coli* based studies of *mre/mrd* essentiality, induction of increased PG biosynthesis by introducing the key divisome gene *ftsZ* on an expression plasmid, facilitated tolerance of *mre/mrd* knockout (Bendezú and de Boer, 2008). I hypothesised that increased divisome PG biosynthesis could facilitate tolerance to *mre/mrd* mutations in *B. pertussis*. However, in *B. pertussis* this does not appear to be the case with divisome PG biosynthesis genes not being significantly differentially expressed in wildtype BP536 across BVG+ and BVG- plate and broth growth conditions (Figure 4.2).

4.2.2-What is the BVG regulated mechanism of tolerance to *mre/mrd* mutation during plate growth?-

Mre/mrd mutant strains are viable during plate growth under BVG+ but not BVG- conditions. Unfortunately, hundreds of genes are differentially expressed between these two conditions, effecting dozens of cellular processes making it very difficult to identify possible tolerance mechanisms from BVG regulon analysis by transcriptomics.

Due to BVG+ genes being fundamental in host infection, genes upregulated under these growth conditions occupy similar functional niches, key to *B. pertussis* adhering to the airway epithelium and manipulating this environment to persist and replicate. This is highlighted by the fact that many of the genes identified by differential expression analysis were classed in the COG categories M, N and U, representing membrane associated molecules, motility related proteins including adhesion and intracellular trafficking and secretion machinery related to toxin production (Table 4.1).

Pertussis expresses a variety of virulence factors all of which play a role in the infection of the respiratory tract with FHA, PT, PRN, FIM2, FIM3 and BrkA all being observed to be involved in this process (Relman et al., 1989, van den Berg et al., 1999, Tuomanen and Weiss, 1985, Leininger et al., 1991, Fernandez and Weiss, 1994).

Some of these proteins have been implicated as important factors in the formation of *B. pertussis* biofilms (Arnal et al., 2015, Cattelan et al., 2016a, Cattelan et al., 2017). This poses the question whether increased bacterial adherence to both the plate and surrounding bacteria provides a community associated mechanism of maintaining cell envelope stability (Figure 4.18)?

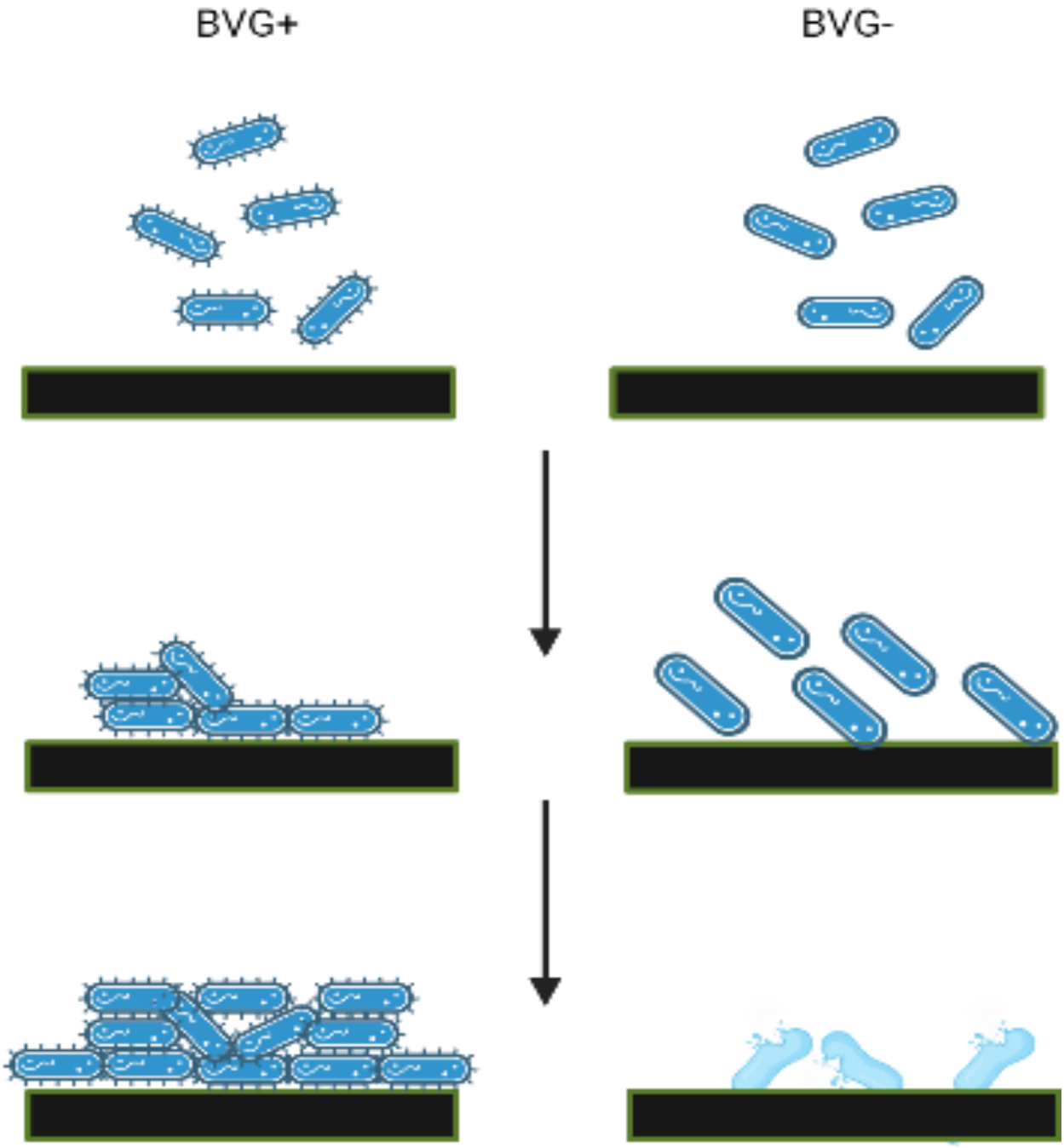

Figure 4.18- Hypothesised role of increased adhesin synthesis on BVG+ plate *mre/mrd* mutants viability. Increased adhesin expression may allow increased cell to cell and cell to plate binding. This could introduce a community induced bacterial viability where they provide structural support to neighbouring bacteria facilitating tolerance to instability of the bacterial cell envelope. Created with BioRender.com

The underlying mechanisms of *B. pertussis* biofilm formation has become an areas of increasing research due to observed links with infection persistence and colonisation of the nasal cavity *in vivo.* During these studies, analysis of the role of BVG+ induced genes were characterised in relation to biofilm formation (Arnal et al., 2015, Cattelan et al., 2016a, Cattelan et al., 2017, Irie et al., 2004, Serra et al., 2011).

FHA was identified as important, with *Δfha* strains displaying reduced bacterial biofilm formation suggesting the adhesive properties of this protein is important in bacteria-bacteria and bacteria-surface interactions (Serra et al., 2011). Findings in *B. bronchiseptica,* a closely related *Bordetella* species to *B. pertussis,* adds a layer of complexity to the mechanisms of biofilm formation in *Bordetella.* The BVG+ upregulated toxin ACT has an inhibitory effect on biofilm formation in *B. bronchiseptica* (Irie et al., 2004). If this finding translates to *B. pertussis,* it would suggest that biofilm formation is not purely a BVG+ induced phenomenon, with two highly upregulated proteins FHA and ACT having biofilm inductor and inhibitor effects respectively. The role of *ompQ,* an BVG+ upregulated gene has also been characterised in *B. bronchiseptica.* Loss of *ompQ* expression did not hinder the bacteria's ability to form early biofilm structures but hindered the formation of mature biofilm (Cattelan et al., 2016b). Fimbriae like those encoded by *fim2* and *fim3* in other gram-negative bacteria have been displayed to play key roles in biofilm formation and development (Schroll et al., 2010). Interestingly in *B. bronchiseptica,* genes involved in flagellum synthesis were upregulated during initial biofilm formation (Nicholson et al., 2012). Flagella biosynthesis is classically a BVG- regulated process contradicting the thinking that biofilm formation and maturation is a BVG+ phenomenon.

In my analysis of differential gene expression during BVG+ vs BVG- plate growth I observed FHA, ACT and OmpQ to be upregulated (Table 4.1). This is not surprising due to them all being classical BVG+ induced genes. However, as discussed FHA and OmpQ have been linked with a pro-biofilm phenotype in broth *in vitro* and murine *in vivo* models, and their upregulation could suggest an increase in the bacteria's ability to adhere to each other as well as the plate. This adherence is a key factor in how biofilms can facilitate bacteria to tolerate stress in their surrounding environment, and therefore may play a role in the ability of *B. pertussis* to tolerate mutagenesis of fundamental cell wall biosynthesis mechanisms.

However, this may not be the case during plate growth. Characterisation of bacterial adhesion and biofilm formation has been classically studied during static broth culturing. During broth culture conditions I have observed *mre/mrd* mutant strains to be comparably viable to wildtype (Figure 3.4). Therefore, factors key in biofilm formation under broth conditions, may not translate to adhesion related tolerance of *mre/mrd* mutants during plate growth.

It is also worthy to note that in highly related *B. bronchiseptica,* two piece of evidence contradict biofilm/adhesion as a mechanism of *mre/mrd* mutation tolerance. Firstly, BVG-

induction of flagellum biosynthesis is required for biofilm formation, a growth phase in which the *mre/mrd* mutant strains are non-viable in plate culture mediums. Secondly, ACT toxin secretion is displayed to have an inhibitory effect on biofilm formation, a mechanism that was upregulated during BVG+ plate growth (Table 4.1).

Therefore, it is unclear whether increased bacterial adhesion plays a role in *mre/mrd* mutation tolerance due to the limited scope of our current understanding of factors in *B. pertussis* biofilm formation. Future experimental investigation could target the most highly characterised adhesin involved in biofilm formation, FHA, for functional genomic analysis.

Identifying the BVG regulated mechanism of tolerance during *B. pertussis* plate growth, is hindered by the number of BVG regulated genes identified as differentially expressed, many whom occupy similar functional niches. Due to this as well as time restrictions I decided to concentrate my research onto the medium dependent mechanism of tolerance between BVG- broth and plate growth.

4.2.3-What is the medium dependent mechanism of tolerance to *mre/mrd* mutations during BVG- broth vs plate growth?-

As *mre/mrd* mutant strains are viable during BVG- broth growth, but nonviable during BVG- plate growth, I compared the transcriptome of these growth conditions to try and identify the mechanism of *mre/mrd* mutation tolerance that is induced during broth growth. Differential expression analysis identified one mechanism related to maintenance of bacterial osmotic stability which was upregulated during BVG- broth growth, betaine/glycine uptake (Table 4.2). The hypothetical mechanism of *mre/mrd* mutation tolerance identified by transcriptomic analysis was the uptake of the well characterised osmoprotectant betaine glycine. Osmoprotection can be divided into stages, the initial stage being the uptake of K^+ ions into the bacteria via low affinity transport systems (Epstein, 1986, Whatmore et al., 1990). This response is limited by the concentration of K^+ that can accumulate in the bacterial cytoplasm to around 400mM, anything above this will have detrimental effects on cytoplasmic enzymatic reactions (Dinnbier et al., 1988). When this salt concentration is reached the secondary stage of osmoprotection is induced which involves the uptake of neutral osmoprotectants into the bacterium (Yancey et al., 1982, Arnal et al., 2015). These molecules can be taken up at much greater concentrations than salts due to their neutral charges meaning they won't interfere with intracellular pH.

Betaine glycine is the most highly utilised neutral osmoprotectant for the majority of bacteria, due to this they have developed mechanism of uptake of glycine betaine from the external environment. This system consists of three genes in *B. pertussis BP2055*, *BP2056* and *BP2057* encoding a substrate binding protein, a permease, and an ATP-binding protein respectively (Table 4.2).

Through transcriptomic analysis of BP536 during BVG- broth vs plate growth conditions it was observed that B/G was significantly upregulated during BVG- broth conditions. As *mre/mrd* mutagenesis reduces osmotic stability of gram-negative bacteria, I hypothesised that the improved ability of *B. pertussis* strains to maintain osmotic homeostasis, by betaine glycine uptake, could be key in restoring BVG- viability during broth growth (Figure 4.19). This was found to be the case, with supplementation of BVG- plates with betaine glycine restoring BP_{536}*ΔmreB* viability (Figure 4.8 & 4.9). This restoration was observed to be a betaine glycine specific process, with supplementation with the alternate osmoprotectant proline not restoring BP_{536}*ΔmreB* viability (Figure 4.10).

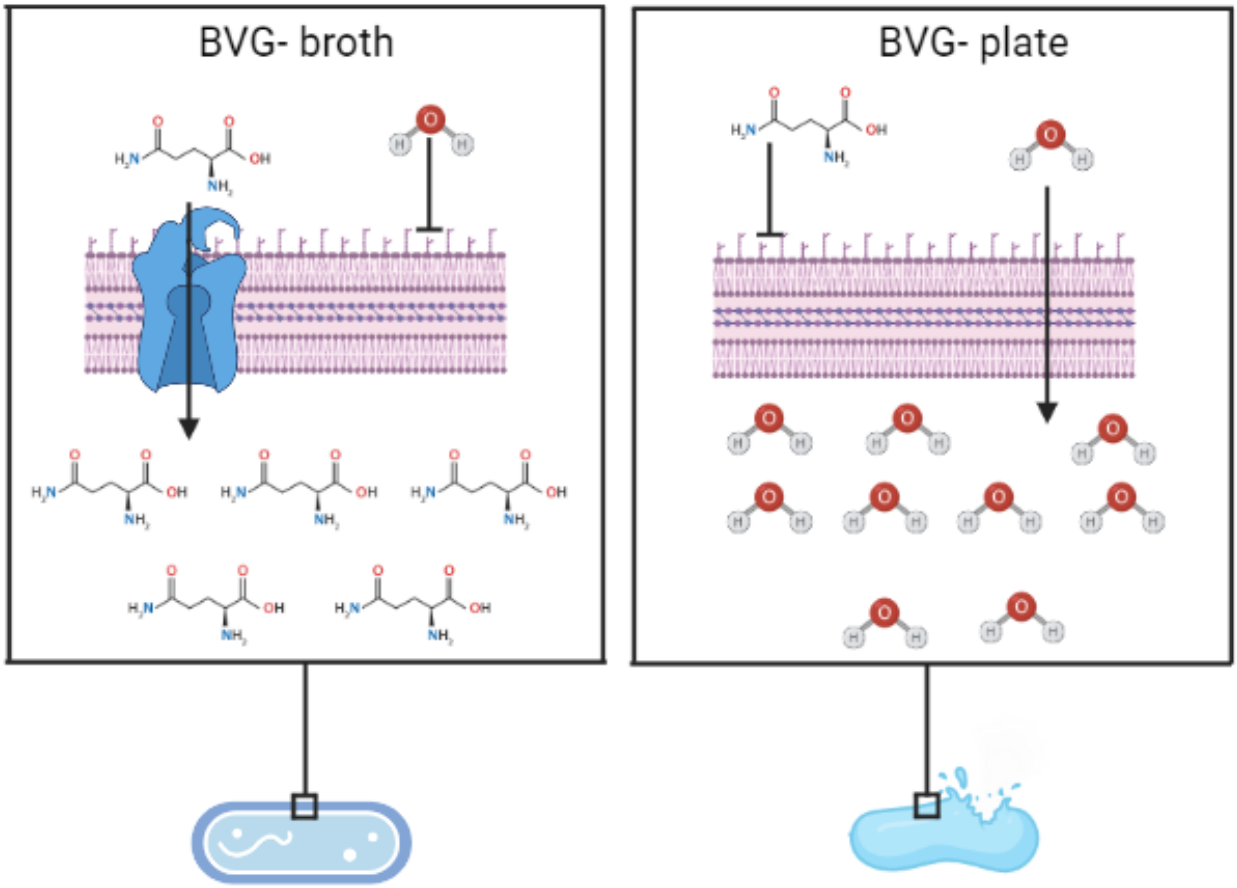

Figure 4.19 – Hypothesised mechanism of betaine uptake induced viability of *mre/mrd* mutants. Betaine can accumulate at high levels intracellularly, reducing water influx into the bacterial cell. Increased betaine uptake could facilitate *mre/mrd* mutants to tolerate BVG- broth growth. Created with BioRender.com

Whether induction of the uptake system was enough to restore BP_{536}*ΔmreB* BVG- plate viability was assessed by introduction of B/G on an inducible plasmid into wildtype and BP_{536}*ΔmreB* strains. Induction of B/G restored viability to a comparable level to that observed upon betaine supplementation (Figure 4.12). This suggests that induction of the betaine uptake system may restore mutant viability independent of supplementation with betaine.

To determine whether functional betaine uptake was required for *B. pertussis* broth viability I knocked out the ATP binding protein BP2057, which fuels the ABC transport of betaine glycine, in BP536 wildtype and BP_{536}*ΔmreB* strains (Figure 4.13 & 4.14). Broth growth of these mutant strains was observed to be unaltered upon loss of betaine uptake (Figure 4.16). This suggests that the increased ability for BP_{536}*ΔmreB* to maintain its osmotic balance is not solely dependent on functional betaine uptake.

4.2.4-Does tolerance of the mutation of *mreC* require a significant alteration in gene expression during BVG+ broth growth?-

To assess whether tolerance of BP_{536}*ΔmreC* in *B. pertussis* requires large-scale alterations in gene expression to tolerate the loss of elongasome PG biosynthesis, I analysed the transcriptome of BP536 wildtype and BP_{536}*ΔmreC* strains during broth culture growth. I hypothesised that due to the fundamental essentiality of the *mre/mrd* operon that *B. pertussis* must display upregulation of genes key in stress responses that maintain cell envelope integrity, facilitating tolerance of *mre/mrd* mutations. Contrastingly, we observed only one gene to be differential expressed, that being the gene knocked out, *mreC*. This illustrates that the BP_{536}*ΔmreC* gene expression is almost identical to that of the wildtype strain (Figure 4.17). This suggests that during BVG+ broth culture, *B. pertussis* is remarkably tolerant to the loss of *mre/mrd* expression with no hallmarks of bacterial stress responses identified. This data further supports the idea that broth growth conditions support tolerance of *mre/mrd* mutations, highlighted by their comparable growth phenotypes compared to wildtype. This is despite the large-scale morphological changes observed upon *mreB* mutation.

4.3-Conclusions and Future Directions

Tolerance of *mre/mrd* mutations without perturbation of growth or OM structural integrity, despite morphological and architectural changes to the bacterial envelope, is a novel phenotype in *B. pertussis.* I hypothesised that this tolerance could be due to an alteration in gene expression between conditions where *mre/mrd* mutations are tolerable and intolerable.

Transcriptomic analysis of wildtype *B. pertussis* allowed me to identify hypothetical mechanisms of tolerance dependent on BVG activation phase and growth medium.

Alternate PG biosynthesis mechanisms were not differentially expression between conditions where the mutants are viable and non-viable, suggesting they don't contribute to *B. pertussis* tolerance of *mre/mrd* mutations.

The mechanism of BVG induced tolerance of *mre/mrd* mutations during *in vitro* plate growth is still undetermined. BVG+ vs BVG- plate analysis suggested that increased adhesin expression could play a role in the mechanism of BVG+ induced tolerance to *mre/mrd* mutations. However, due to the overlapping functionality of many *B. pertussis* adhesins and the poorly understood nature of *B. pertussis* biofilm formation, how to approach this analysis from a functional genomic standpoint was difficult. Future studies where deletion of key bacterial adhesins in *mre/mrd* mutant strains would elaborate on the role these proteins play in BVG+ plate viability.

BVG- broth vs plate analysis identified the ability for *B. pertussis* to uptake the osmoprotectant betaine glycine as highly upregulated during broth growth. This suggests that BVG- broth induced viability may be due to the bacterium having an increased ability to regulate its osmolarity through betaine glycine uptake. This theory was supported by the fact that supplementation with betaine glycine restored mutant BVG- plate viability. However, betaine glycine uptake may not be the sole mechanism of tolerance to *mre/mrd* mutation, as *BP2057* deletion did not alter BP_{536}*ΔmreB* bacterial growth during broth culture. Therefore, other factors that contribute to *mre/mrd* mutation tolerance during broth culturing are to be elucidated in future work.

The hypothesis that *mre/mrd* mutations were tolerated in *B. pertussis* during BVG+ broth growth due to the induction of a transcriptomic change was disproved by direct comparison of the BP_{536}*ΔmreC* transcriptome to wildtype. This analysis displayed remarkably little alteration in transcriptome between mutant and wildtype strains, suggesting that mutation of *mreC* is inherently tolerated in *B. pertussis.* Future transcriptomic analysis of BVG- broth grown BP_{536}*ΔmreC* strains would further validate this finding.

Chapter 5- Analysis of *mre/mrd* and *rpsA* mutant hypervesiculating phenotype.

5.1- Results

As OMVs have been identified as promising vaccine antigens against *B. pertussis* and could be utilised to bolster the current vaccine regimen, the generation of hypervesiculating mutants is of particular interest. Therefore, the characterisation of mutant strains for their vesiculating phenotype and OMVs produced is important in assessing whether they could be utilised for OMV production for vaccine development.

As OM stability has been strongly linked with OMV biogenesis I hypothesised that upon *mre/mrd* mutation a hypervesiculating phenotype may be induced. I aimed to characterise *mre/mrd* mutants vesiculation phenotype and OMVs produced in the BP536 and PTg *B. pertussis* strains.

In parallel I assessed the vesiculation phenotype of *rpsA* mutant strains identified by my collaborators at GSK. I aimed to assess the characterise OMVs produced and elucidate the mechanism of how truncation of the ribosomal protein RpsA induced a hypervesiculating phenotype in *B. pertussis.*

5.1.1-Do *mre/mrd* mutations result in a hypervesiculating phenotypes in *B. pertussis*?-

To assess whether *mre/mrd* mutant strains display an increased secretion of lipid structures into the culture supernatant, eluding to a hypervesiculating phenotype, analysis of lipid content of purified supernatant from deep well growth assays was carried out. Quantification of lipid structures using the lipophilic fluorescent dye, FM4-64, acts as indirect measurement of OMVs produced by strains during culture growth. We observed that all strains displayed a significant increase in fluorescence intensity over wildtype (FIOW), suggesting a hypervesiculating phenotype was induced upon *mre/mrd* mutation (Figure 5.1). For further analysis of OMVs, mutant strains will be grown in large cultures from which supernatant will be extracted. Therefore, selection of the most highly vesiculating strain to take into this analysis is key. I selected BP_{536}*ΔmreC* for further analysis because it displayed one of the highest level of lipids in the culture supernatant.

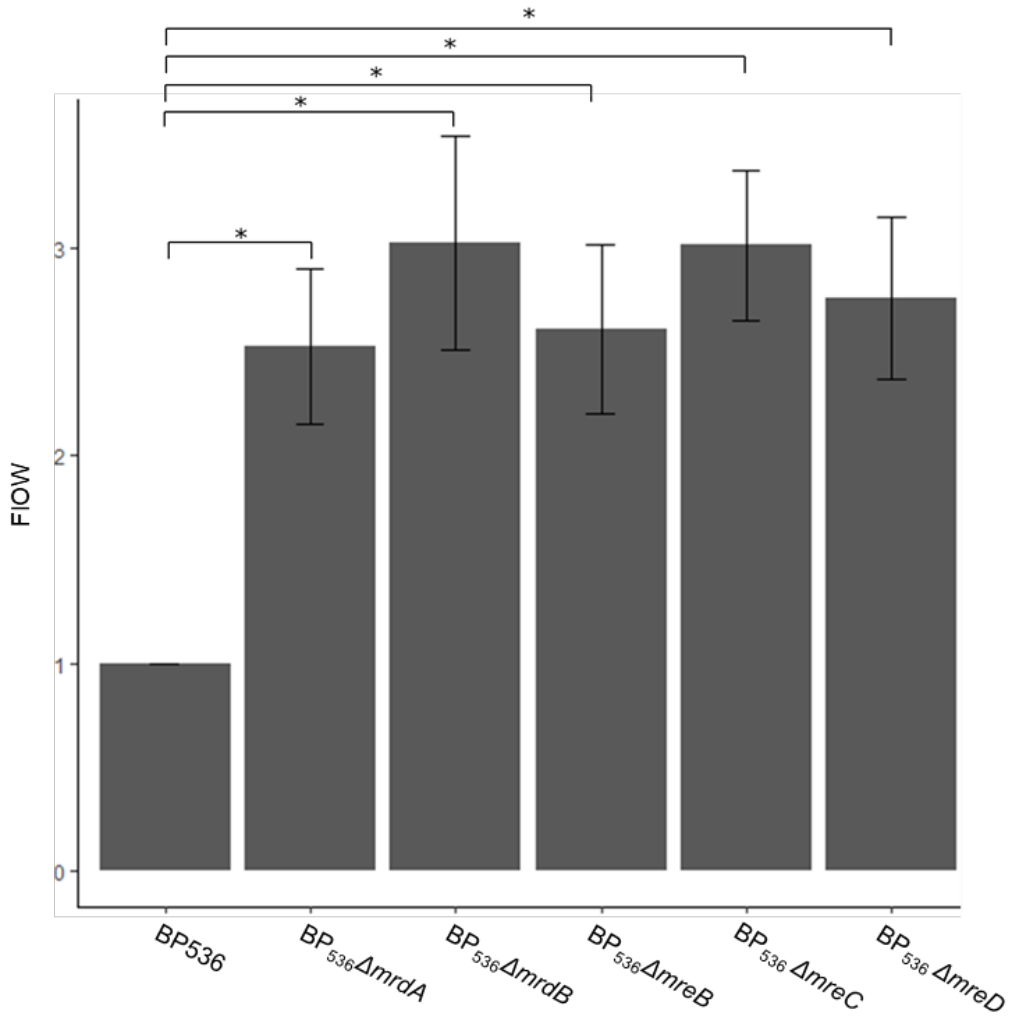

Figure 5.1– Lipid quantification of *mre/mrd* mutants culture supernatant relative to BP536 wildtype during deep well culture growth. Fluorescence intensity over wildtype (FIOW) per strain. Strains were grown in SSCH media in deep well plates. Culture supernatant was extracted at 24 hours and analysed by FM4-64 assay. Results are representative of three biological replicates*=p≤0.05, Students T-test. Error bars = Standard error of the mean.

To assess the optimum timepoint for harvesting supernatant to purify OMVs from 50ml cultures, I quantified lipid structure across a 72-hour period by FM4-64 assay. BP_{536}*ΔmreC* had significantly increased lipid concentrations at 48 hours and 52 hours of growth when compared to BP536 (Figure 5.2). During this growth period strains were observed to reach early stationary phase. At 69- and 72-hours, where mutants have reached late stationary/early death growth phases, highlighted by a plateauing of the culture OD_{600}, we see the highest level of lipid contents in culture supernatant with no significant difference between wildtype and mutant levels. However, whether lipid structures quantified are indeed OMVs at this phase required further analysis due to the fact that cellular debris released during cell death

may contribute to the high lipid levels observed. From this I selected 52- and 72-hours growth as key timepoints for OMV purification.

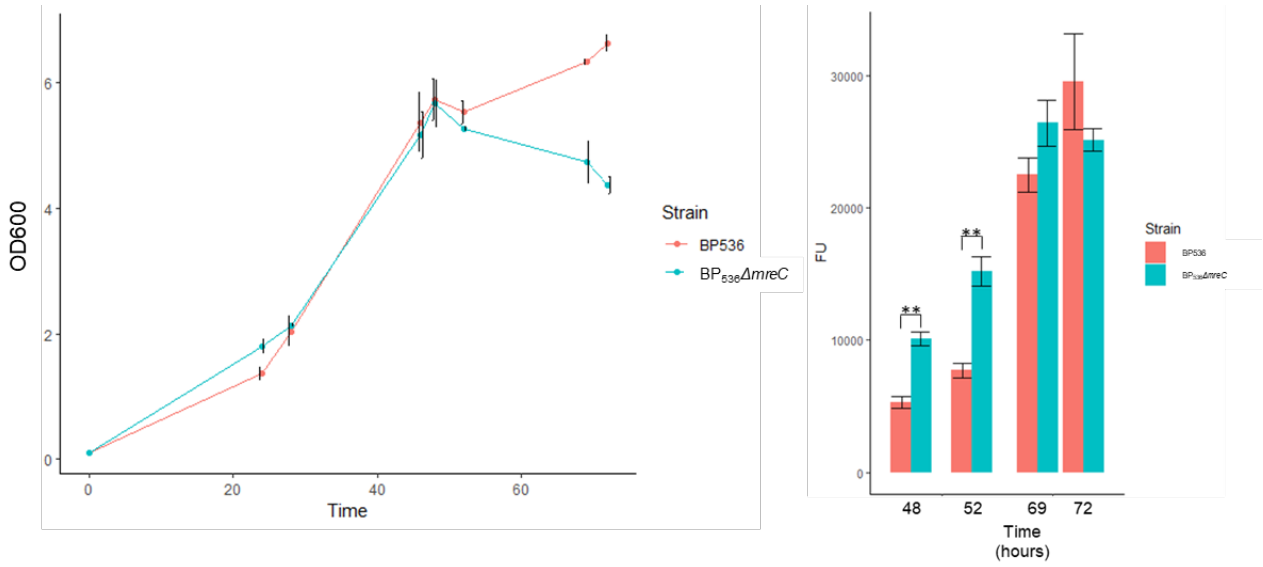

Figure 5.2- Analysis of BP_{536}*ΔmreC* and BP536 growth and secretion of lipid structures across 72 hours of growth in 50ml cultures to identify optimum timepoints to purify OMVs. OD readings were taken, and supernatant extracted across the 72-hour growth period. OD_{600} and Fluorescence intensity units plotted against time of sampling of wildtype and mutant stains. FU data representative of three biological replicates. **=p<0.01, One way ANOVA, Tukeys post-hoc. Error bars = Standard error of the mean.

I then purified OMVs from BP_{536}*ΔmreC* and BP536 50ml cultures at 52- and 72-hours of growth, by ultracentrifugation of filtered culture supernatant. Purified OMVs were analysed by lipid and protein quantification assays. The protein concentration of purified OMVs increased significantly at 72 hours (Figure 5.3). Lipid quantification displayed a significant increase in lipid structures at 52 hours compared to wildtype, with only a slight increase observed between the 52- and 72-hour timepoints. Increased lipid and protein concentrations suggest the presence of increased OMV structures in bacterial supernatant.

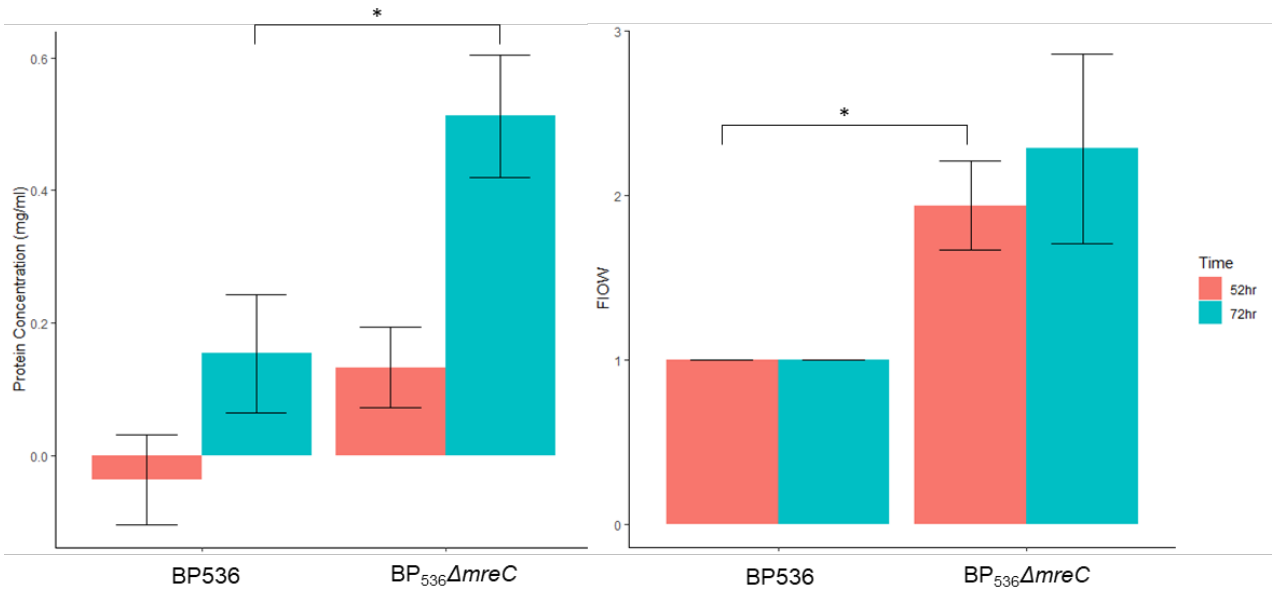

Figure 5.3- Analysis of protein and lipid concentrations of BP_{536}*ΔmreC and* BP536 purified OMVs. Protein and lipid quantification of purified OMVs from 50ml cultures of wildtype and mutant *B. pertussis* strains at 52 and 72hrs of growth. Lipid quantification depicted as Fluorescence intensity over wildtype. Data representative of three biological replicates. *=$p<0.05$, One way ANOVA, Tukeys post-hoc. Error bars = Standard error of the mean.

To determine whether the structures quantified by protein and lipid assays were indeed OMVs, I visualised purified OMV samples by SEM analysis. This analysis displayed OMV structures were present in both the wildtype and mutant samples, with similar OMV species of comparable size observed (Figure 5.4).

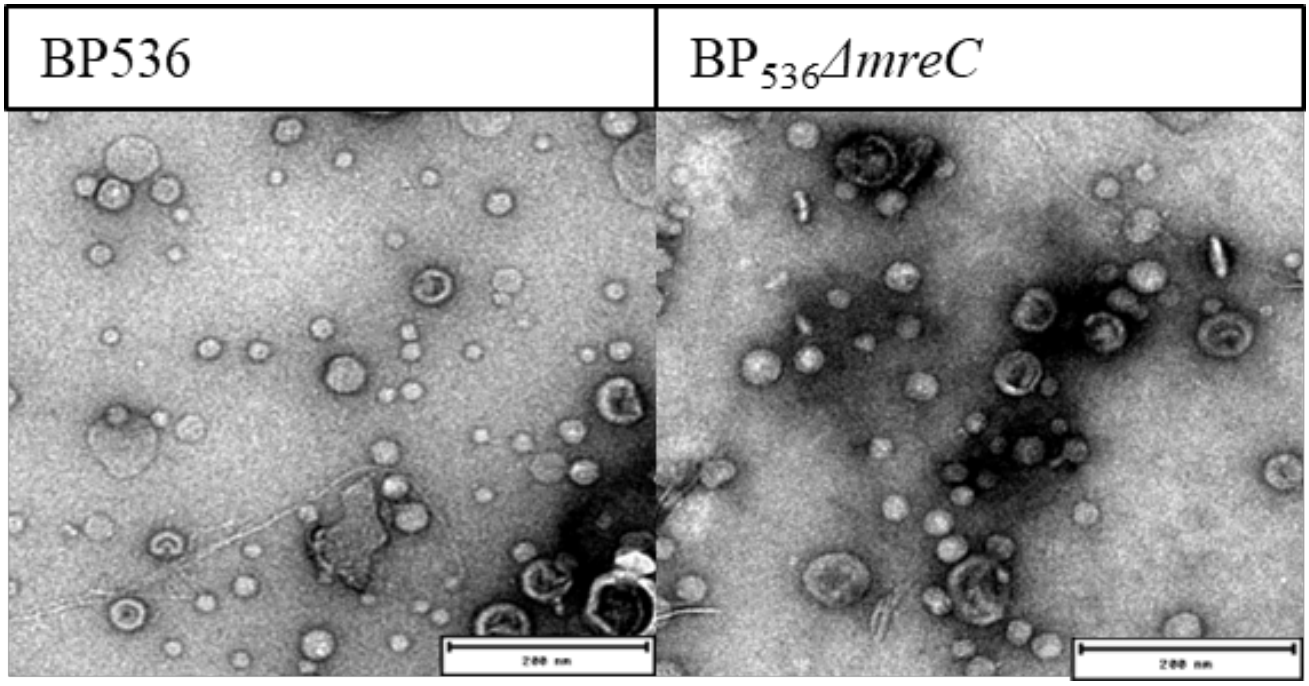

Figure 5.4- Visualisation of OMVs purified from BP536 and $BP_{536}\Delta mreC$ by SEM analysis. Quantity of purified OMVs loaded for imaging standardised to volume.

As OMVs have potential to be utilised as vaccine antigens, I wanted to verify that alteration of PG biosynthesis did not alter the protein composition of OMVs produced. I assessed this by SDS-page analysis of OMVs. OMVs were standardised to lipid concentrations or protein concentrations prior to loading. There were no large variations in band intensity or band pattern of OMVs extracted from wildtype or mutant strains suggesting mutation of *mreC* does not effect protein composition of OMVs (Figure 5.5).

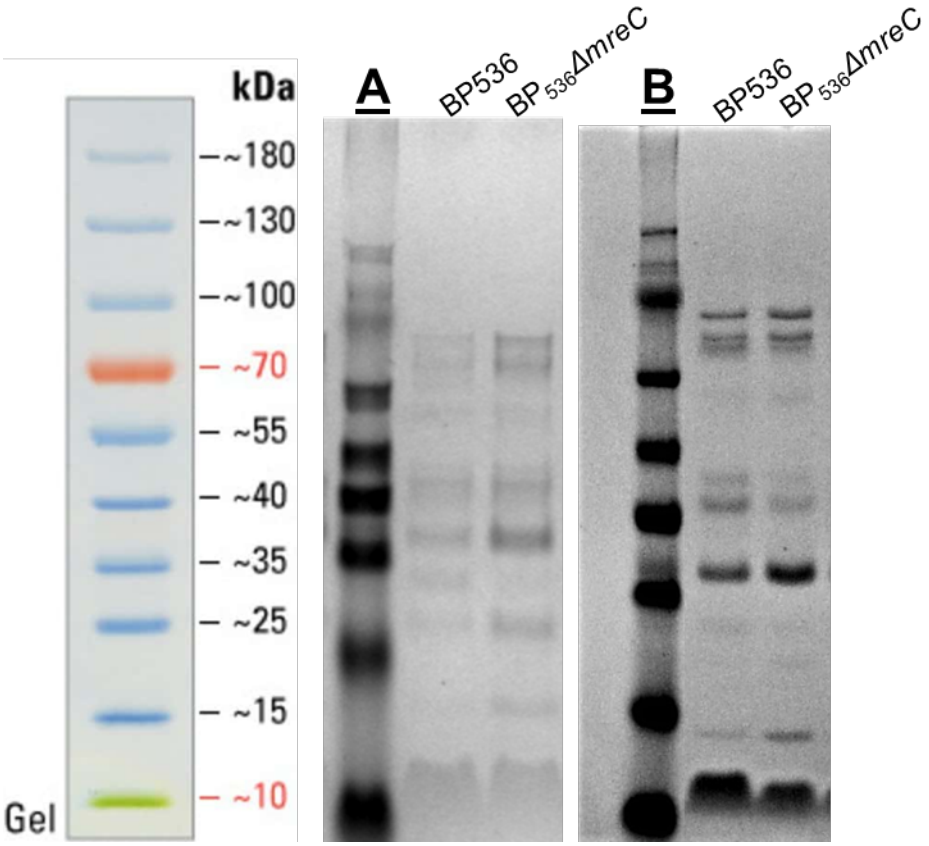

Figure 5.5- SDS page analysis of protein composition of purified OMVs from BP536 and BP$_{536}$*ΔmreC*. A) Standardised to protein concentration. B) Standardised to lipid concentration.

Dynamic light scattering (DLS) analysis was utilised to characterise OMV species produced by *B. pertussis* strains. DLS utilises the Brownian motion of particles suspended in a solution to allow for accurate measurement of particle size. I aimed to utilise this technique to determine whether mutation of *mreC* resulted in different populations of OMVs. I hypothesised that due to altered OM stability BP$_{536}$*ΔmreC* may produce OMVs of differing size to wildtype OMVs, increased OM instability would allow for the blebbing process to occur more readily. Whether these populations would be larger than or smaller than BP536 OMVs was difficult to predict, increased OM instability could theoretically increase the production of smaller OMV populations due to increased rate of OM bulging, or larger OMV populations due to larger OM bulges occurring.

In this analysis BP$_{536}$*ΔmreC* OMVs displayed a more heterogeneous population with variation observed between the three biological replicates. This is highlighted by the BP$_{536}$*ΔmreC* OMVs displaying a broader peak in the chromatograph, with higher percentages of larger and smaller OMV populations compared to the uniform peaks displayed by the

wildtype OMVs (Figure 5.6). This increased variance of OMV size and shape is further represented by an increased average OMV diameter and increase polydispersion index, a measurement of the breadth of the dispersion of particle molecular weight in the sample. However, these values were not significantly different to that of BP536 OMVs. Therefore, from this analysis I cannot conclude that the *mreC* mutation significantly alters the size of OMVs produced during bacterial growth.

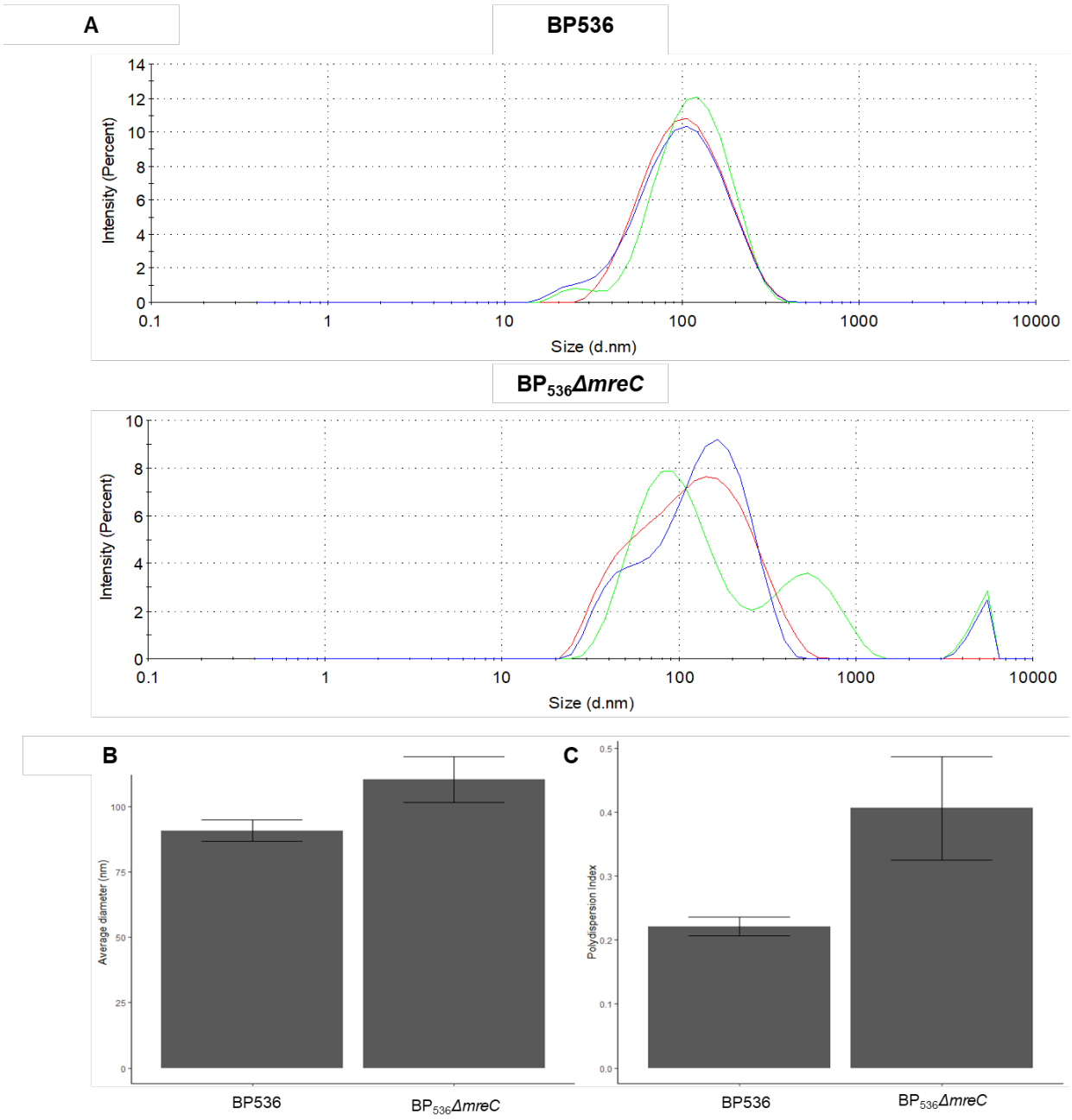

Figure 5.6- Measurement of purified OMVs from BP536 and BP$_{536}$*ΔmreC* by DLS analysis. A) Graph of Intensity of scattering (percent) vs Size (diameter in nm). B) Average diameter of OMV. C) Polydispersion index of samples. Data representative of three biological replicates. Error bars = Standard error of the mean.

To accurately quantify purified OMVs, I utilised Nanoparticle tracking analysis (NTA). NTA uses a laser beam to illuminate particles in suspension which are pumped across a cell upon which a high magnification camera is aimed. This camera records the flow of particles across the cell allowing accurate quantification of OMVs. As OMVs pelleted by ultracentrifugation were resuspended in equal volumes of PBS this analysis allows for direct quantification of OMV concentrations. This analysis displayed that BP$_{536}$*ΔmreC* had significantly higher levels of OMVs further supporting the finding that *mreC* mutation induces a hypervesiculating phenotype in *B. pertussis* (Figure 5.7).

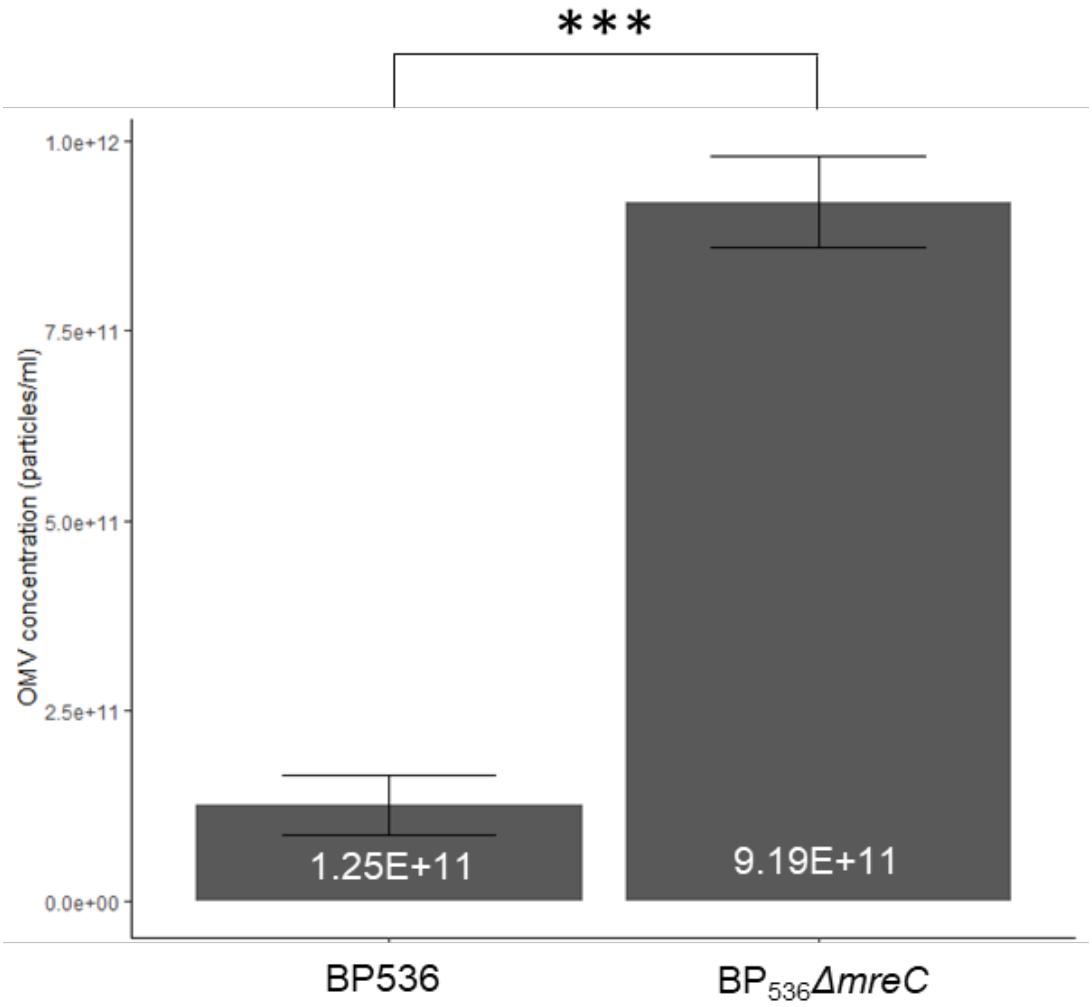

Figure 5.7- Quantification of OMVs in BP536 and BP$_{536}$*ΔmreC* samples by NTA. OMV concentration (particle/ml) graphed against sample. Internal bar labels= average OMV concentration. Data representative of

three biological replicates. ***=p<0.001 One way ANOVA, Tukeys post-hoc. Error bars = Standard error of the mean.

5.1.2-Comparative analysis of the vesiculation phenotype of BP_{PTg}*ΔmreB*, BP_{PTg}50D6 and BP_{PTg}C7 *B. pertussis* strains.-

Work by my collaborators at GSK identified novel hypervesiculating mutants upon truncation of the ribosomal protein RpsA. I wanted to directly compare the vesiculation phenotype and OMV characteristics of the *mre/mrd* mutant strains to those of the *rpsA* mutant strains.

To directly compare the vesiculation phenotypes of *mre/mrd* mutant strains to the *rpsA* mutant strains identified by GSK, I firstly had to transfer a *mre/mrd* mutant allele into the PTg strain which *rpsA* mutants was generated in. I did this by introducing an internally deleted version of the *mreB* gene, carrying a kanamycin cassette, by allelic exchange into PTg using the suicide vector pSS4940. Verification of *mreB* deletion was done by

amplification of the mutant allele and the kanamycin cassette from mutant gDNA (Figure 5.8).

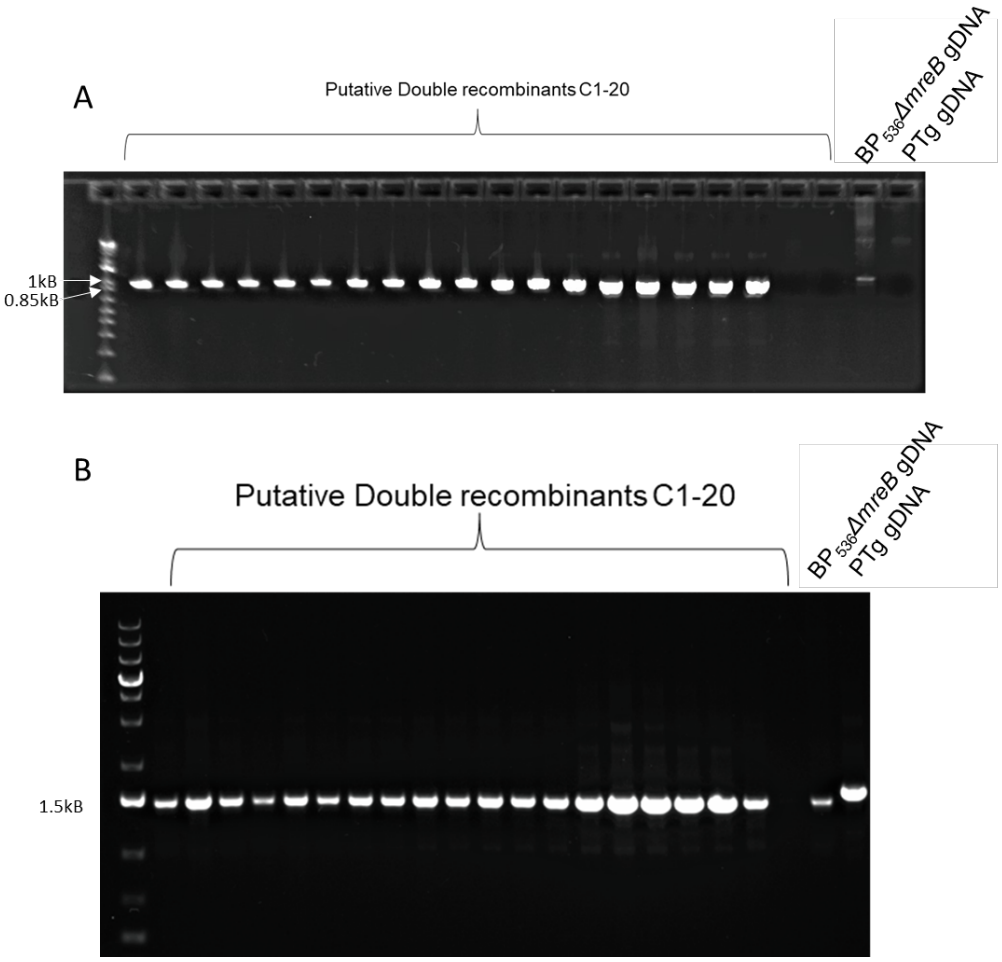

Figure 5.8- Verification of *mreB* deletion in PTg strain background by colony PCR. Colonies 1-20 (C1-20) A) Kan cassette amplification wildtype=0bp Mutant=830bp B) *mreB* coding region amplification wildtype= 1548bp, Mutant= 1305bp

To assess the optimum timepoint for harvesting supernatant to purify OMVs from the *rpsA* truncation mutants, BP_{PTg}50D6 and BP_{PTg}C7, in 50ml cultures, I quantified lipid structure secretion across a 72-hour period by FM4-64 assay. In both the transposon mutant BP_{PTg}50D6 and the confirmatory mutant BP_{PTg}C7 lipid structures in the supernatant was observed at 48 hours of growth, where mutant strains are reaching late logarithmic growth phases (Figure 5.9). At 72- and 76-hour timepoints, I observed the highest level of lipid structures with no significant difference to PTg. From this analysis I selected 52- and 72-hours growth as key timepoints for OMV purification.

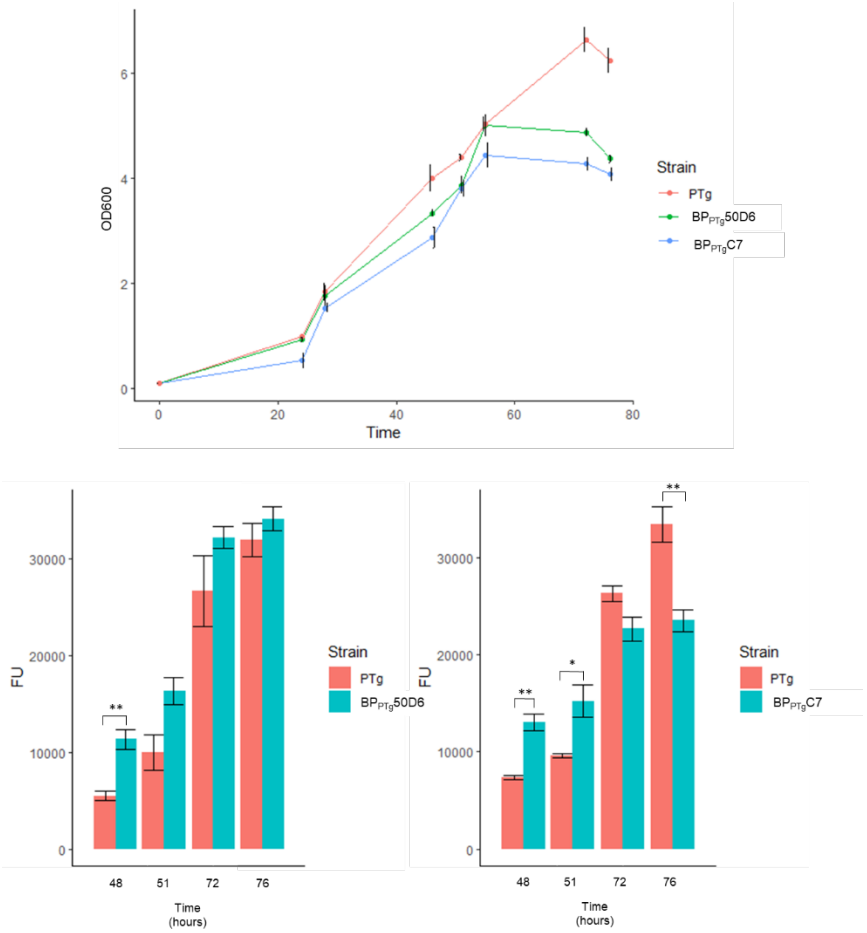

Figure 5.9- Analysis of BP_{PTg}50D6, BP_{PTg}C7 and PTg growth and secretion of lipid structures across 72 hours of growth in 50ml cultures to identify optimum timepoints to purify OMVs. OD_{600} and Fluorescence intensity units plotted against time of sampling of PTg and mutant stains. FU data representative of three biological replicates. *=p<0.05, **=p<0.01, One way ANOVA, Tukeys post-hoc. Error bars = Standard error of the mean.

Purified OMVs were then assessed at these timepoints by lipid and protein quantification assays. We observed that protein concentrations of purified OMVs increased significantly at 52 and 72 hours in the BP_{PTg}*ΔmreB* strain, with no significant increase in OMV protein concentrations in the *rpsA* mutant strains BP_{PTg}50D6 and BP_{PTg}C7 (Figure 5.10). Lipid quantification displayed that there was a significant increase in lipid content in the OMV purified samples at 52 hours in BP_{PTg}C7, and 52 and 72 hours in BP_{PTg}*ΔmreB*. Interestingly BP_{PTg}50D6 displayed no significant increase in supernatant lipid content.

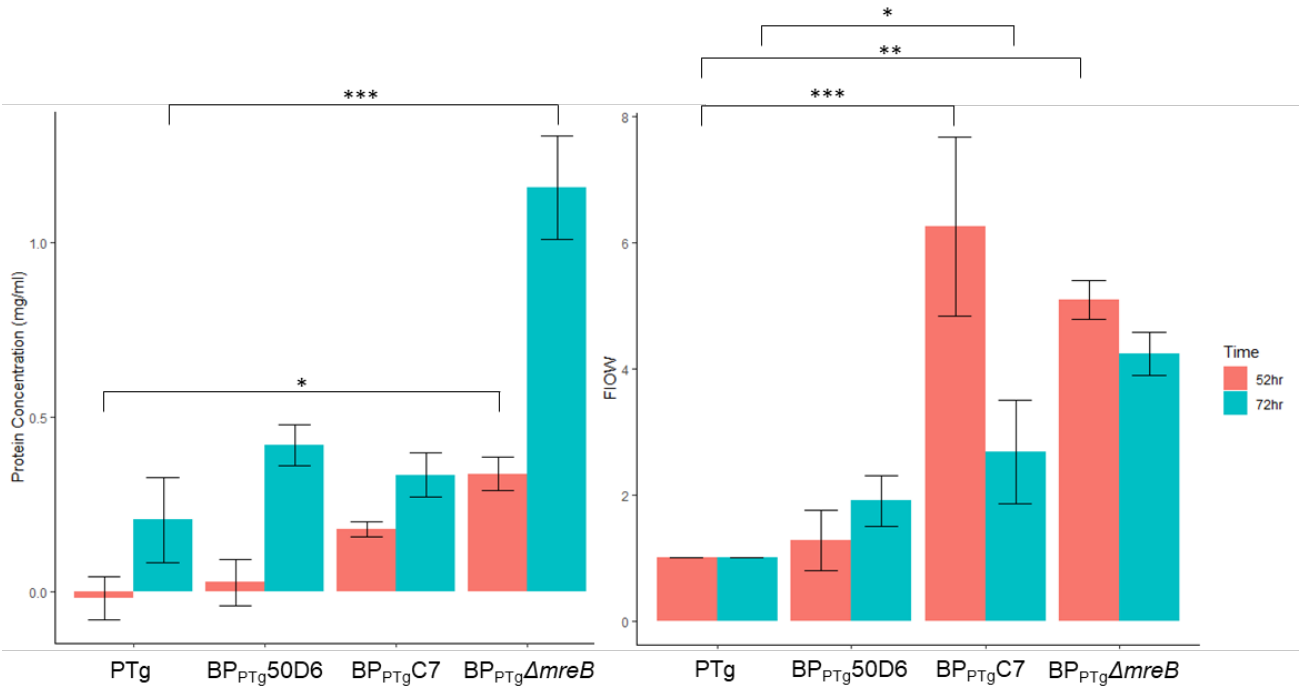

Figure 5.10- Analysis of the protein and lipid concentration of purified OMVs from 50ml cultures of PTg, BP$_{PTg}$50D6, BP$_{PTg}$C7 and BP$_{PTg}$*ΔmreB B. pertussis* strains. OMVs purified at 52 and 72 hours of growth. Lipid quantification depicted as Fluorescence intensity over wildtype. Data representative of three biological replicates. *=p<0.05, **=p<0.01, ***=p<0.001 One way ANOVA, Tukeys post-hoc. Error bars = Standard error of the mean.

EM analysis of purified OMVs displayed quantified structures were indeed OMVs. As samples were standardised to volume this analysis is semi quantitative with purifications that had the highest lipid and protein levels (BP$_{PTg}$C7 and BP$_{PTg}$*ΔmreB)* displaying the highest density of OMVs imaged (Figure 5.11).

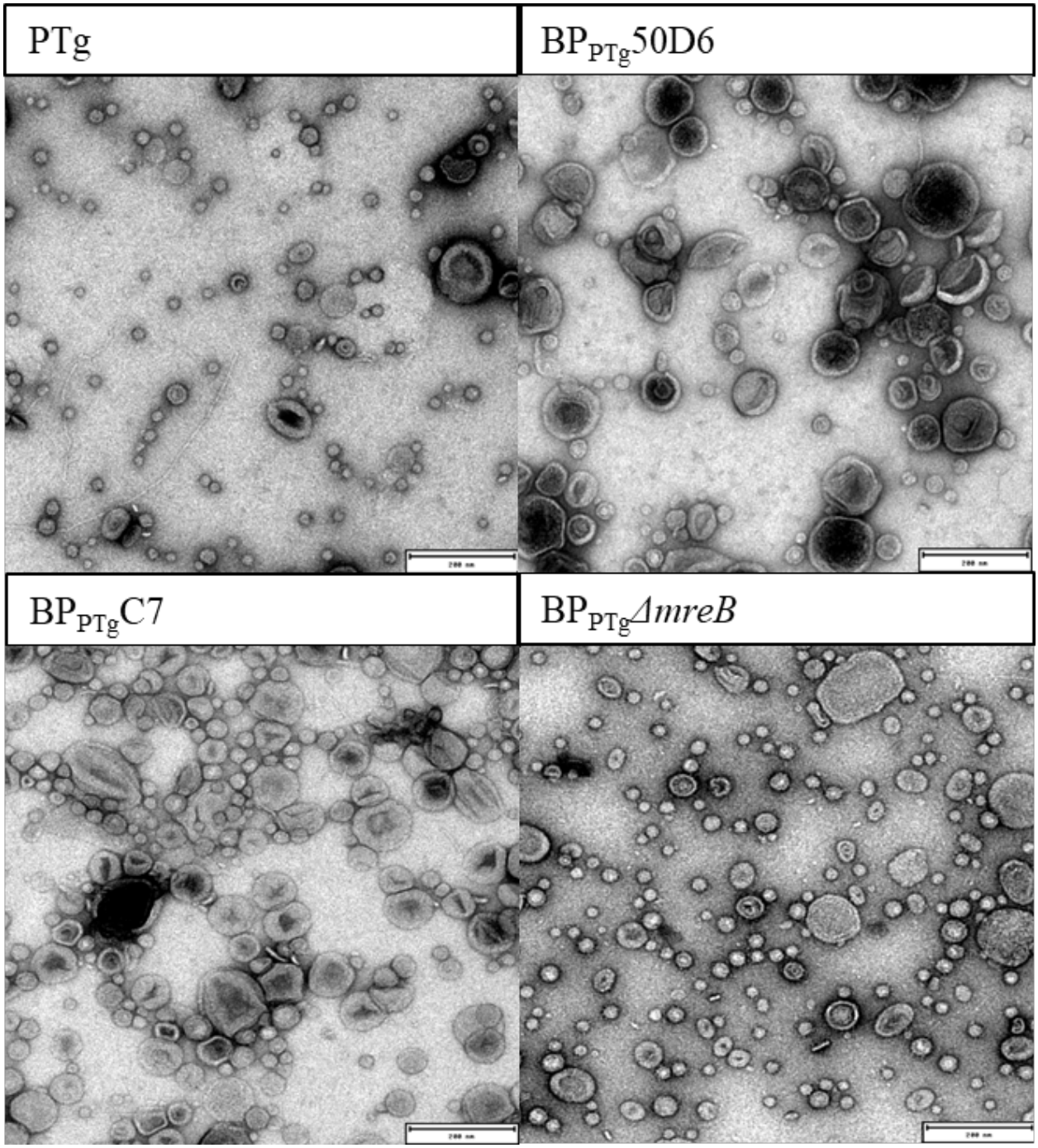

Figure 5.11- Visualisation of purified OMVs of PTg, BP$_{PTg}$50D6, BP$_{PTg}$C7 and *BPΔmreB* by EM. Samples standardised to volume.

As I observed differing protein and lipid levels between OMVs purified from different strains, I wanted to analyse whether the protein species in the OMV samples were altered. I did this by comparing protein profiles by SDS page analysis standardising volume loaded to a set protein or lipid concentration. Standardising to protein concentration allows analysis of the ratio of protein species to each other and allows insight into whether this is altered by the hypervesiculating mutations. Standardising to lipid concentrations allows me to assess

whether protein species concentrations change in purified OMVs, as a set lipid concentration roughly equates to a comparable amount of OMVs per sample.

When samples were standardised to protein concentration, OMVs purified from $BP_{PTg}C7$ and BP_{PTg}*ΔmreB* strains had similar band patterns as PTg, suggesting that the same proteins were present in the mutants compared to PTg. Alternatively, in $BP_{PTg}50D6$ there appears to be an alteration in band pattern when compared to PTg OMVs. Analysis of band intensity displayed different protein species were enriched in mutants compared to PTg, suggesting the hypervesiculating mutations has resulted in alterations of OMV protein profiles (Figure 5.12A). In $BP_{PTg}C7$ and $BP_{PTg}50D6$ a ~40kDa protein is enriched when compared to PTg and BP_{PTg}*ΔmreB.* In $BP_{PTg}C7$ a ~27kDa, ~90kDa are also enriched. In BP_{PTg}*ΔmreB* OMVs a ~27kDa and ~90kDa protein species are enriched.

When I standardise OMV volumes loaded to lipid content the alteration in protein band intensity was further highlighted between samples along with additional enriched protein species being identified (Figure 5.12B). In all mutant strains ~80kDa protein species is enriched. In both $BP_{PTg}C7$ and BP_{PTg}*ΔmreB* OMVs a protein band of around 35kDa is enriched, this band is absent in the $BP_{PTg}50D6$ OMVs. Finally, in BP_{PTg}*ΔmreB* OMVs a protein of ~12kDa is observed to be enriched.

Overall, this analysis suggest that protein compositions are altered in purified OMVs from mutant strains. In $BP_{PTg}C7$ and BP_{PTg}*ΔmreB* OMVs this alteration appears to be limited to a change in protein species concentration, with band patterns of OMVs being comparable to wildtype with only a variation in band intensity between mutant and PTg extracted OMVs. However, in $BP_{PTg}50D6$ OMVs this is not the case with both band pattern and intensity having changed when compared to PTg OMVs.

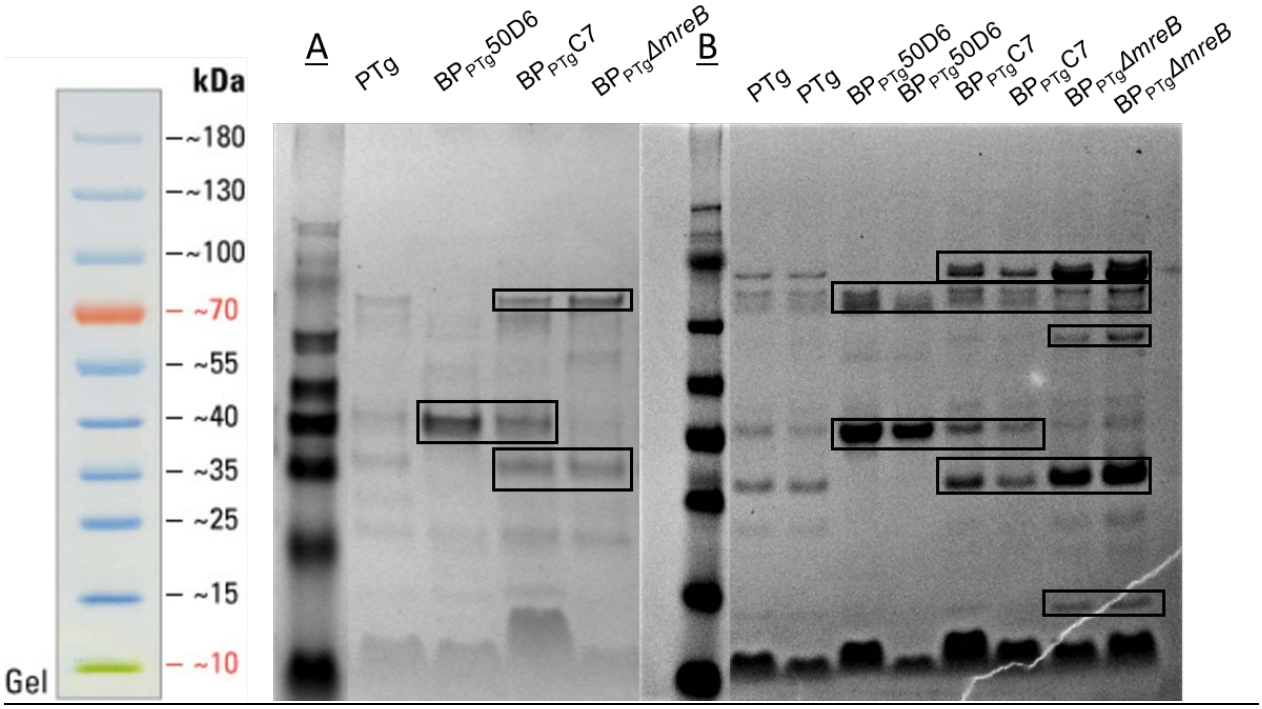

Figure 5.12- SDS page analysis of protein composition of OMVs purified from PTg, BP_{PTg}50D6, BP_{PTg}C7 and BP_{PTg}*ΔmreB*. A) Loading standardised to protein concentration. B) Loading standardised to lipid concentration.

DLS analysis of purified OMVs displayed that BP_{PTg}C7 and BP_{PTg}50D6 OMVs were slightly less diverse in size, with a smaller range of size distribution, an increased OMV diameter and a decreased polydispersion index (Figure 5.13). The opposite was observed in BP_{PTg}*ΔmreB* OMVs with a broader peak displaying increased proportions of smaller and larger OMV species. This was further highlighted by an increased polydispersion index when compared to PTg and the BP_{PTg}50D6 and BP_{PTg}C7 *rpsA* mutant strains. This analysis suggests that there may be a difference in the threshold of bleb size before OM pinching to release the OMV from bacterial surface.

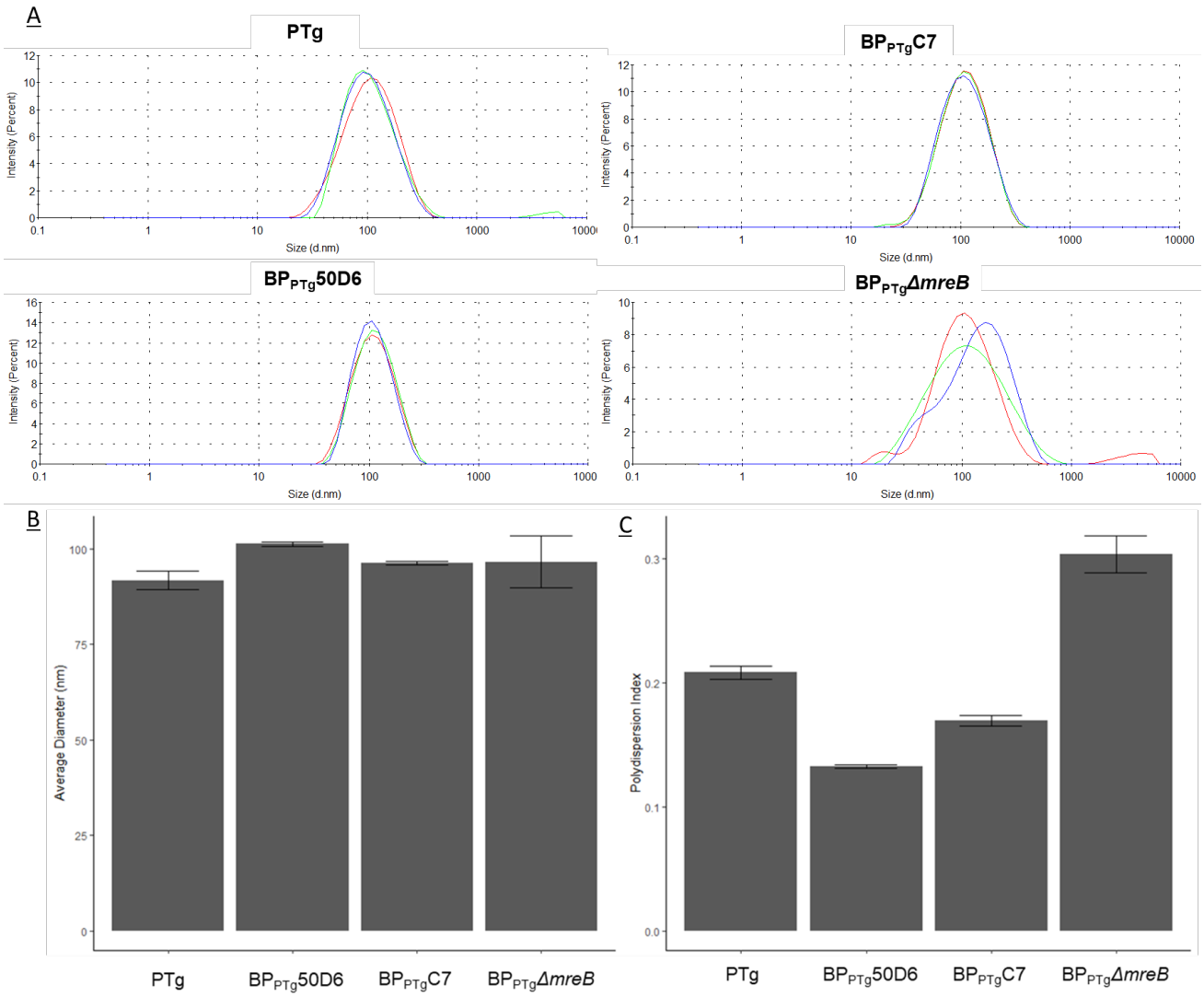

Figure 5.13- Measurement of OMV populations by DLS analysis of purified OMVs from PTg, BP$_{PTg}$50D6, BP$_{PTg}$C7 and BP$_{PTg}$*ΔmreB* samples. A) Graph of Intensity of scattering (percent) vs Size (diameter in nm). B) Average diameter of OMV. C) Polydispersion index of samples. Data representative of three biological replicates. Error bars = Standard error of the mean.

Having characterised OMV lipid and protein composition and OMV size, I wanted to accurately quantify OMVs purified from mutant culture supernatant by NTA. All three mutant strains had significantly increased levels of OMVs displaying that they all display a hypervesiculating phenotype (Figure 5.14). The BP$_{PTg}$C7 *rpsA* mutant displayed the highest level of OMVs, however, there is no significant difference observed between all three strains analysed.

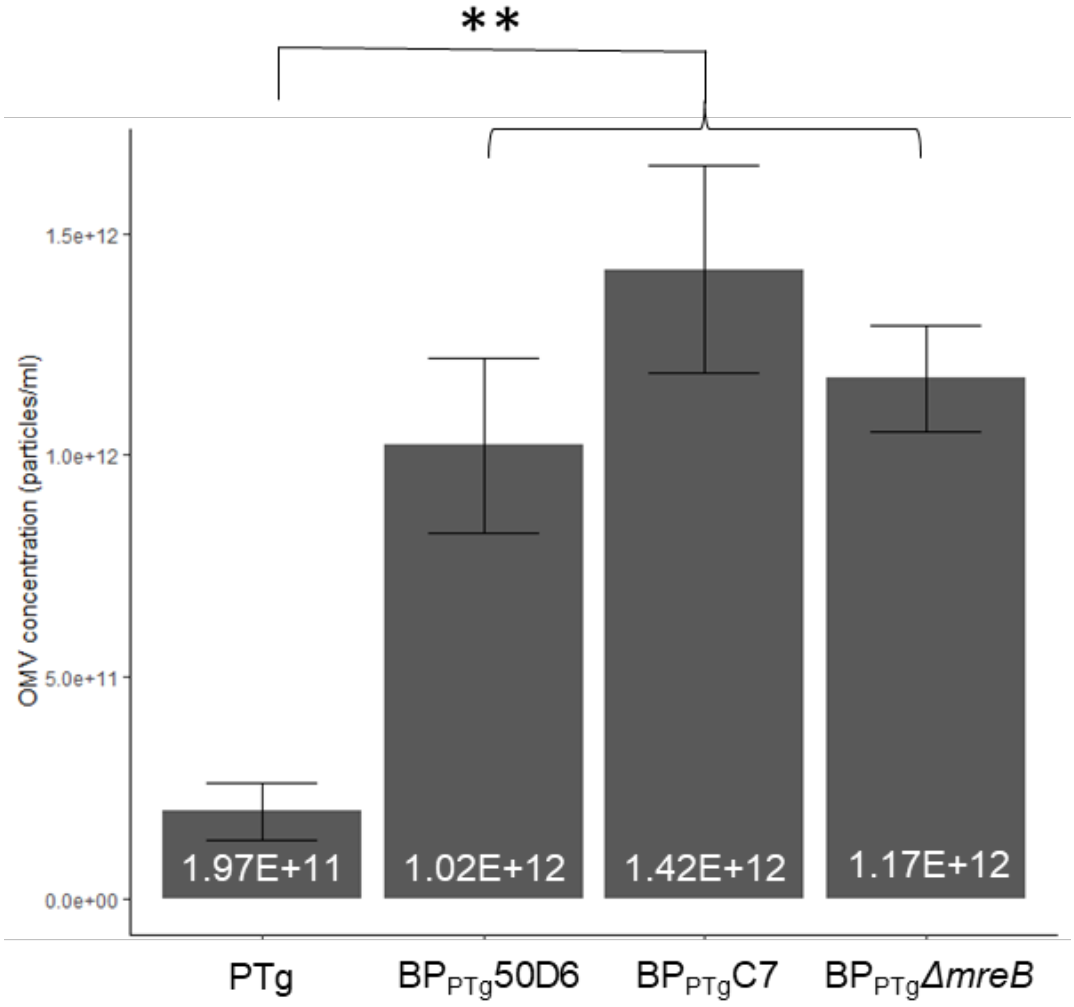

Figure 5.14- Quantification of OMVs in samples purified from PTg, BP$_{PTg}$50D6, BP$_{PTg}$C7 and BP$_{PTg}$*ΔmreB* by Nanoparticle tracking analysis (NTA). OMV concentration (particle/ml) graphed against sample. Bars labelled with mean value. Data representative of three biological replicates. **=p<0.01, One way ANOVA, Tukeys post-hoc. Error bars = Standard error of the mean.

As protein concentrations were observed to only be significantly increased in BP$_{PTg}$*ΔmreB* purified OMVs, with no significant increase in BP$_{PTg}$50D6 or BP$_{PTg}$C7 purified OMVs (Figure 5.10), I decided to analyse protein concentrations standardised to OMV numbers (Figure 5.14) to determine whether there was a significant change in protein concentration per OMV in the different hypervesiculating strains. To do this I standardised the protein concentration per ml to the number of particles per ml quantified by NTA analysis (Figure 5.15). This analysis displayed that there was significantly more protein per OMV in those purified from BP$_{PTg}$*ΔmreB* when compared those purified from PTg, BP$_{PTg}$50D6 and BP$_{PTg}$C7 strains.

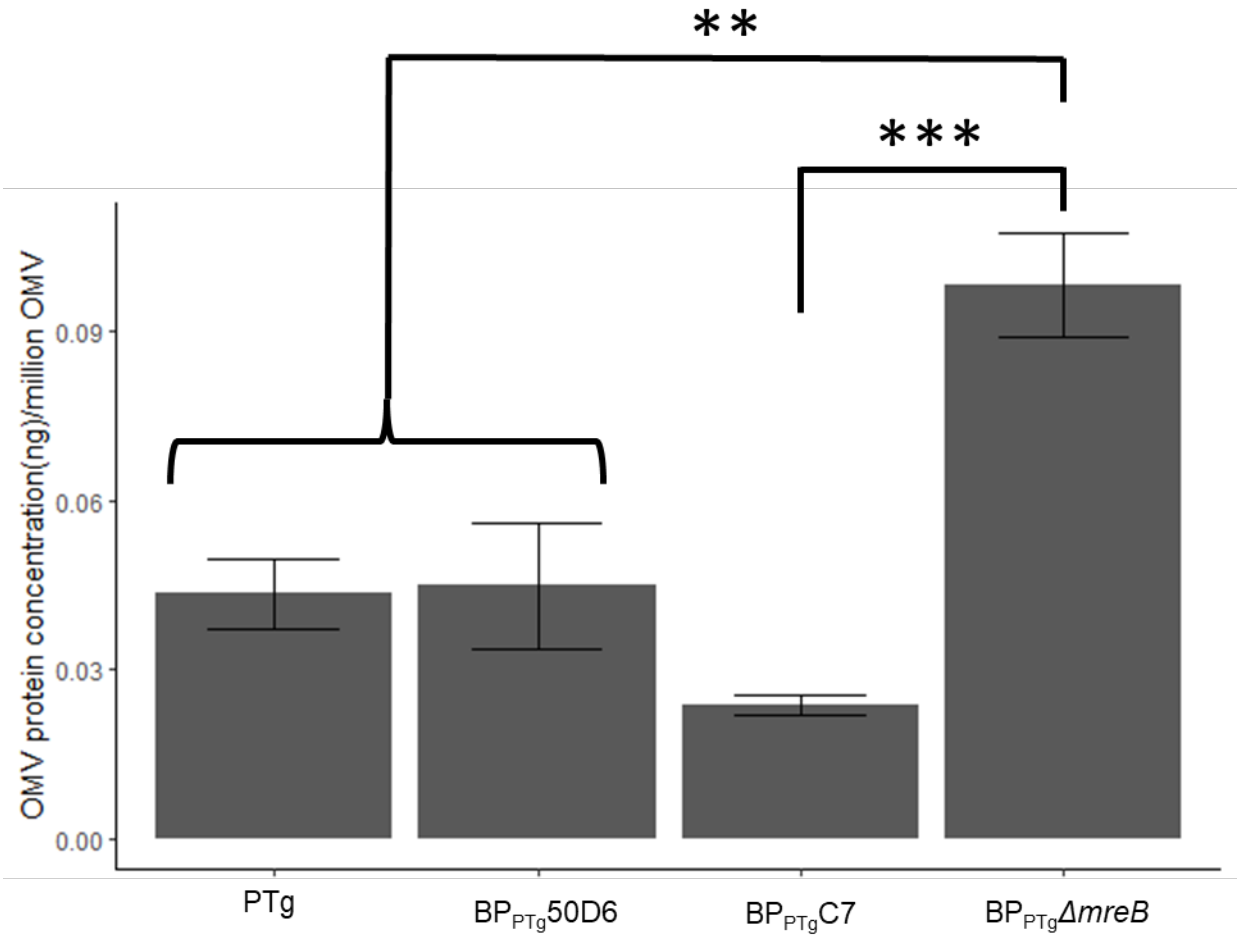

Figure 5.15- Analysis of the ratio of protein (ng/ml) to number of OMV particles (million OMV particles/ml) in samples purified from PTg, BP_{PTg}50D6, BP_{PTg}C7 and BP_{PTg}*ΔmreB* strains. Protein quantification of purified OMVs by DC assay and NTA OMV quantfication data utilised to standrdise protein concentration to OMV number. Data representative of three biological replicates. **=p<0.01, ***=p<0.001, One way ANOVA, Tukeys post-hoc. Error bars = Standard error of the mean.

5.1.3-Can transcriptomic analysis of *rpsA* mutants facilitate the identification of the mechanism of how *rpsA* truncation induces the hypervesiculating phenotype?-

RpsA is a ribosomal protein that has been characterised to be involved in translation initiation, mRNA recognition, and *trans*-translation processes. RpsA is made up of six functional domains. GSK identified that truncation of the sixth domain at the C-terminus resulted in a hypervesiculating phenotype in deep well plate growth, that I have now verified in 50ml culture growth. As *rpsA* is not directly involved in OM stability I decided to utilise transcriptomic analysis to see if truncation altered gene expression of processes involved in OM biosynthesis or remodelling, which may result in OMV biogenesis. BP_{PTg}50D6 and

$BP_{PTg}C7$ mutant strains were grown in triplicate in parallel to PTg in BVG+ 50ml broth cultures. RNA for transcriptomic profiling was extracted at mid-Log growth phases.

At this growth phase it was observed that in both the $BP_{PTg}50D6$ transposon truncation mutant of *rpsA* and the confirmatory mutant $BP_{PTg}C7$, two main BVG- associated pathways were significantly upregulated compared to PTg: capsule biosynthesis and flagellum biosynthesis (Figure 5.16, 5.17, 5.18 and 5.19, Table 5.1 and 5.2). Interestingly the differential expression of these two pathways is not accompanied by the upregulation of other BVG- regulons or the downregulation of BVG+ regulons, suggesting that truncation of *rpsA* has a direct effect on these two pathways independently of the BVG two component system.

Flagellum biosynthesis displayed the highest level of upregulation in both $BP_{PTg}50D6$ and $BP_{PTg}C7$ mutant strains, with genes upregulated in flagella functional and structural apparatus; the membrane associated basal body (*fliEFGHIJLMNOPQ* operon), the flagellar hook (*flgABCDEHIJKL* operon), the filament (*fliC* and *fliDST)* and the stator (*motAB)* (Table 5.1 and 5.2) (Macnab, 2003, Deme et al., 2020).

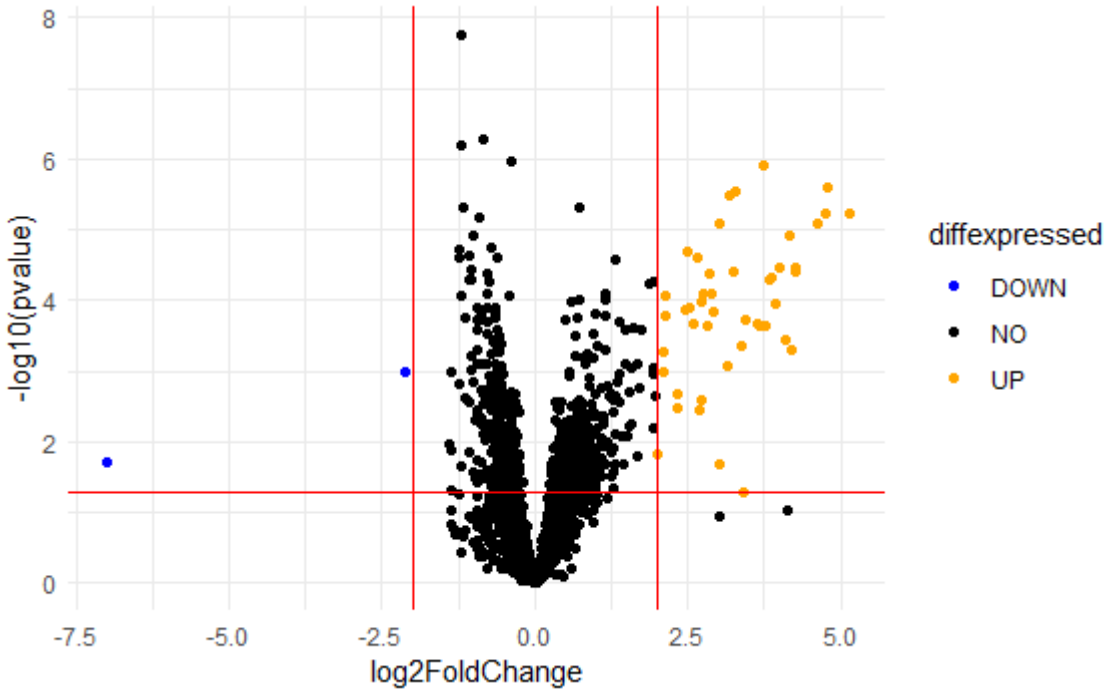

Figure 5.16- Distribution of differentially expressed genes in $BP_{PTg}50D6$ when compared to PTg. Red lines depict values of selection for differential expression Log_2 Fold change > 2 or <-2, p <0.05 the Wald Test.

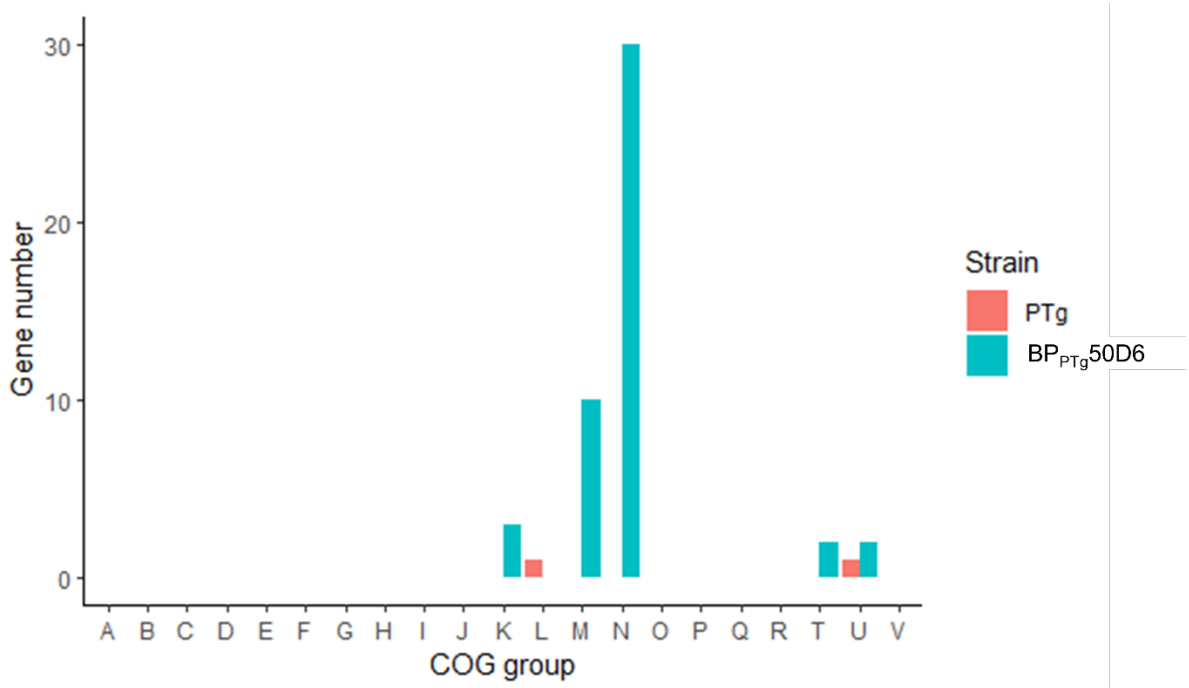

COG category	Function	COG category	Function
A	RNA processing and modification	L	Replication and repair
B	Chromatin structure and dynamics	M	Cell wall/membrane/envelope biogenesis
C	Energy production and conversion	N	Cell motility
D	Cell cycle control and mitosis	O	PTM, protein turnover and chaperones
E	Amino acid metabolism and transport	P	Inorganic ion transport and metabolism
F	Nucleotide metabolism and transport	Q	Secondary structure
G	Carbohydrate metabolism and transport	R	General function prediction only
H	Coenzyme metabolism	S	Unknown
I	Lipid metabolism	T	Signal transduction
J	Translation	U	Intracellular trafficking and secretion
K	Transcription	V	Defence mechanisms

Figure 5.17– Grouping of differentially expressed genes in BP$_{PTg}$50D6 when compared to PTg by COG category.

Table 5.1 – Genes upregulate in $BP_{PTg}50D6$ in M (Cell envelope biogenesis) and N (Cell motility) COG categories.

Gene	Log2 Fold Change	P value	COG category	Description	Preferred name
BP1399	2.10035	0.02673092	N	Flagellar FliJ protein	*fliJ*
BP1620	2.123277	0.005969222	M	glycosyltransferase	NA
BP1021	2.139439	0.008370908	N K	RNA polymerase sigma factor for flagellar operon	*fliA*
BP1631	2.322576	0.042965071	M	Capsular polysaccharide biosynthesis	*wcbA*
BP1408	2.338695	0.050130686	N	flagellar protein	*fliT*
BP1394	2.515312	0.007199864	N	Flagellar motor switch	*fliM*
BP1382	2.597314	0.009424719	N	Flagellar hook-associated protein	*flgK*
BP1767	2.643939	0.003331538	MU	cell adhesion	*phg*
BP1393	2.720148	0.006610608	N	Flagellar motor switch	*fliN*
BP1383	2.733492	0.045866937	N	Flagellin and related hook-associated proteins	*flgL*
BP1028	2.751697	0.005894138	NT	Chemotaxis protein histidine kinase	*cheA*
BP1026	2.824694	0.009465753	N	chemotaxis protein	*cheY*
BP1410	2.853269	0.004100331	N	flagellar biosynthesis protein	*fliD*
BP1628	2.882657	0.005894138	M	Polysaccharide biosynthesis/export protein	*wza*
BP1401	2.934841	0.007930497	N	Flagellar biosynthesis type III secretory pathway protein	*fliH*
BP1367	3.016011	0.001744174	N	flagellar biosynthesis protein	*flhA*
BP1625	3.137531	0.022573814	M	COG3524 Capsule polysaccharide export protein	*kpsE*
BP1366	3.242218	0.004100331	N	flagellar biosynthesis protein	*flhB*
BP1395	3.386072	0.014788399	N	flagellar protein	*fliL*
BP1626	3.432173	0.008557043	M	glycosyltransferase group 1 family	*wbpT*
BP1030	3.635268	0.009278591	NT	Methyl-accepting chemotaxis protein	*tsr*
BP1402	3.674346	0.009465753	N	flagellar rotation	*fliG*
BP1025	3.72493	0.000803151	N	chemotaxis motB protein	*motB*
BP1029	3.760265	0.009465753	N	chemotaxis protein	*cheW*
BP1379	3.851792	0.004507724	N	flagellar protein	*flgH*
BP1403	3.866035	0.004507724	N	The M ring may be actively involved in energy transduction	*fliF*
BP1381	3.927807	0.006884107	N	Flagellum-specific muramidase, peptidoglycan hydrolysis	*flgJ*
BP1377	3.99871	0.004080618	N	flagellar basal body rod	*flgF*
BP1627	4.100319	0.012836678	M	Vi biosynthesis protein	*vipC*
BP1024	4.17477	0.002315311	N	chemotaxis motA protein	*motA*
BP1405	4.203348	0.015954424	M	Flagellar regulator YcgR	*ycgR*
BP1380	4.262732	0.004100331	N	flagellar scaffolding protein	*flgI*
BP1378	4.27317	0.004063799	N	flagellar basal body rod	*flgG*
BP1376	4.610043	0.001744174	N	Flagellar hook protein FlgE	*flgE*
BP1375	4.744591	0.001553223	N	flagellar scaffolding protein	*flgD*
BP1374	4.777041	0.001257271	N	Flagellar basal body rod	*flgC*
BP1373	5.144899	0.001553223	N	Structural component of flagellum	*flgB*

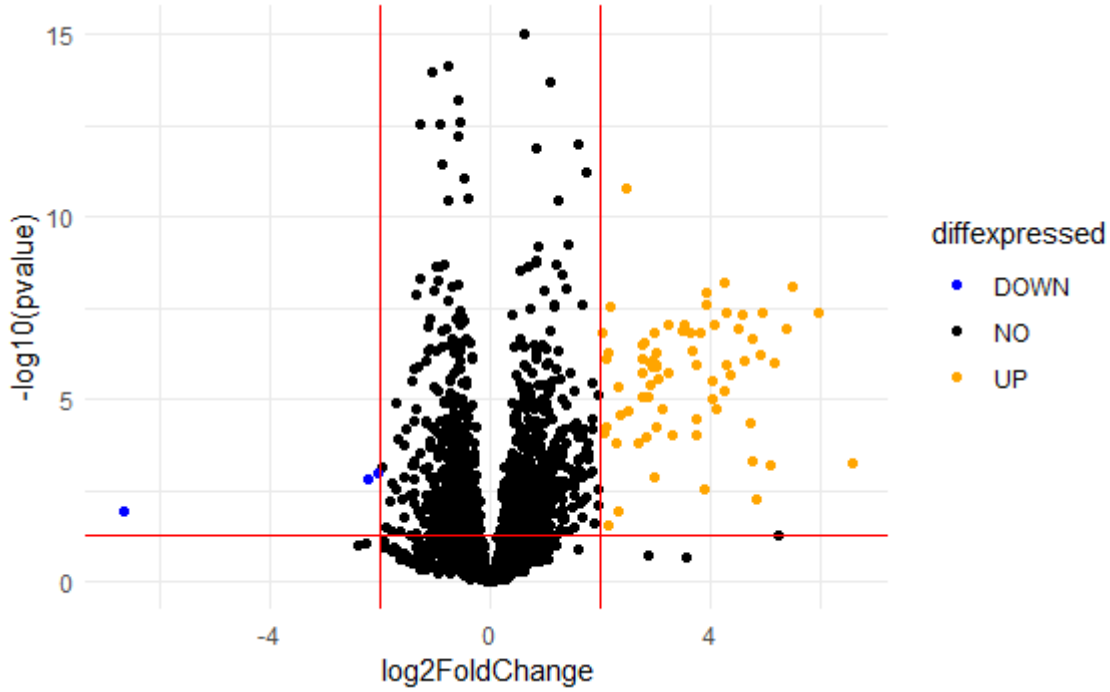

Figure 5.18- Distribution of differentially expressed genes in $BP_{PTg}C7$ when compared to PTg. Red lines depict values of selection for differential expression Log_2 Fold change > 2 or <-2, p <0.05 the Wald Test.

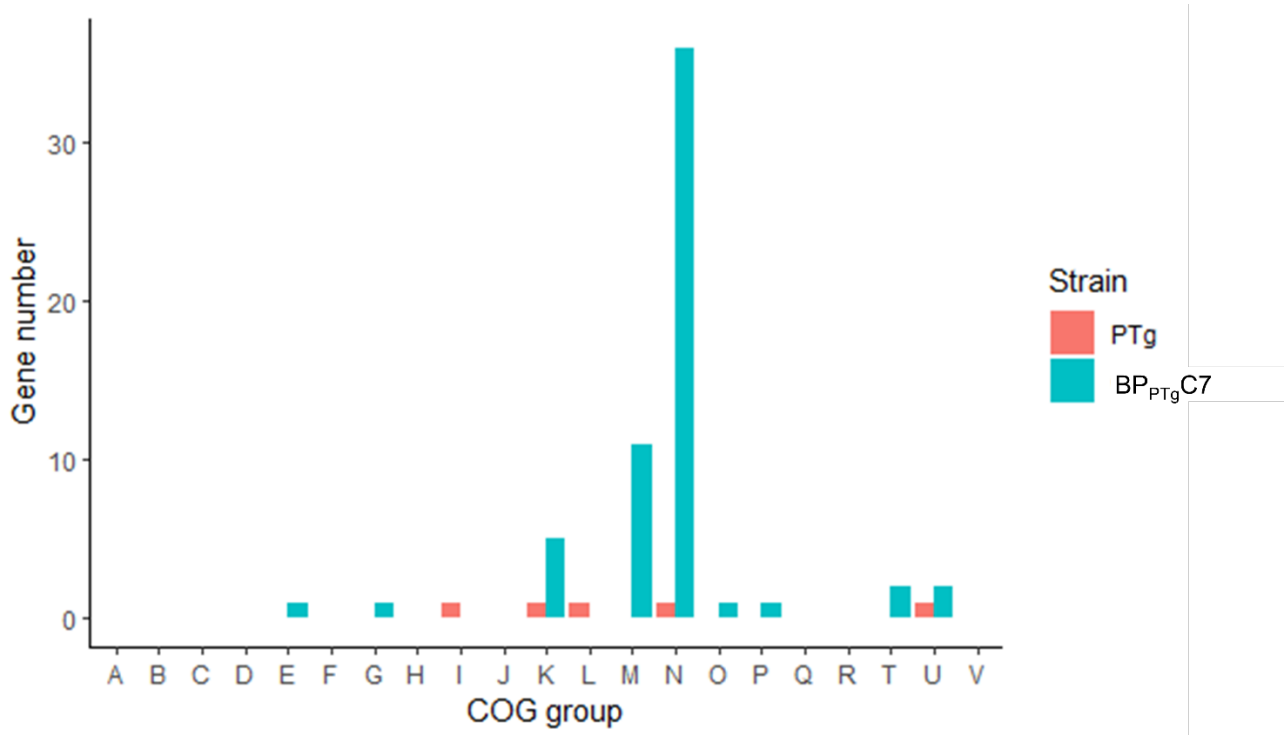

COG category	Function	COG category	Function
A	RNA processing and modification	L	Replication and repair
B	Chromatin structure and dynamics	M	Cell wall/membrane/envelope biogenesis
C	Energy production and conversion	N	Cell motility
D	Cell cycle control and mitosis	O	PTM, protein turnover and chaperones
E	Amino acid metabolism and transport	P	Inorganic ion transport and metabolism
F	Nucleotide metabolism and transport	Q	Secondary structure
G	Carbohydrate metabolism and transport	R	General function prediction only
H	Coenzyme metabolism	S	Unknown
I	Lipid metabolism	T	Signal transduction
J	Translation	U	Intracellular trafficking and secretion
K	Transcription	V	Defence mechanisms

Figure 5.19- Grouping of differentially expressed genes in $BP_{PTg}C7$ when compared to PTg by COG category.

Table 5.2- Genes upregulate in $BP_{PTg}C7$ in M (Cell envelope biogenesis) and N (Cell motility) COG categories.

Gene	Log2 Fold Change	p value	COG category	Description	Preferred name
BP1404	6.599912	0.004798	N	Flagellar hook-basal body	*fliE*
BP1373	5.977433	2.99E-06	N	Structural component of flagellum	*flgB*
BP1627	5.502548	8.30E-07	M	Vi biosynthesis protein	*vipC*
BP1374	5.402011	6.34E-06	N	Flagellar basal body rod	*flgC*
BP1375	5.164882	2.97E-05	N	flagellar scaffolding protein	*flgD*
BP1376	4.935167	2.99E-06	N	Flagellar hook protein FlgE	*flgE*
BP1024	4.909779	2.11E-05	N	chemotaxis motA protein	*motA*
BP1378	4.763034	9.80E-06	N	flagellar basal body rod	*flgG*
BP1405	4.720438	0.000675	M	Flagellar regulator YcgR	*ycgR*
BP1380	4.627254	2.80E-05	N	flagellar basal body rod	*flgI*
BP1403	4.569948	2.99E-06	N	flagellar M ring	*fliF*
BP1626	4.497171	5.90E-06	M	glycosyltransferase group 1 family	*wbpT*
BP1377	4.359187	5.29E-05	N	flagellar basal body rod	*flgF*
BP1379	4.301249	3.30E-05	N	Flagellar L-ring	*flgH*
BP1025	4.280911	2.99E-06	N	chemotaxis motB protein	*motB*
BP1395	4.267519	7.20E-07	N	flagellar protein	*fliL*
BP1629	4.247665	0.000125	M	UDP-glucose GDP-mannose dehydrogenase	*wbpO*
BP1029	4.128038	0.000318	N	chemotaxis protein	*cheW*
BP1381	4.087406	4.94E-06	N	Flagellum-specific muramidase	*flgJ*
BP1625	4.037282	7.90E-05	M	Capsule polysaccharide export protein	*kpsE*
BP1030	3.94035	1.06E-06	NT	Methyl-accepting chemotaxis protein	*tsr*
BP1402	3.927034	2.10E-06	N	flagellar rotation protein	*fliG*
BP1628	3.805418	7.29E-06	M	Polysaccharide biosynthesis/export protein	*wza*
BP1406	3.741722	0.001272	N	Flagellar biosynthesis protein	*flhB_1*
BP1366	3.646071	7.00E-06	N	export apparatus of flagellin	*flhB*
BP1410	3.51483	4.94E-06	N	flagellar filament	*fliD*
BP1367	3.48148	6.86E-06	N	flagellar biosynthesis protein	*flhA*
BP1401	3.297102	0.001202	N	type III secretory pathway protein	*fliH*
BP1631	3.248903	4.94E-06	M	biosynthesis of a cell envelope polysaccharide,	*wcbA*
BP1618	3.137389	0.000324	M	Vi polysaccharide biosynthesis protein tviD	*tviD*
BP1026	3.041524	6.96E-05	N	chemotaxis protein	*cheY*
BP1624	3.021075	0.000784	GM	ATPases	*kpsT*
BP1383	3.015733	3.51E-05	N	Flagellin and related hook-associated proteins	*flgL*
BP1393	3.004241	3.24E-05	N	Flagellar motor switch	*fliN*
BP1767	3.001332	7.00E-06	MU	cell adhesion	*phg*
BP1620	2.937151	3.79E-05	M	glycosyltransferase	*NA*
BP1028	2.936367	2.86E-05	NT	Chemotaxis protein histidine kinase	*cheA*
BP1394	2.913948	3.09E-05	N	Flagellar motor switch	*fliM*
BP1382	2.865263	0.000184	N	Flagellar hook-associated protein	*flgK*
BP1392	2.834122	0.001302	N	flagellar protein	*fliO*
BP1371	2.78625	1.22E-05	N	Anti-sigma-28 factor, FlgM	*flgM*
BP1021	2.773167	2.47E-05	N K	RNA polymerase sigma factor for flagellar operon	*fliA*
BP1372	2.771921	1.27E-05	N	flagellar P-ring.	*flgA*
BP1408	2.679488	0.001861	N	flagellar protein	*fliT*
BP1409	2.339187	0.000109	N	Flagellar protein FliS	*fliS*
BP1368	2.313628	0.04725	N	flagellar biosynthesis protein	*flhF*
BP1399	2.281694	0.00183	N	Flagellar FliJ protein	*fliJ*

5.2-Discussion

Through this experimental work I have characterised the vesiculation phenotype induced upon *mre/mrd* mutation in both BP536 and PTg *B. pertussis* strains.

The BP_{536}*ΔmreC* strain had significant increases in lipids in culture supernatant during deep well plate and 50ml culture growth (Figure 5.1, 5.2 and 5.3). This increase in lipid structures was further supported by an increase in protein concentrations in purified OMVs (Figure 5.3). These structures were verified to be OMVs via visualisation by electron microscopy, and accurately quantified by NTA, which proved that *mreC* mutation induced a hypervesiculating phenotype in BP536 *B. pertussis* (Figure 5.4 & Figure 5.7).

In the PTg background introduction of the *mreB* mutation was also found to induce a hypervesiculating phenotype, with significant increase in lipids and proteins in OMVs compared to PTg OMVs (Figure 5.9 and 5.10). When compared to *rpsA* mutants BP_{PTg}50D6 and BP_{PTg}C7, lipid structures were at a comparable level but only the *mreB* mutation resulted in significantly increased levels of protein. This was further highlighted upon standardising to number of particles per ml with BP_{PTg}*ΔmreB* OMVs displaying significantly increased protein concentrations per million OMVs when compared to PTg, BP_{PTg}50D6 and BP_{PTg}C7 purified OMVs (Figure 5.15). This finding suggest BP_{PTg}*ΔmreB* OMV antigens could be promising as vaccine antigen, as enriched protein composition of OMV may be beneficial in inducing a protective immune response. However, to verify this further analysis will be required to determine whether proteins increasing in concentrations are protective antigens on the OMVs OM surface, and not internalised proteins with no protective effect.

Perturbations in OM stability have previously been observed to induce hyper vesiculating phenotypes in *B. pertussis* and other gram-negative bacteria, with knockout of in integral crosslinking proteins and alteration of OM phospholipid symmetry resulting in hypervesiculation phenotypes (de Jonge et al., 2022a, de Jonge et al., 2022b). However, this is the first time that disruption of PG biosynthesis has been characterised to induce a hypervesiculating phenotype. This may be due to the fact elongasome PG biosynthesis mechanisms are essential in many gram-negative bacterial species. Therefore, the ability to knockout elongasome PG biosynthesis to induce a hypervesiculating phenotype may be specific to *B. pertussis.*

As these OMVs would hypothetically be utilised in a novel vaccine it is important to characterise OMV morphology and antigen profiles. I looked at whether OMV size was

effected in hypervesiculating mutant strains. OMV size could contribute to their effectiveness as novel vaccine antigens. Studies have displayed that particle size can contribute to localisation of particles within the body, rate of uptake by immune cells and immune response induction. Firstly, particle size has been shown to be a determining factor in where particles ends up in the body, with large particles of greater than 1µm being observed to accumulate in capillaries, which can cause dangerous side effects such as thrombosis (Benne et al., 2016). Particles of ~100nm dissipate at a quicker rate from circulation (Epstein-Barash et al., 2010). This is thought to be due to particles of this size being taken up more readily by circulating immune cells. This was verified by the comparative analysis of the rate of uptake of 80nm and 100nm liposomal particles, in which the 80nm particles persisted significantly longer in circulation. Particle size has also been displayed to be an important contributor to immune induction, with larger particles of 200nm displaying a more robust cytokine response when compared to smaller ~80nm liposomes (Epstein-Barash et al., 2010, Shima et al., 2013). Overall, this work suggests that OMVs of a size range of ~100nm-200nm could be optimum for vaccine antigens because they display more effective induction of immune responses.

DLS analysis displayed that BP_{536}*ΔmreC* and BP_{PTg}*ΔmreB* OMVs were more polydispersed with an increased number of OMVs in larger and smaller OMV populations (Figure 5.6 and 5.13). However, average OMV size was not drastically altered when compared to BP536 and PTg OMVs respectively, displaying that despite increased number of smaller and larger OMV populations the majority of OMVs produced are of a similar size. BP_{PTg}50D6 and BP_{PTg}C7 strains OMVs conversely displayed a less polydispersed population suggesting OMV blebbing and release was more uniform than in PTg. Overall, this analysis displayed that the hypervesiculating mutations did not greatly alter OMV morphology, with the average OMV diameter falling between 90-110nm for all strains.

Another key characteristic of OMVs that contributed to their feasibility as vaccine components is the presence of wildtype OM antigens. OMVs purified from *B. pertussis* cultures have been displayed to be protective in murine models (Zurita et al., 2019). Therefore, OMVs generated by hypervesiculating strains would ideally display wildtype antigen profiles on the OMV surface. SDS page analysis displayed that BP_{536}*ΔmreC,* BP_{PTg}*ΔmreB* and BP_{PTg}C7 OMVs displayed the same pattern of proteins as wildtype OMVs with only a change in protein intensity being observed in some of the mutant strains (Figure 5.5 and 5.12). Interestingly in the BP_{PTg}50D6 *rpsA* mutant strain an alteration in the protein

pattern was observed along with changes in protein intensity suggesting OMVs from this hypervesiculating strain may have an alternate antigen profile to protective OMVs purified from *B. pertussis* wildtype (Figure 5.12). Therefore, OMVs from BP_{PTg}50D6 may not evoke as broad and protective immune response as OMVs from other hypervesiculating strains. During this body of work, I did not utilise immunoblotting to identify known *B. pertussis* antigens.

In BP_{536}*ΔmreC* OMVs no proteins were observed to be enriched when compared to BP536 wildtype (Figure 5.5). However, in BP_{PTg}*ΔmreB* OMVs a ~27kDa, ~70kDa, and~90kDa protein species are enriched suggesting there may be an alteration in OMV antigen profiles (Figure 5.12). What these protein bands correspond to is unable to be eluded without proteomic or immunoblotting analysis as many OM proteins have sizes comparable to these bands.

The transcriptomic profiling of BP_{PTg}C7 and BP_{PTg}50D6 strains identified flagella biosynthesis mechanisms to be highly upregulated in the mutant strains (Figure 5.16, 5.17, 5.18, and 5.19, Table 5.1 and 5.2). In previous studies of motile *B. pertussis,* flagellum biosynthesis was characterised by the expression of ~40kDa flagellin protein. In BP_{PTg}50D6 and BP_{PTg}C7 OMVs one of the most highly enriched protein is around ~40kDa suggesting flagellin may be expressed on purified OMVs from these strains (Figure 5.12).

In *B. pertussis,* flagellum and capsule biosynthesis are BVG- induced responses. Interestingly in the r*psA* mutant strains these classically BVG- induced responses have been shown to be significantly upregulated during BVG+ broth culture. As the BVG- regulon is not expressed during *B. pertussis* infection, no BVG- OM antigens are included in the current vaccine regimen. As flagellum associated motility and capsule biosynthesis are not known to be important in the natural course of *B. pertussis* infection, their presence in OMVs may be detrimental to the ability of the vaccine to protect against *B. pertussis*. This is because both capsule and flagella components are highly immunostimulatory in other gram-negative bacteria, therefore their presence as OMV antigens may direct a substantial proportion of the immune response towards antigens not expressed during *B. pertussis* infection (Wilson et al., 2008, Mizel and Bates, 2010, Hajam et al., 2017). However, as I have not directly verified the presence of either capsule or flagellin antigens on OMVs produced by *rpsA* mutants, I cannot conclusively say that characterised transcriptomic changes have altered OMV antigen profiles.

Transcriptomic analysis of BP_{536}*ΔmreC* during broth culture displayed only *mreC* to be differentially expressed (Figure 4.20). This suggests that BP_{536}*ΔmreC* strains display wildtype gene expression and therefore OMVs produced by these strains may display the same antigens as wildtype OMVs which have previously characterised as protective. Whether this lack of transcriptomic change is mirrored in the BP_{PTg}*ΔmreB* strain is yet to be determined, with the enrichment of different proteins observed by SDS-page of OMVs suggesting there may be changes to gene expression.

The transcriptomic analysis of the *rpsA* mutant strains could elucidate the mechanism of OMV biogenesis induced by truncation of *rpsA,* as there was no direct link with alteration of ribosomal proteins to OM stability. Transcriptomic analysis identified two pathways which were highly upregulated upon *rpsA* truncation both in the BP_{PTg}50D6 transposon mutant and the BP_{PTg}C7 confirmatory mutant (Figure 5.16, 5.17, 5.18, and 5.19, Table 5.1 and 5.2). These were capsule and flagella biosynthesis pathways both of which have been previously characterised as BVG- associated. Interestingly the upregulation of these two classical BVG- pathways does not appear to be due to a shift to the BVG- regulon in the *rpsA* mutant strains. This is displayed by the fact that there is no change in the expression of the BVG+ virulence associated genes between PTg and the *rpsA* mutant strains. How these BVG- regulated pathways come to be upregulated during BVG+ broth growth of the *rpsA* mutant strains is unclear.

Capsule biosynthesis is not well understood in *B. pertussis,* with initial research suggesting *B. pertussis* to be un-encapsulated with only recent studies alluding to a microcapsule being present during BVG- growth (Hoo et al., 2014, Neo et al., 2010). To date there has been no link between increased capsule biosynthesis and OMV biogenesis in any gram-negative bacteria.

Flagellum biosynthesis is also not well understood in *B. pertussis. B. pertussis* is thought to be a nonmotile bacteria which was further supported by a stop codon interrupting the coding sequence of *flhA,* a gene which is key in flagellar biosynthesis due to its role in export of the flagellum filament component (Parkhill et al., 2003). However, motility has been observed in some *B. pertussis* strains under BVG- modulating conditions, but this motility is yet to be verified as flagellum dependent (Hoffman et al., 2019). Interestingly a study in *E. coli* identified OMVs produced to contained abundant levels of FliC in the OMV lumen. Null mutants of both *fliC* and *flgK* were observed to produce lower levels of OMV in culture

supernatant suggesting a link between flagellar biosynthesis and OMV production (Manabe et al., 2013). In *Vibrio fischeri* similar findings were observed, with flagellum biosynthesis being found to be inherently linked with OMV biogenesis (Aschtgen et al., 2016). However, the exact mechanism of how flagellar biosynthesis relates to OMV production is unclear.

As FliC was found to be enriched in OMV lumen it suggests that the presence of flagellar proteins in the bacterial periplasmic space is important in OMV production, not their presentation on the bacterial surface (Manabe et al., 2013). In *B. pertussis* Tohama I derivative strains such as BP536 and PTg this accumulation may be exaggerated by the fact that the key transporter *flhA* is truncated by an internal stop codon (Parkhill et al., 2003).

From this body of work, it suggests that the hypervesiculating phenotype induced by *rpsA* truncation could be due to the upregulation of flagellum biosynthesis observed in transcriptomic analysis. The fact that enrichment of a ~40kDa protein is observed in purified OMVs from these strains further supports this, as this is the correct size for flagellin (Figure 5.12). However, direct verification of flagellin presence is yet to be carried out.

Another potential mechanism for flagellum biosynthesis induced hypervesiculation is the increased expression of *flgJ,* a PG muramidase, which is involved in the hydrolysis of PG at the site of flagellum assembly (Hirano et al., 2001). As shown in *mre/mrd* mutant strains, disruption or alteration of the PG sacculus can induce a hypervesiculating phenotype. Therefore, high levels of expression of a PG muramidase could play a role in the hypervesiculation observed in the *rpsA* mutant strains.

It also worthy to note that the hypervesiculating phenotype could be pleotropic with flagellum biosynthesis only partly being responsible. The fact that *rpsA* plays a role in protein biogenesis via translational regulation means that transcriptomic analysis may not directly correspond to protein profiles as translation of mRNA may be altered. It would be interesting to do proteomic analysis of *rpsA* mutant strains in the future to analyse whether truncation alters the synthesis of proteins involved in OM stability and therefore OMV biogenesis.

5.3-Conclusions

It was hypothesised that *mre/mrd* mutations would result in a hypervesiculating phenotype as reduced OM stability has been inherently linked to OMV biogenesis. Quantification through indirect and direct methods displayed that this was indeed the case, displaying *mre/mrd* mutants as hypervesiculating mutant strains. *rpsA* mutant strains also displayed

hypervesiculating phenotypes with no significant difference in vesiculation levels between BP_{PTg}*ΔmreB* and the *rpsA* mutant strains.

Characterisation of size distribution and antigen composition of OMVs produced by BP_{PTg}*ΔmreB* and *rpsA* mutants, displayed OMVs produced by BP_{PTg}*ΔmreB* to be promising candidates for vaccine antigens with comparable antigen profiles to wildtype and optimal size for uptake by immune cells. In the future it would be relevant to do more robust characterisation of OMV protein compositions to verify the presence of key vaccine antigens.

Transcriptomic analysis of *rpsA* mutant strains to try and elucidate the mechanisms of OMV biogenesis displayed enrichment of BVG- associated pathways, capsule and flagellar biosynthesis. Flagellin accumulation in the bacterial periplasm has been previously identified to induce OMV biogenesis and may be the mechanism of hypervesiculation induced by *rpsA* truncation. In the future determination of the presence of flagellin in the purified OMVs from the *rpsA* mutant strains would aid to validate its proposed role in the hypervesiculating phenotype induced.

6- Conclusions and future directions.

Characterisation of the effect of *mre/mrd* mutation on *B. pertussis*-

Characterisation of the effect of the loss of elongasome PG biosynthesis on bacterial growth displayed that the *mre/mrd* operon was conditionally essential dependent on the activation state of the BVG two component system and the culture medium. Under nonessential growth conditions mutants grew comparably to wildtype, suggesting that bacterial viability wasn't altered upon the loss of elongasome PG biosynthesis despite clear alterations in bacterial morphology. Despite a significantly increased periplasmic area being induced upon elongasome loss, the OM of mutant strains was observed to tolerate detergent treatment comparably to wildtype.

Overall, this work displays that the loss of elongasome PG biosynthesis results in morphological changes to the overall shape of the bacterium and the membrane architecture. However, these changes don't result in a reduction of bacterial viability. In the future it would be interesting to further analyse the cell wall characteristics of the mutant strains to determine whether its functionality is altered upon elongasome PG biosynthesis loss.

It would be relevant to characterise the ability of mutant strains to tolerate growth in mediums of increasing osmolarity, to determine whether osmotic stability is perturbed upon the loss of elongasome PG biosynthesis, as this is a phenotype observed in *mreB* mutant *E. coli* strains. It would also be interesting to determine whether the minimum inhibitory concentration (MIC) of cell wall targeting antibiotics, such as vancomycin, is altered in mutant strains. A decreased MIC in mutant strains would elude to an increased reliance on alternate PG biosynthesis mechanisms to maintain the PG sacculus.

Identification of the mechanisms of tolerance to the loss of elongasome PG biosynthesis-

Tolerance of the loss of elongasome PG biosynthesis, despite morphological and architectural changes to the bacterial envelope, is a novel phenotype in *B. pertussis.* Differential expression analysis of *B. pertussis* transcriptomes, between viable and unviable growth conditions, facilitated the investigation of mechanisms of tolerance to *mre/mrd* knockout.

The mechanism of BVG induced tolerance of the loss of the elongasome during *in vitro* plate growth is yet to be determined. Analysis displayed during the BVG+ plate growth, where mutants are viable, adhesin expression was significantly increased. Increased adhesin expression may facilitate BVG+ induced tolerance to *mre/mrd* mutations through stronger

bacterium-plate and bacterium-bacterium interactions. However, this hasn't been investigated experimentally. In the future it would be interesting to analyse the potential link between increased expression of bacterial adhesins and tolerance of *mre/mrd* mutation by targeted mutagenesis of a number of key bacterial adhesins, such as FHA, FIM2/3 and OmpQ, and analysing the result of the loss of adhesin expression on mutant viability in plate growth conditions.

The medium induced mechanism of tolerance was partially elucidated by this body of work. Transcriptomic analysis of BVG- broth vs plate growth identified the ability for *B. pertussis* to uptake the osmoprotectant betaine glycine as highly upregulated during broth growth. From this finding we hypothesised that the tolerance of *mre/mrd* knockout induced upon broth culturing may be due to the bacterium having an increased ability to regulate its osmolarity through betaine glycine uptake. This was displayed to be partially true as supplementation with betaine glycine restoring *mre/mrd* mutant BVG- plate viability, suggesting osmotic instability to play a factor on BVG- plate induced *mre/mrd* mutant death. However, this does not appear to be the sole mechanism of tolerance induced during broth culture growth as *mreB* mutants displayed no loss of viability in broth upon the knockout of this betaine uptake system. The future directions of this work would proceed in two directions. Firstly, it would be interesting to probe other potential mechanisms of tolerance induced upon broth growth such as capsule biosynthesis. Secondly it would be interesting to determine whether betaine supplementation facilitates tolerance of *mre/mrd* knockout in other gram-negative bacterial species and whether these strains display a hypervesiculating phenotype. This study would have relevance to the development of OMV based vaccines against other gram-negative bacteria.

Utilising comparative transcriptomic analysis of wildtype and BP_{536}*ΔmreC* gene expression during BVG+ broth growth we observed that there was remarkably little difference between their transcriptomes, suggesting that mutation of *mreC* is inherently tolerated in *B. pertussis* without the induction of stress response related to OM instability. It would be interesting to determine whether this is the case during BVG- broth growth or whether a transcriptomic alteration is required for tolerance.

<u>*B. pertussis* hypervesiculating mutants and their relevance to vaccine development-</u>

In this body of work, we have characterised the hypervesiculating phenotypes of strains in which the *mre/mrd* operon, or RpsA, was mutated. Analysis displayed that all strains had a

significant increase in OMV production, producing OMVs of an optimum size for immune cell uptake. Therefore, this body of work has verified two novel mechanisms for induction of a hypervesiculating phenotype in *B. pertussis* via mutagenesis of the *mre/mrd* operon, or truncation of *rpsA.* As antigen profiling of these OMVs was done by SDS page analysis it would be interesting in the future to directly identify and quantify the specific antigens present on OMVs utilising proteomic techniques. This investigation would be especially relevant to for the OMVs produced by the *rpsA* mutant strains, as transcriptomic analysis suggested increased expression of the flagellum biosynthesis pathway during culture. Whether this increased expression correlates to increased flagellar assembly on the bacterial OM is yet to be verified in *B. pertussis.* Once OMV antigenic profiles are determined it would be interesting to utilise OMVs produced by these mutant strains as vaccine components in animal challenge models to assess their efficacy.

Transcriptomic investigation of the mechanisms of OMV biogenesis induced by *rpsA* truncation. highlighted enrichment in capsule and flagellar biosynthesis pathways expression as potential inducers of OMV biogenesis. In the future it would be interesting to determine the contribution of these pathways to OMV biogenesis via the quantification of OMVs produced by wildtype *B. pertussis* upon the overexpression of capsule and flagellar biosynthesis. As RpsA is a ribosomal protein there is also potential for translational alterations being key in the induction of the hypervesiculating phenotype. Therefore, it would be valuable to analyse the proteome of the *rpsA* mutant strains to determine whether any proteomic changes occur upon *rpsA* truncation and whether these changes could alter OM stability and therefore induce OMV biogenesis.

7-References

ALEXANDER, C. & RIETSCHEL, E. T. 2001. Invited review: bacterial lipopolysaccharides and innate immunity. *Journal of endotoxin research,* 7**,** 167-202.

ALIPRANDI, P., SIZUN, C., PEREZ, J., MAREUIL, F., CAPUTO, S., LEROY, J.-L., ODAERT, B., LAALAMI, S., UZAN, M. & BONTEMS, F. 2008. S1 ribosomal protein functions in translation initiation and ribonuclease RegB activation are mediated by similar RNA-protein interactions: an NMR and SAXS analysis. *Journal of Biological Chemistry,* 283**,** 13289-13301.

ALLEN, A. & MASKELL, D. 1996. The identification, cloning and mutagenesis of a genetic locus required for lipopolysaccharide biosynthesis in Bordetella pertussis. *Molecular microbiology,* 19**,** 37-52.

ANDREASEN, C. & CARBONETTI, N. H. 2008. Pertussis toxin inhibits early chemokine production to delay neutrophil recruitment in response to Bordetella pertussis respiratory tract infection in mice. *Infection and immunity,* 76**,** 5139-5148.

ANDREASEN, C., POWELL, D. A. & CARBONETTI, N. H. 2009. Pertussis toxin stimulates IL-17 production in response to Bordetella pertussis infection in mice. *PLoS One,* 4**,** e7079.

ANGERT, E. R. 2005. Alternatives to binary fission in bacteria. *Nature Reviews Microbiology,* 3**,** 214-224.

APPLEBY, J. L., PARKINSON, J. S. & BOURRET, R. B. 1996. Signal transduction via the multi-step phosphorelay: not necessarily a road less traveled. *Cell,* 86**,** 845-848.

ARNAL, L., GRUNERT, T., CATTELAN, N., DE GOUW, D., VILLALBA, M. I., SERRA, D. O., MOOI, F. R., EHLING-SCHULZ, M. & YANTORNO, O. M. 2015. Bordetella pertussis isolates from argentinean whooping cough patients display enhanced biofilm formation capacity compared to Tohama I reference strain. *Frontiers in microbiology,* 6**,** 1352.

ASCHTGEN, M.-S., LYNCH, J. B., KOCH, E., SCHWARTZMAN, J., MCFALL-NGAI, M. & RUBY, E. 2016. Rotation of Vibrio fischeri flagella produces outer membrane vesicles that induce host development. *Journal of bacteriology,* 198**,** 2156-2165.

BARTON, B., GRINNELL, A. & MORGENSTEIN, R. M. 2021. Disruption of the MreB elongasome is overcome by mutations in the tricarboxylic acid cycle. *Frontiers in microbiology,* 12**,** 664281.

BASLER, M., MASIN, J., OSICKA, R. & SEBO, P. 2006. Pore-forming and enzymatic activities of Bordetella pertussis adenylate cyclase toxin synergize in promoting lysis of monocytes. *Infect Immun,* 74**,** 2207-14.

BECK, T. C., GOMES, A. C., CYSTER, J. G. & PEREIRA, J. P. 2014. CXCR4 and a cell-extrinsic mechanism control immature B lymphocyte egress from bone marrow. *J Exp Med,* 211**,** 2567-81.

BELCHER, T., MACARTHUR, I., KING, J. D., LANGRIDGE, G. C., MAYHO, M., PARKHILL, J. & PRESTON, A. 2020. Fundamental differences in physiology of Bordetella pertussis dependent on the two-component system Bvg revealed by gene essentiality studies. *Microbial Genomics,* 6.

BENDEZÚ, F. O. & DE BOER, P. A. 2008. Conditional lethality, division defects, membrane involution, and endocytosis in mre and mrd shape mutants of Escherichia coli. *Journal of bacteriology,* 190**,** 1792-1811.

BENNE, N., VAN DUIJN, J., KUIPER, J., JISKOOT, W. & SLÜTTER, B. 2016. Orchestrating immune responses: How size, shape and rigidity affect the immunogenicity of particulate vaccines. *Journal of Controlled Release,* 234**,** 124-134.

BERNADAC, A., GAVIOLI, M., LAZZARONI, J.-C., RAINA, S. & LLOUBÈS, R. 1998. Escherichia coli tol-pal mutants form outer membrane vesicles. *Journal of bacteriology,* 180**,** 4872-4878.

BISSON-FILHO, A. W., HSU, Y.-P., SQUYRES, G. R., KURU, E., WU, F., JUKES, C., SUN, Y., DEKKER, C., HOLDEN, S. & VANNIEUWENHZE, M. S. 2017. Treadmilling by FtsZ filaments drives peptidoglycan synthesis and bacterial cell division. *Science,* 355**,** 739-743.

BONE, M. A., WILK, A. J., PERAULT, A. I., MARLATT, S. A., SCHELLER, E. V., ANTHOUARD, R., CHEN, Q., STIBITZ, S., COTTER, P. A. & JULIO, S. M. 2017. Bordetella PlrSR regulatory system controls BvgAS activity and virulence in the lower respiratory tract. *Proceedings of the National Academy of Sciences,* 114**,** E1519-E1527.

BORDET, J. & GENGOU, O. 1906. Le microbe de la coqueluche. *Bulletin de l'Académie royale de médecine de Belgique*.
BORKNER, L., CURHAM, L. M., WILK, M. M., MORAN, B. & MILLS, K. H. 2021. IL-17 mediates protective immunity against nasal infection with Bordetella pertussis by mobilizing neutrophils, especially Siglec-F+ neutrophils. *Mucosal immunology,* 14**,** 1183-1202.
BOULANGER, A., CHEN, Q., HINTON, D. M. & STIBITZ, S. 2013. In vivo phosphorylation dynamics of the B ordetella pertussis virulence-controlling response regulator BvgA. *Molecular microbiology,* 88**,** 156-172.
BRAUN, V. 1975. Covalent lipoprotein from the outer membrane of Escherichia coli. *Biochimica et Biophysica Acta (BBA)-Reviews on Biomembranes,* 415**,** 335-377.
BRAY, N. L., PIMENTEL, H., MELSTED, P. & PACHTER, L. 2016. Near-optimal probabilistic RNA-seq quantification. *Nature biotechnology,* 34**,** 525-527.
BRUMMELMAN, J., WILK, M. M., HAN, W. G., VAN ELS, C. A. & MILLS, K. H. 2015. Roads to the development of improved pertussis vaccines paved by immunology. *Pathogens and disease,* 73.
CARBONETTI, N. H., ARTAMONOVA, G. V., VAN ROOIJEN, N. & AYALA, V. I. 2007. Pertussis toxin targets airway macrophages to promote Bordetella pertussis infection of the respiratory tract. *Infection and immunity,* 75**,** 1713-1720.
CARPENTER, T. S., PARKIN, J. & KHALID, S. 2016. The free energy of small solute permeation through the Escherichia coli outer membrane has a distinctly asymmetric profile. *The journal of physical chemistry letters,* 7**,** 3446-3451.
CARVER, T., HARRIS, S. R., BERRIMAN, M., PARKHILL, J. & MCQUILLAN, J. A. 2012. Artemis: an integrated platform for visualization and analysis of high-throughput sequence-based experimental data. *Bioinformatics,* 28**,** 464-469.
CASCALES, E., BERNADAC, A., GAVIOLI, M., LAZZARONI, J.-C. & LLOUBES, R. 2002. Pal lipoprotein of Escherichia coli plays a major role in outer membrane integrity. *Journal of bacteriology,* 184**,** 754-759.
CATTELAN, N., DUBEY, P., ARNAL, L., YANTORNO, O. M. & DEORA, R. 2016a. Bordetella biofilms: a lifestyle leading to persistent infections. *FEMS Pathogens and Disease,* 74**,** ftv108.
CATTELAN, N., JENNINGS-GEE, J., DUBEY, P., YANTORNO, O. M. & DEORA, R. 2017. Hyperbiofilm formation by Bordetella pertussis strains correlates with enhanced virulence traits. *Infection and Immunity,* 85**,** e00373-17.
CATTELAN, N., VILLALBA, M. I., PARISI, G., ARNAL, L., SERRA, D. O., AGUILAR, M. & YANTORNO, O. 2016b. Outer membrane protein OmpQ of Bordetella bronchiseptica is required for mature biofilm formation. *Microbiology,* 162**,** 351-363.
CDC 2012. Epidemiology and prevention of vaccine-preventable ciseases In: CDC (Hrsg). The Pink Book: Course Textbook. *Public Health Foundation. S***,** 139-150.
CDC. 2019. *Pertussis | Surveillance Trend Reporting and Case Definition | CDC* [Online]. [Accessed 05.01.2023].
CERNY, O., KAMANOVA, J., MASIN, J., BIBOVA, I., SKOPOVA, K. & SEBO, P. 2015. Bordetella pertussis Adenylate Cyclase Toxin Blocks Induction of Bactericidal Nitric Oxide in Macrophages through cAMP-Dependent Activation of the SHP-1 Phosphatase. *J Immunol,* 194**,** 4901-13.
CHEN, Y. & ERICKSON, H. P. 2005. Rapid in vitro assembly dynamics and subunit turnover of FtsZ demonstrated by fluorescence resonance energy transfer. *Journal of Biological Chemistry,* 280**,** 22549-22554.
CHEN, Z., ZHANG, J., CAO, L., ZHANG, N., ZHU, J., PING, G., ZHAO, J., LI, S. & HE, Q. 2016. Seroprevalence of pertussis among adults in China where whole cell vaccines have been used for 50 years. *Journal of Infection,* 73**,** 38-44.
CHERRY, J. D. 1999. Pertussis in the Preantibiotic and Prevaccine Era, with Emphasis on Adult Pertussis. *Clinical Infectious Diseases,* 28**,** S107-S111.

CHERRY, J. D. 2015. The history of pertussis (whooping cough); 1906–2015: facts, myths, and misconceptions. *Current Epidemiology Reports,* 2**,** 120-130.
CHERRY, J. D., BRUNELL, P. A., GOLDEN, G. S. & KARZON, D. T. 1988. Report of the task force on pertussis and pertussis immunization—1988. *Pediatrics,* 81**,** 933-984.
CHIANG, S. L. & MEKALANOS, J. J. 1998. Use of signature-tagged transposon mutagenesis to identify Vibrio cholerae genes critical for colonization. *Molecular microbiology,* 27**,** 797-805.
CHUNG, D. R., KASPER, D. L., PANZO, R. J., CHTINIS, T., GRUSBY, M. J., SAYEGH, M. H. & TZIANABOS, A. O. 2003. CD4+ T cells mediate abscess formation in intra-abdominal sepsis by an IL-17-dependent mechanism. *The Journal of Immunology,* 170**,** 1958-1963.
COLAVIN, A., SHI, H. & HUANG, K. C. 2018. RodZ modulates geometric localization of the bacterial actin MreB to regulate cell shape. *Nature communications,* 9**,** 1-11.
CONNELLY, C. E., SUN, Y. & CARBONETTI, N. H. 2012. Pertussis toxin exacerbates and prolongs airway inflammatory responses during Bordetella pertussis infection. *Infect Immun,* 80**,** 4317-32.
COOKSON, B. T., TYLER, A. N. & GOLDMAN, W. E. 1989. Primary structure of the peptidoglycan-derived tracheal cytotoxin of Bordetella pertussis. *Biochemistry,* 28**,** 1744-1749.
COTTER, P. & MILLER, J. 2001. Bordetella, p 619–674. *Principles of bacterial pathogenesis. Academic Press, San Diego, CA*.
COTTER, P. A. & MILLER, J. F. 1994. BvgAS-mediated signal transduction: analysis of phase-locked regulatory mutants of Bordetella bronchiseptica in a rabbit model. *Infection and immunity,* 62**,** 3381-3390.
COUTTE, L., ANTOINE, R., DROBECQ, H., LOCHT, C. & JACOB-DUBUISSON, F. 2001. Subtilisin-like autotransporter serves as maturation protease in a bacterial secretion pathway. *The EMBO journal,* 20**,** 5040-5048.
CUMMINGS, C., BOOTSMA, H., RELMAN, D. & MILLER, J. 2006. Species-and strain-specific control of a complex, flexible regulon by Bordetella BvgAS. *Journal of bacteriology,* 188**,** 1775-1785.
DE BOER, P., CROSSLEY, R. & ROTHFIELD, L. 1992. The essential bacterial cell-division protein FtsZ is a GTPase. *Nature,* 359**,** 254-256.
DE GREEFF, S. C., MOOI, F. R., WESTERHOF, A., VERBAKEL, J., PEETERS, M. F., HEUVELMAN, C., NOTERMANS, D. W., ELVERS, L., SCHELLEKENS, J. F. & DE MELKER, H. E. 2010. Pertussis disease burden in the household: how to protect young infants. *Clinical infectious diseases,* 50**,** 1339-1345.
DE JONGE, E. F., VAN BOXTEL, R., BALHUIZEN, M. D., HAAGSMAN, H. P. & TOMMASSEN, J. 2022a. Pal depletion results in hypervesiculation and affects cell morphology and outer-membrane lipid asymmetry in bordetellae. *Research in Microbiology,* 173**,** 103937.
DE JONGE, E. F., VOGRINEC, L., VAN BOXTEL, R. & TOMMASSEN, J. 2022b. Inactivation of the Mla system and outer-membrane phospholipase A results in disrupted outer-membrane lipid asymmetry and hypervesiculation in Bordetella pertussis. *Current Research in Microbial Sciences,* 3**,** 100172.
DEME, J. C., JOHNSON, S., VICKERY, O., ARON, A., MONKHOUSE, H., GRIFFITHS, T., JAMES, R. H., BERKS, B. C., COULTON, J. W., STANSFELD, P. J. & LEA, S. M. 2020. Structures of the stator complex that drives rotation of the bacterial flagellum. *Nature Microbiology,* 5**,** 1553-1564.
DEN BLAAUWEN, T., AARSMAN, M. E., VISCHER, N. O. & NANNINGA, N. 2003. Penicillin-binding protein PBP2 of Escherichia coli localizes preferentially in the lateral wall and at mid-cell in comparison with the old cell pole. *Molecular microbiology,* 47**,** 539-547.
DEN BLAAUWEN, T., DE PEDRO, M. A., NGUYEN-DISTECHE, M. & AYALA, J. A. 2008. Morphogenesis of rod-shaped sacculi. *FEMS microbiology reviews,* 32**,** 321-344.
DEN HARTOG, G., SCHIJF, M. A., BERBERS, G. A., VAN DER KLIS, F. R. & BUISMAN, A.-M. 2022. Bordetella pertussis induces interferon gamma production by natural killer cells, resulting in chemoattraction by respiratory epithelial cells. *The Journal of Infectious Diseases,* 225**,** 1248-1260.

DENOME, S. A., ELF, P. K., HENDERSON, T. A., NELSON, D. E. & YOUNG, K. D. 1999. Escherichia coli mutants lacking all possible combinations of eight penicillin binding proteins: viability, characteristics, and implications for peptidoglycan synthesis. *Journal of bacteriology,* 181**,** 3981-3993.

DEPIENNE, C., TROUILLARD, O., SAINT-MARTIN, C., GOURFINKEL-AN, I., BOUTEILLER, D., CARPENTIER, W., KEREN, B., ABERT, B., GAUTIER, A. & BAULAC, S. 2009. Spectrum of SCN1A gene mutations associated with Dravet syndrome: analysis of 333 patients. *Journal of medical genetics,* 46**,** 183-191.

DINNBIER, U., LIMPINSEL, E., SCHMID, R. & BAKKER, E. P. 1988. Transient accumulation of potassium glutamate and its replacement by trehalose during adaptation of growing cells of Escherichia coli K-12 to elevated sodium chloride concentrations. *Archives of Microbiology,* 150**,** 348-357.

DUPRE, E., HERROU, J., LENSINK, M. F., WINTJENS, R., VAGIN, A., LEBEDEV, A., CROSSON, S., VILLERET, V., LOCHT, C. & ANTOINE, R. 2015. Virulence regulation with Venus flytrap domains: structure and function of the periplasmic moiety of the sensor-kinase BvgS. *PLoS pathogens,* 11**,** e1004700.

EBY, J. C., GRAY, M. C. & HEWLETT, E. L. 2014. Cyclic AMP-mediated suppression of neutrophil extracellular trap formation and apoptosis by the Bordetella pertussis adenylate cyclase toxin. *Infection and immunity,* 82**,** 5256-5269.

EGAN, A. J., ERRINGTON, J. & VOLLMER, W. 2020. Regulation of peptidoglycan synthesis and remodelling. *Nature Reviews Microbiology,* 18**,** 446-460.

EL-AZAMI-EL-IDRISSI, M., BAUCHE, C., LOUCKA, J., OSICKA, R., SEBO, P., LADANT, D. & LECLERC, C. 2003. Interaction of Bordetella pertussis adenylate cyclase with CD11b/CD18: role of toxin acylation and identification of the main integrin interaction domain. *Journal of Biological Chemistry,* 278**,** 38514-38521.

EL BAYÂ, A., BRÜCKENER, K. & SCHMIDT, M. A. 1999. Nonrestricted differential intoxication of cells by pertussis toxin. *Infection and immunity,* 67**,** 433-435.

EMSLEY, P., MCDERMOTT, G., CHARLES, I. G., FAIRWEATHER, N. F. & ISAACS, N. W. 1994. Crystallographic characterization of pertactin, a membrane-associated protein from Bordetella pertussis. *Journal of molecular biology,* 235**,** 772-773.

ENGLER, C., KANDZIA, R. & MARILLONNET, S. 2008. A one pot, one step, precision cloning method with high throughput capability. *PloS one,* 3**,** e3647.

EPSTEIN-BARASH, H., GUTMAN, D., MARKOVSKY, E., MISHAN-EISENBERG, G., KOROUKHOV, N., SZEBENI, J. & GOLOMB, G. 2010. Physicochemical parameters affecting liposomal bisphosphonates bioactivity for restenosis therapy: internalization, cell inhibition, activation of cytokines and complement, and mechanism of cell death. *Journal of controlled release,* 146**,** 182-195.

EPSTEIN, W. 1986. Osmoregulation by potassium transport in Escherichia coli. *FEMS microbiology reviews,* 2**,** 73-78.

FERNANDEZ, R. C. & WEISS, A. A. 1994. Cloning and sequencing of a Bordetella pertussis serum resistance locus. *Infection and Immunity,* 62**,** 4727-4738.

FINNE, J., LEINONEN, M. & MÄKELÄ, P. H. 1983. Antigenic similarities between brain components and bacteria causing meningitis: implications for vaccine development and pathogenesis. *The Lancet,* 322**,** 355-357.

FISER, R., MASIN, J., BUMBA, L., POSPISILOVA, E., FAYOLLE, C., BASLER, M., SADILKOVA, L., ADKINS, I., KAMANOVA, J., CERNY, J., KONOPASEK, I., OSICKA, R., LECLERC, C. & SEBO, P. 2012. Calcium influx rescues adenylate cyclase-hemolysin from rapid cell membrane removal and enables phagocyte permeabilization by toxin pores. *PLoS Pathog,* 8**,** e1002580.

GAMBA, P., VEENING, J.-W., SAUNDERS, N. J., HAMOEN, L. W. & DANIEL, R. A. 2009. Two-step assembly dynamics of the Bacillus subtilis divisome. *Journal of bacteriology,* 191**,** 4186-4194.

GARDE, S., CHODISETTI, P. K. & REDDY, M. 2021. Peptidoglycan: Structure, synthesis, and regulation. *EcoSal Plus,* 9.

GEUIJEN, C., WILLEMS, R., BONGAERTS, M., TOP, J., GIELEN, H. & MOOI, F. R. 1997. Role of the Bordetella pertussis minor fimbrial subunit, FimD, in colonization of the mouse respiratory tract. *Infection and immunity,* 65**,** 4222-4228.

GLASER, P., ELMAOGLOU-LAZARIDOU, A., KRIN, E., LADANT, D., BARZU, O. & DANCHIN, A. 1989. Identification of residues essential for catalysis and binding of calmodulin in Bordetella pertussis adenylate cyclase by site-directed mutagenesis. *The EMBO Journal,* 8**,** 967-972.

GLAUERT, A. M. & THORNLEY, M. J. 1969. The topography of the bacterial cell wall. *Annual review of microbiology,* 23**,** 159-198.

GRAF, R., CODINA, J. & BIRNBAUMER, L. 1992. Peptide inhibitors of ADP-ribosylation by pertussis toxin are substrates with affinities comparable to those of the trimeric GTP-binding proteins. *Molecular pharmacology,* 42**,** 760-764.

GROSS, R. 1993. Signal transduction and virulence regulation in human and animal pathogens. *FEMS microbiology reviews,* 10**,** 301-326.

GUERMONPREZ, P., KHELEF, N., BLOUIN, E., RIEU, P., RICCIARDI-CASTAGNOLI, P., GUISO, N., LADANT, D. & LECLERC, C. 2001. The adenylate cyclase toxin of Bordetella pertussis binds to target cells via the αMβ2 integrin (CD11b/CD18). *The Journal of experimental medicine,* 193**,** 1035-1044.

GUSTAFSSON, L., HESSEL, L., STORSAETER, J. & OLIN, P. 2006. Long-term follow-up of Swedish children vaccinated with acellular pertussis vaccines at 3, 5, and 12 months of age indicates the need for a booster dose at 5 to 7 years of age. *Pediatrics,* 118**,** 978-984.

HAJAM, I. A., DAR, P. A., SHAHNAWAZ, I., JAUME, J. C. & LEE, J. H. 2017. Bacterial flagellin—a potent immunomodulatory agent. *Experimental & molecular medicine,* 49**,** e373-e373.

HAMIDOU SOUMANA, I., LINZ, B. & HARVILL, E. T. 2017. Environmental origin of the genus Bordetella. *Frontiers in microbiology,* 8**,** 28.

HARDY-FAIRBANKS, A. J., PAN, S. J., DECKER, M. D., JOHNSON, D. R., GREENBERG, D. P., KIRKLAND, K. B., TALBOT, E. A. & BERNSTEIN, H. H. 2013. Immune responses in infants whose mothers received Tdap vaccine during pregnancy. *The Pediatric infectious disease journal,* 32**,** 1257-1260.

HEIJENOORT, J. V. 2001. Formation of the glycan chains in the synthesis of bacterial peptidoglycan. *Glycobiology,* 11**,** 25R-36R.

HIGGINS, S. C., JARNICKI, A. G., LAVELLE, E. C. & MILLS, K. H. 2006. TLR4 mediates vaccine-induced protective cellular immunity to Bordetella pertussis: role of IL-17-producing T cells. *The Journal of Immunology,* 177**,** 7980-7989.

HINDS, P. W., 2ND, YIN, C., SALVATO, M. S. & PAUZA, C. D. 1996. Pertussis toxin induces lymphocytosis in rhesus macaques. *J Med Primatol,* 25**,** 375-81.

HIRANO, T., MINAMINO, T. & MACNAB, R. M. 2001. The role in flagellar rod assembly of the N-terminal domain of Salmonella FlgJ, a flagellum-specific muramidase. *J Mol Biol,* 312**,** 359-69.

HODGE, G., HODGE, S., MARKUS, C., LAWRENCE, A. & HAN, P. 2003. A marked decrease in L-selectin expression by leucocytes in infants with Bordetella pertussis infection: leucocytosis explained? *Respirology,* 8**,** 157-62.

HOFFMAN, C. L., GONYAR, L. A., ZACCA, F., SISTI, F., FERNANDEZ, J., WONG, T., DAMRON, F. H. & HEWLETT, E. L. 2019. Bordetella pertussis can be motile and express flagellum-like structures. *MBio,* 10**,** e00787-19.

HOO, R., LAM, J. H., HUOT, L., PANT, A., LI, R., HOT, D. & ALONSO, S. 2014. Evidence for a role of the polysaccharide capsule transport proteins in pertussis pathogenesis. *PLoS One,* 9**,** e115243.

HOT, D., ANTOINE, R., RENAULD-MONGENIE, G., CARO, V., HENNUY, B., LEVILLAIN, E., HUOT, L., WITTMANN, G., PONCET, D. & JACOB-DUBUISSON, F. 2003. Differential modulation of Bordetella pertussis virulence genes as evidenced by DNA microarray analysis. *Molecular Genetics and Genomics,* 269**,** 475-486.

HUANG, Y., CHING, G. & INOUYE, M. 1983. Comparison of the lipoprotein gene among the enterobacteriaceae. DNA sequence of Morganella morganii lipoprotein gene and its expression in Escherichia coli. *Journal of Biological Chemistry,* 258**,** 8139-8145.
HUERTA-CEPAS, J., SZKLARCZYK, D., HELLER, D., HERNÁNDEZ-PLAZA, A., FORSLUND, S. K., COOK, H., MENDE, D. R., LETUNIC, I., RATTEI, T. & JENSEN, L. J. 2019. eggNOG 5.0: a hierarchical, functionally and phylogenetically annotated orthology resource based on 5090 organisms and 2502 viruses. *Nucleic acids research,* 47**,** D309-D314.
IIJIMA, N. & IWASAKI, A. 2014. A local macrophage chemokine network sustains protective tissue-resident memory CD4 T cells. *Science,* 346**,** 93-98.
IRIE, Y., MATTOO, S. & YUK, M. H. 2004. The Bvg virulence control system regulates biofilm formation in Bordetella bronchiseptica. *Journal of bacteriology,* 186**,** 5692-5698.
ISHIBASHI, Y., CLAUS, S. & RELMAN, D. A. 1994. Bordetella pertussis filamentous hemagglutinin interacts with a leukocyte signal transduction complex and stimulates bacterial adherence to monocyte CR3 (CD11b/CD18). *The Journal of experimental medicine,* 180**,** 1225-1233.
ISHIBASHI, Y. & NISHIKAWA, A. 2002. Bordetella pertussis infection of human respiratory epithelial cells up-regulates intercellular adhesion molecule-1 expression: role of filamentous hemagglutinin and pertussis toxin. *Microbial pathogenesis,* 33**,** 115-125.
ISHIBASHI, Y., YOSHIMURA, K., NISHIKAWA, A., CLAUS, S., LAUDANNA, C. & RELMAN, D. A. 2002. Role of phosphatidylinositol 3-kinase in the binding of Bordetella pertussis to human monocytes. *Cellular Microbiology,* 4**,** 825-833.
JADHAV, S. & GAIROLA, S. 1999. Composition of acellular pertussis and combination vaccines: a general review. *Biologicals,* 27**,** 105-110.
KAMANOVA, J., KOFRONOVA, O., MASIN, J., GENTH, H., VOJTOVA, J., LINHARTOVA, I., BENADA, O., JUST, I. & SEBO, P. 2008. Adenylate cyclase toxin subverts phagocyte function by RhoA inhibition and unproductive ruffling. *The Journal of Immunology,* 181**,** 5587-5597.
KAO, C.-Y., CHEN, Y., THAI, P., WACHI, S., HUANG, F., KIM, C., HARPER, R. W. & WU, R. 2004. IL-17 markedly up-regulates β-defensin-2 expression in human airway epithelium via JAK and NF-κB signaling pathways. *The Journal of Immunology,* 173**,** 3482-3491.
KARATAEV, G., SINYASHINA, L., MEDKOVA, A. Y., SEMIN, E., SHEVTSOVA, Z., MATUA, A., KONDZARIYA, I., AMICHBA, A., KUBRAVA, D. & MIKVABIA, Z. Y. 2016. Insertional inactivation of virulence operon in population of persistent Bordetella pertussis bacteria. *Russian journal of genetics,* 52**,** 370-377.
KATADA, T. 2012. The inhibitory G protein Gi identified as pertussis toxin-catalyzed ADP-ribosylation. *Biological and Pharmaceutical Bulletin,* 35**,** 2103-2111.
KAWAZURA, T., MATSUMOTO, K., KOJIMA, K., KATO, F., KANAI, T., NIKI, H. & SHIOMI, D. 2017. Exclusion of assembled M re B by anionic phospholipids at cell poles confers cell polarity for bidirectional growth. *Molecular microbiology,* 104**,** 472-486.
KENT, A., LADHANI, S. N., ANDREWS, N. J., MATHESON, M., ENGLAND, A., MILLER, E., HEATH, P. T. & GROUP, P. S. 2016. Pertussis antibody concentrations in infants born prematurely to mothers vaccinated in pregnancy. *Pediatrics,* 138.
KILGORE, P. E., SALIM, A. M., ZERVOS, M. J. & SCHMITT, H.-J. 2016. Pertussis: microbiology, disease, treatment, and prevention. *Clinical microbiology reviews,* 29**,** 449-486.
KIRIMANJESWARA, G. S., AGOSTO, L. M., KENNETT, M. J., BJORNSTAD, O. N. & HARVILL, E. T. 2005. Pertussis toxin inhibits neutrophil recruitment to delay antibody-mediated clearance of Bordetella pertussis. *The Journal of clinical investigation,* 115**,** 3594-3601.
KOBAYASHI, K., EHRLICH, S. D., ALBERTINI, A., AMATI, G., ANDERSEN, K., ARNAUD, M., ASAI, K., ASHIKAGA, S., AYMERICH, S. & BESSIERES, P. 2003. Essential Bacillus subtilis genes. *Proceedings of the National Academy of Sciences,* 100**,** 4678-4683.
KOTNIK, M., ANDERLUH, P. S. & PREZELJ, A. 2007. Development of novel inhibitors targeting intracellular steps of peptidoglycan biosynthesis. *Current pharmaceutical design,* 13**,** 2283-2309.

KOTOB, S. I., HAUSMAN, S. Z. & BURNS, D. L. 1995. Localization of the promoter for the ptl genes of Bordetella pertussis, which encode proteins essential for secretion of pertussis toxin. *Infection and immunity,* 63**,** 3227-3230.

KRUSE, T., MØLLER-JENSEN, J., LØBNER-OLESEN, A. & GERDES, K. 2003. Dysfunctional MreB inhibits chromosome segregation in Escherichia coli. *The EMBO journal,* 22**,** 5283-5292.

KUCHAR, E., KARLIKOWSKA-SKWARNIK, M., HAN, S. & NITSCH-OSUCH, A. 2016. Pertussis: history of the disease and current prevention failure. *Pulmonary dysfunction and disease***,** 77-82.

LADANT, D., MICHELSON, S., SARFATI, R., GILLES, A., PREDELEANU, R. & BARZU, O. 1989. Characterization of the calmodulin-binding and of the catalytic domains of Bordetella pertussis adenylate cyclase. *Journal of Biological Chemistry,* 264**,** 4015-4020.

LEE, J.-C. & STEWART, G. C. 2003. Essential nature of the mreC determinant of Bacillus subtilis. *Journal of bacteriology,* 185**,** 4490-4498.

LEININGER, E., ROBERTS, M., KENIMER, J. G., CHARLES, I. G., FAIRWEATHER, N., NOVOTNY, P. & BRENNAN, M. J. 1991. Pertactin, an Arg-Gly-Asp-containing Bordetella pertussis surface protein that promotes adherence of mammalian cells. *Proceedings of the National Academy of Sciences,* 88**,** 345-349.

LESLIE, P. & GARDNER, A. 1931. The phases of Haemophilus pertussis. *Epidemiology & Infection,* 31**,** 423-434.

LESNE, E., CAVELL, B. E., FREIRE-MARTIN, I., PERSAUD, R., ALEXANDER, F., TAYLOR, S., MATHESON, M., VAN ELS, C. A. & GORRINGE, A. 2020. Acellular pertussis vaccines induce anti-pertactin bactericidal antibodies which drives the emergence of pertactin-negative strains. *Frontiers in microbiology,* 11**,** 2108.

LIANG, J. L., TIWARI, T., MORO, P., MESSONNIER, N. E., REINGOLD, A., SAWYER, M. & CLARK, T. A. 2018. Prevention of pertussis, tetanus, and diphtheria with vaccines in the United States: recommendations of the Advisory Committee on Immunization Practices (ACIP). *MMWR Recommendations and Reports,* 67**,** 1.

LOCHT, C., COUTTE, L. & MIELCAREK, N. 2011. The ins and outs of pertussis toxin. *The FEBS journal,* 278**,** 4668-4682.

LOVE, M. I., HUBER, W. & ANDERS, S. 2014. Moderated estimation of fold change and dispersion for RNA-seq data with DESeq2. *Genome biology,* 15**,** 1-21.

MA, X., EHRHARDT, D. W. & MARGOLIN, W. 1996. Colocalization of cell division proteins FtsZ and FtsA to cytoskeletal structures in living Escherichia coli cells by using green fluorescent protein. *Proceedings of the National Academy of Sciences,* 93**,** 12998-13003.

MA, X., SUN, Q., WANG, R., SINGH, G., JONIETZ, E. L. & MARGOLIN, W. 1997. Interactions between heterologous FtsA and FtsZ proteins at the FtsZ ring. *Journal of bacteriology,* 179**,** 6788-6797.

MACNAB, R. M. 2003. How bacteria assemble flagella. *Annual Reviews in Microbiology,* 57**,** 77-100.

MADSEN, T. 1933. Vaccination against whooping cough. *Journal of the American Medical Association,* 101**,** 187-188.

MAGALHAES, J. G., PHILPOTT, D. J., NAHORI, M. A., JÉHANNO, M., FRITZ, J., BOURHIS LE, L., VIALA, J., HUGOT, J. P., GIOVANNINI, M. & BERTIN, J. 2005. Murine Nod1 but not its human orthologue mediates innate immune detection of tracheal cytotoxin. *EMBO reports,* 6**,** 1201-1207.

MAHON, B. P., SHEAHAN, B. J., GRIFFIN, F., MURPHY, G. & MILLS, K. H. 1997. Atypical disease after Bordetella pertussis respiratory infection of mice with targeted disruptions of interferon-γ receptor or immunoglobulin μ chain genes. *The Journal of experimental medicine,* 186**,** 1843-1851.

MALINVERNI, J. C. & SILHAVY, T. J. 2009. An ABC transport system that maintains lipid asymmetry in the gram-negative outer membrane. *Proceedings of the National Academy of Sciences,* 106**,** 8009-8014.

MANABE, T., KATO, M., UENO, T. & KAWASAKI, K. 2013. Flagella proteins contribute to the production of outer membrane vesicles from Escherichia coli W3110. *Biochemical and biophysical research communications,* 441**,** 151-156.
MANGMOOL, S. & KUROSE, H. 2011. Gi/o protein-dependent and-independent actions of pertussis toxin (PTX). *Toxins,* 3**,** 884-899.
MARTIN, S. W., PAWLOSKI, L., WILLIAMS, M., WEENING, K., DEBOLT, C., QIN, X., REYNOLDS, L., KENYON, C., GIAMBRONE, G. & KUDISH, K. 2015. Pertactin-negative Bordetella pertussis strains: evidence for a possible selective advantage. *Clinical Infectious Diseases,* 60**,** 223-227.
MARTINEZ DE TEJADA, G., COTTER, P. A., HEININGER, U., CAMILLI, A., AKERLEY, B. J., MEKALANOS, J. J. & MILLER, J. F. 1998. Neither the Bvg− phase nor the vrg6 locus of Bordetella pertussis is required for respiratory infection in mice. *Infection and immunity,* 66**,** 2762-2768.
MASCART, F., HAINAUT, M., PELTIER, A., VERSCHEURE, V., LEVY, J. & LOCHT, C. 2007. Modulation of the infant immune responses by the first pertussis vaccine administrations. *Vaccine,* 25**,** 391-398.
MASHBURN-WARREN, L., HOWE, J., GARIDEL, P., RICHTER, W., STEINIGER, F., ROESSLE, M., BRANDENBURG, K. & WHITELEY, M. 2008. Interaction of quorum signals with outer membrane lipids: insights into prokaryotic membrane vesicle formation. *Molecular microbiology,* 69**,** 491-502.
MASHBURN-WARREN, L. M. & WHITELEY, M. 2006. Special delivery: vesicle trafficking in prokaryotes. *Molecular microbiology,* 61**,** 839-846.
MATTOO, S. & CHERRY, J. D. 2005. Molecular pathogenesis, epidemiology, and clinical manifestations of respiratory infections due to Bordetella pertussis and other Bordetella subspecies. *Clinical microbiology reviews,* 18**,** 326-382.
MATTOO, S., FOREMAN-WYKERT, A. K., COTTER, P. A. & MILLER, J. F. 2001. Mechanisms of Bordetella pathogenesis. *Frontiers in Bioscience-Landmark,* 6**,** 168-186.
MAZAR, J. & COTTER, P. A. 2006. Topology and maturation of filamentous haemagglutinin suggest a new model for two-partner secretion. *Molecular microbiology,* 62**,** 641-654.
MAZURKIEWICZ, P., TANG, C. M., BOONE, C. & HOLDEN, D. W. 2006. Signature-tagged mutagenesis: barcoding mutants for genome-wide screens. *Nature Reviews Genetics,* 7**,** 929-939.
MCBROOM, A. J., JOHNSON, A. P., VEMULAPALLI, S. & KUEHN, M. J. 2006. Outer membrane vesicle production by Escherichia coli is independent of membrane instability. *Journal of bacteriology,* 188**,** 5385-5392.
MCBROOM, A. J. & KUEHN, M. J. 2007. Release of outer membrane vesicles by Gram-negative bacteria is a novel envelope stress response. *Molecular microbiology,* 63**,** 545-558.
MEBERG, B. M., SAILER, F. C., NELSON, D. E. & YOUNG, K. D. 2001. Reconstruction of Escherichia coli mrcA (PBP 1a) mutants lacking multiple combinations of penicillin binding proteins. *Journal of Bacteriology,* 183**,** 6148-6149.
MEI, J. M., NOURBAKHSH, F., FORD, C. W. & HOLDEN, D. W. 1997. Identification of Staphylococcus aureus virulence genes in a murine model of bacteraemia using signature-tagged mutagenesis. *Molecular microbiology,* 26**,** 399-407.
MENGIN-LECREULX, D. & LEMAITRE, B. 2005. Structure and metabolism of peptidoglycan and molecular requirements allowing its detection by the Drosophila innate immune system. *Journal of endotoxin research,* 11**,** 105-111.
MIELCAREK, N., DEBRIE, A. S., RAZE, D., BERTOUT, J., ROUANET, C., YOUNES, A. B., CREUSY, C., ENGLE, J., GOLDMAN, W. E. & LOCHT, C. 2006. Live attenuated B. pertussis as a single-dose nasal vaccine against whooping cough. *PLoS Pathog,* 2**,** e65.
MILLS, K., BARNARD, A., WATKINS, J. & REDHEAD, K. 1993. Cell-mediated immunity to Bordetella pertussis: role of Th1 cells in bacterial clearance in a murine respiratory infection model. *Infection and immunity,* 61**,** 399-410.

MISIAK, A., WILK, M. M., RAVERDEAU, M. & MILLS, K. H. 2017. IL-17–Producing innate and pathogen-specific tissue resident memory γδ T cells expand in the lungs of Bordetella pertussis–infected mice. *The Journal of Immunology,* 198**,** 363-374.

MIURA, T. & MIZUSHIMA, S. 1968. Separation by density gradient centrifugation of two types of membranes from spheroplast membrane of Escherichia coli K12. *Biochimica et Biophysica Acta (BBA)-Biomembranes,* 150**,** 159-161.

MIYAMOTO, M., PRAUSE, O., SJÖSTRAND, M., LAAN, M., LÖTVALL, J. & LINDÉN, A. 2003. Endogenous IL-17 as a mediator of neutrophil recruitment caused by endotoxin exposure in mouse airways. *The Journal of Immunology,* 170**,** 4665-4672.

MIZEL, S. B. & BATES, J. T. 2010. Flagellin as an adjuvant: cellular mechanisms and potential. *The Journal of Immunology,* 185**,** 5677-5682.

MOON, K., BONOCORA, R. P., KIM, D. D., CHEN, Q., WADE, J. T., STIBITZ, S. & HINTON, D. M. 2017. The BvgAS regulon of Bordetella pertussis. *MBio,* 8**,** e01526-17.

MORALES, V. M., BÄCKMAN, A. & BAGDASARIAN, M. 1991. A series of wide-host-range low-copy-number vectors that allow direct screening for recombinants. *Gene,* 97**,** 39-47.

MORGENSTEIN, R. M., BRATTON, B. P., NGUYEN, J. P., OUZOUNOV, N., SHAEVITZ, J. W. & GITAI, Z. 2015. RodZ links MreB to cell wall synthesis to mediate MreB rotation and robust morphogenesis. *Proceedings of the National Academy of Sciences,* 112**,** 12510-12515.

MORGENSTEIN, R. M., BRATTON, B. P., SHAEVITZ, J. W. & GITAI, Z. 2017. RodZ promotes MreB polymer formation and curvature localization to determine the cylindrical uniformity of E. coli shape. *bioRxiv***,** 226290.

MUELLER, S. N. & MACKAY, L. K. 2016. Tissue-resident memory T cells: local specialists in immune defence. *Nature Reviews Immunology,* 16**,** 79-89.

NANNINGA, N. 1998. Morphogenesis of Escherichia coli. *Microbiology and molecular biology reviews,* 62**,** 110-129.

NEO, Y., LI, R., HOWE, J., HOO, R., PANT, A., HO, S. & ALONSO, S. 2010. Evidence for an intact polysaccharide capsule in Bordetella pertussis. *Microbes and infection,* 12**,** 238-245.

NEUHAUS, F. C. & HAMMES, W. P. 1981. Inhibition of cell wall biosynthesis by analogues of alanine. *Pharmacology & therapeutics,* 14**,** 265-319.

NICHOLSON, T. L., CONOVER, M. S. & DEORA, R. 2012. Transcriptome profiling reveals stage-specific production and requirement of flagella during biofilm development in Bordetella bronchiseptica. *PLoS One,* 7**,** e49166.

NIKAIDO, H. 2003. Molecular basis of bacterial outer membrane permeability revisited. *Microbiology and molecular biology reviews,* 67**,** 593-656.

OSBORN, M., GANDER, J., PARISI, E. & CARSON, J. 1972. Mechanism of assembly of the outer membrane of Salmonella typhimurium: isolation and characterization of cytoplasmic and outer membrane. *Journal of Biological Chemistry,* 247**,** 3962-3972.

OSICKOVÁ, A., OSICKA, R., MAIER, E., BENZ, R. & SEBO, P. 1999. An amphipathic alpha-helix including glutamates 509 and 516 is crucial for membrane translocation of adenylate cyclase toxin and modulates formation and cation selectivity of its membrane channels. *J Biol Chem,* 274**,** 37644-50.

OUZOUNOV, N., NGUYEN, J. P., BRATTON, B. P., JACOBOWITZ, D., GITAI, Z. & SHAEVITZ, J. W. 2016. MreB orientation correlates with cell diameter in Escherichia coli. *Biophysical journal,* 111**,** 1035-1043.

PACCANI, S. R., MOLIN, F. D., BENAGIANO, M., LADANT, D., D'ELIOS, M. M., MONTECUCCO, C. & BALDARI, C. T. 2008. Suppression of T-lymphocyte activation and chemotaxis by the adenylate cyclase toxin of Bordetella pertussis. *Infection and immunity,* 76**,** 2822-2832.

PARK, J. T. 1993. Turnover and recycling of the murein sacculus in oligopeptide permease-negative strains of Escherichia coli: indirect evidence for an alternative permease system and for a monolayered sacculus. *Journal of bacteriology,* 175**,** 7-11.

PARKHILL, J., SEBAIHIA, M., PRESTON, A., MURPHY, L. D., THOMSON, N., HARRIS, D. E., HOLDEN, M. T., CHURCHER, C. M., BENTLEY, S. D. & MUNGALL, K. L. 2003. Comparative analysis of the genome sequences of Bordetella pertussis, Bordetella parapertussis and Bordetella bronchiseptica. *Nature genetics,* 35**,** 32-40.

PECK, A. & MELLINS, E. D. 2010. Precarious balance: Th17 cells in host defense. *Infection and immunity,* 78**,** 32-38.

PETERSEN, J. W., IBSEN, P. H., HASLØV, K. & HERON, I. 1992. Proliferative responses and gamma interferon and tumor necrosis factor production by lymphocytes isolated from tracheobroncheal lymph nodes and spleen of mice aerosol infected with Bordetella pertussis. *Infect Immun,* 60**,** 4563-70.

PETOUSIS-HARRIS, H. 2018. Impact of meningococcal group B OMV vaccines, beyond their brief. *Human vaccines & immunotherapeutics,* 14**,** 1058-1063.

PIZZA, M., COVACCI, A., BARTOLONI, A., PERUGINI, M., NENCIONI, L., DE MAGISTRIS, M. T., VILLA, L., NUCCI, D., MANETTI, R. & BUGNOLI, M. 1989. Mutants of pertussis toxin suitable for vaccine development. *Science,* 246**,** 497-500.

PLAUT, R. D., SCANLON, K. M., TAYLOR, M., TETER, K. & CARBONETTI, N. H. 2016. Intracellular disassembly and activity of pertussis toxin require interaction with ATP. *FEMS Pathogens and Disease,* 74**,** ftw065.

RASBAND, W. S. 2011. National Institutes of Health, Bethesda, Maryland, USA. *http://imagej. nih. gov/ij/*.

RELMAN, D., TUOMANEN, E., FALKOW, S., GOLENBOCK, D. T., SAUKKONEN, K. & WRIGHT, S. D. 1990. Recognition of a bacterial adhesin by an integrin: macrophage CR3 (αMβ2, CD11bCD18) binds filamentous hemagglutinin of Bordetella pertussis. *Cell,* 61**,** 1375-1382.

RELMAN, D. A., DOMENIGHINI, M., TUOMANEN, E., RAPPUOLI, R. & FALKOW, S. 1989. Filamentous hemagglutinin of Bordetella pertussis: nucleotide sequence and crucial role in adherence. *Proceedings of the national academy of sciences,* 86**,** 2637-2641.

REYES, I. S., HSIEH, D. T., LAUX, L. C. & WILFONG, A. A. 2011. Alleged cases of vaccine encephalopathy rediagnosed years later as Dravet syndrome. *Pediatrics,* 128**,** e699-e702.

ROIER, S., ZINGL, F. G., CAKAR, F., DURAKOVIC, S., KOHL, P., EICHMANN, T. O., KLUG, L., GADERMAIER, B., WEINZERL, K. & PRASSL, R. 2016a. A novel mechanism for the biogenesis of outer membrane vesicles in Gram-negative bacteria. *Nature communications,* 7**,** 10515.

ROIER, S., ZINGL, F. G., CAKAR, F. & SCHILD, S. 2016b. Bacterial outer membrane vesicle biogenesis: a new mechanism and its implications. *Microbial Cell,* 3**,** 257.

ROMAGNANI, S. 2000. T-cell subsets (Th1 versus Th2). *Annals of allergy, asthma & immunology,* 85**,** 9-21.

ROSS, P. J., SUTTON, C. E., HIGGINS, S., ALLEN, A. C., WALSH, K., MISIAK, A., LAVELLE, E. C., MCLOUGHLIN, R. M. & MILLS, K. H. 2013. Relative contribution of Th1 and Th17 cells in adaptive immunity to Bordetella pertussis: towards the rational design of an improved acellular pertussis vaccine. *PLoS pathogens,* 9**,** e1003264.

ROWE, S. L., TAY, E. L., FRANKLIN, L. J., STEPHENS, N., WARE, R. S., KACZMAREK, M. C., LESTER, R. A. & LAMBERT, S. B. 2018. Effectiveness of parental cocooning as a vaccination strategy to prevent pertussis infection in infants: a case-control study. *Vaccine,* 36**,** 2012-2019.

ROWLEY, G., SPECTOR, M., KORMANEC, J. & ROBERTS, M. 2006. Pushing the envelope: extracytoplasmic stress responses in bacterial pathogens. *Nature Reviews Microbiology,* 4**,** 383-394.

RSTUDIO, T. 2020. RStudio: integrated development for R. *Rstudio Team, PBC, Boston, MA URL http://www. rstudio. com*.

RUIZ, N., KAHNE, D. & SILHAVY, T. J. 2006. Advances in understanding bacterial outer-membrane biogenesis. *Nature Reviews Microbiology,* 4**,** 57-66.

RYAN, M., MURPHY, G., RYAN, E., NILSSON, L., SHACKLEY, F., GOTHEFORS, L., OYMAR, K., MILLER, E., STORSAETER, J. & MILLS, K. 1998. Distinct T-cell subtypes induced with whole cell and acellular pertussis vaccines in children. *Immunology,* 93**,** 1.

SAEDI, S., SAFARCHI, A., MOGHADAM, F. T., HEIDARZADEH, S., NIKBIN, V. S. & SHAHCHERAGHI, F. 2021. Fha deficient Bordetella pertussis isolates in Iran with 50 years whole cell pertussis vaccination. *Iranian journal of public health,* 50**,** 1454-1462.

SAFARCHI, A., OCTAVIA, S., LUU, L. D. W., TAY, C. Y., SINTCHENKO, V., WOOD, N., MARSHALL, H., MCINTYRE, P. & LAN, R. 2015. Pertactin negative Bordetella pertussis demonstrates higher fitness under vaccine selection pressure in a mixed infection model. *Vaccine,* 33**,** 6277-6281.

SAFARCHI, A., OCTAVIA, S., WU, S. Z., KAUR, S., SINTCHENKO, V., GILBERT, G. L., WOOD, N., MCINTYRE, P., MARSHALL, H. & KEIL, A. D. 2016. Genomic dissection of Australian Bordetella pertussis isolates from the 2008–2012 epidemic. *Journal of Infection,* 72**,** 468-477.

SAKAMOTO, H., BELLALOU, J., SEBO, P. & LADANT, D. 1992. Bordetella pertussis adenylate cyclase toxin. Structural and functional independence of the catalytic and hemolytic activities. *Journal of Biological Chemistry,* 267**,** 13598-13602.

SAUKKONEN, K., CABELLOS, C., BURROUGHS, M., PRASAD, S. & TUOMANEN, E. 1991. Integrin-mediated localization of Bordetella pertussis within macrophages: role in pulmonary colonization. *The Journal of experimental medicine,* 173**,** 1143-1149.

SCHNEIDER, T. & SAHL, H.-G. 2010. An oldie but a goodie–cell wall biosynthesis as antibiotic target pathway. *International Journal of Medical Microbiology,* 300**,** 161-169.

SCHROLL, C., BARKEN, K. B., KROGFELT, K. A. & STRUVE, C. 2010. Role of type 1 and type 3 fimbriae in Klebsiella pneumoniae biofilm formation. *BMC microbiology,* 10**,** 1-10.

SCHWECHHEIMER, C., RODRIGUEZ, D. L. & KUEHN, M. J. 2015. NlpI-mediated modulation of outer membrane vesicle production through peptidoglycan dynamics in Escherichia coli. *Microbiologyopen,* 4**,** 375-389.

SERRA, D. O., CONOVER, M. S., ARNAL, L., SLOAN, G. P., RODRIGUEZ, M. E., YANTORNO, O. M. & DEORA, R. 2011. FHA-mediated cell-substrate and cell-cell adhesions are critical for Bordetella pertussis biofilm formation on abiotic surfaces and in the mouse nose and the trachea. *PloS one,* 6**,** e28811.

SHI, H., COLAVIN, A., BIGOS, M., TROPINI, C., MONDS, R. D. & HUANG, K. C. 2017. Deep phenotypic mapping of bacterial cytoskeletal mutants reveals physiological robustness to cell size. *Current Biology,* 27**,** 3419-3429. e4.

SHIMA, F., UTO, T., AKAGI, T., BABA, M. & AKASHI, M. 2013. Size effect of amphiphilic poly (γ-glutamic acid) nanoparticles on cellular uptake and maturation of dendritic cells in vivo. *Acta biomaterialia,* 9**,** 8894-8901.

SIEGER, B., SCHUBERT, K., DONOVAN, C. & BRAMKAMP, M. 2013. The lipid II flippase RodA determines morphology and growth in C orynebacterium glutamicum. *Molecular microbiology,* 90**,** 966-982.

SILHAVY, T. J., KAHNE, D. & WALKER, S. 2010. The bacterial cell envelope. *Cold Spring Harbor perspectives in biology,* 2**,** a000414.

SKERRY, C., GOLDMAN, W. E. & CARBONETTI, N. H. 2019. Peptidoglycan Recognition Protein 4 Suppresses Early Inflammatory Responses to Bordetella pertussis and Contributes to Sphingosine-1-Phosphate Receptor Agonist-Mediated Disease Attenuation. *Infect Immun,* 87.

SKOPOVA, K., TOMALOVA, B., KANCHEV, I., ROSSMANN, P., SVEDOVA, M., ADKINS, I., BIBOVA, I., TOMALA, J., MASIN, J., GUISO, N., OSICKA, R., SEDLACEK, R., KOVAR, M. & SEBO, P. 2017. Cyclic AMP-Elevating Capacity of Adenylate Cyclase Toxin-Hemolysin Is Sufficient for Lung Infection but Not for Full Virulence of Bordetella pertussis. *Infect Immun,* 85.

SONNTAG, I., SCHWARZ, H., HIROTA, Y. & HENNING, U. 1978. Cell envelope and shape of Escherichia coli: multiple mutants missing the outer membrane lipoprotein and other major outer membrane proteins. *Journal of bacteriology,* 136**,** 280-285.

SOUFO, H. J. D. & GRAUMANN, P. L. 2003. Actin-like proteins MreB and Mbl from Bacillus subtilis are required for bipolar positioning of replication origins. *Current biology,* 13**,** 1916-1920.
SPANGRUDE, G., SACCHI, F., HILL, H., VAN EPPS, D. & DAYNES, R. 1985. Inhibition of lymphocyte and neutrophil chemotaxis by pertussis toxin. *Journal of immunology (Baltimore, Md.: 1950),* 135**,** 4135-4143.
STEIN, P. E., BOODHOO, A., ARMSTRONG, G. D., COCKLE, S. A., KLEIN, M. H. & READ, R. J. 1994a. The crystal structure of pertussis toxin. *Structure,* 2**,** 45-57.
STEIN, P. E., BOODHOO, A., ARMSTRONG, G. D., HEERZE, L. D., COCKLE, S. A., KLEIN, M. H. & READ, R. J. 1994b. Structure of a pertussis toxin–sugar complex as a model for receptor binding. *Nature structural biology,* 1**,** 591-596.
SU, S. B., SILVER, P. B., ZHANG, M., CHAN, C. C. & CASPI, R. R. 2001. Pertussis toxin inhibits induction of tissue-specific autoimmune disease by disrupting G protein-coupled signals. *J Immunol,* 167**,** 250-6.
SUZUKI, H., NISHIMURA, Y. & HIROTA, Y. 1978a. On the process of cellular division in Escherichia coli: a series of mutants of E. coli altered in the penicillin-binding proteins. *Proceedings of the National Academy of Sciences,* 75**,** 664-668.
SUZUKI, H., NISHIMURA, Y., YASUDA, S., NISHIMURA, A., YAMADA, M. & HIROTA, Y. 1978b. Murein-lipoprotein of Escherichia coli: a protein involved in the stabilization of bacterial cell envelope. *Molecular and General Genetics MGG,* 167**,** 1-9.
SWITZER, C., D'HEILLY, C. & MACINA, D. 2019. Immunological and clinical benefits of maternal immunization against pertussis: a systematic review. *Infectious Diseases and Therapy,* 8**,** 499-541.
SZWEDZIAK, P., WANG, Q., BHARAT, T. A., TSIM, M. & LÖWE, J. 2014. Architecture of the ring formed by the tubulin homologue FtsZ in bacterial cell division. *Elife,* 3**,** e04601.
TAMAKI, S., MATSUZAWA, H. & MATSUHASHI, M. 1980. Cluster of mrdA and mrdB genes responsible for the rod shape and mecillinam sensitivity of Escherichia coli. *Journal of bacteriology,* 141**,** 52-57.
TAU, G. & ROTHMAN, P. 1999. Biologic functions of the IFN-γ receptors. *Allergy,* 54**,** 1233.
TUOMANEN, E. & WEISS, A. 1985. Characterization of two adhesins of Bordetella pertussis for human ciliated respiratory-epithelial cells. *Journal of Infectious Diseases,* 152**,** 118-125.
TURNER, D. L. & FARBER, D. L. 2014. Mucosal resident memory CD4 T cells in protection and immunopathology. *Frontiers in immunology,* 5**,** 331.
UHL, M. A. & MILLER, J. F. 1996. Central role of the BvgS receiver as a phosphorylated intermediate in a complex two-component phosphorelay. *Journal of Biological Chemistry,* 271**,** 33176-33180.
VAN DEN BERG, B. M., BEEKHUIZEN, H., WILLEMS, R. J., MOOI, F. R. & VAN FURTH, R. 1999. Role of Bordetella pertussis virulence factors in adherence to epithelial cell lines derived from the human respiratory tract. *Infection and immunity,* 67**,** 1056-1062.
VAN DER LEE, S., HENDRIKX, L. H., SANDERS, E. A., BERBERS, G. A. & BUISMAN, A.-M. 2018a. Whole-cell or acellular pertussis primary immunizations in infancy determines adolescent cellular immune profiles. *Frontiers in immunology,* 9**,** 51.
VAN DER LEE, S., SANDERS, E. A., BERBERS, G. A. & BUISMAN, A.-M. 2018b. Whole-cell or acellular pertussis vaccination in infancy determines IgG subclass profiles to DTaP booster vaccination. *Vaccine,* 36**,** 220-226.
VAN STRIJP, J., RUSSELL, D., TUOMANEN, E., BROWN, E. & WRIGHT, S. 1993. Ligand specificity of purified complement receptor type three (CD11b/CD18, alpha m beta 2, Mac-1). Indirect effects of an Arg-Gly-Asp (RGD) sequence. *Journal of immunology (Baltimore, Md.: 1950),* 151**,** 3324-3336.
VARMA, A. & YOUNG, K. D. 2009. In Escherichia coli, MreB and FtsZ direct the synthesis of lateral cell wall via independent pathways that require PBP 2. *Journal of bacteriology,* 191**,** 3526-3533.

VOLGERS, C., SAVELKOUL, P. H. & STASSEN, F. R. 2018. Gram-negative bacterial membrane vesicle release in response to the host-environment: different threats, same trick? *Critical Reviews in Microbiology,* 44**,** 258-273.
VOLLMER, W. 2008. Structural variation in the glycan strands of bacterial peptidoglycan. *FEMS microbiology reviews,* 32**,** 287-306.
WACHI, M., DOI, M., TAMAKI, S., PARK, W., NAKAJIMA-IIJIMA, S. & MATSUHASHI, M. 1987. Mutant isolation and molecular cloning of mre genes, which determine cell shape, sensitivity to mecillinam, and amount of penicillin-binding proteins in Escherichia coli. *Journal of bacteriology,* 169**,** 4935-4940.
WALSH, C. 1989. Enzymes in the D-alanine branch of bacterial cell wall peptidoglycan assembly. *Journal of biological chemistry,* 264**,** 2393-2396.
WANG, Y. 2002. The function of OmpA in Escherichia coli. *Biochemical and biophysical research communications,* 292**,** 396-401.
WARFEL, J. M., BEREN, J., KELLY, V. K., LEE, G. & MERKEL, T. J. 2012. Nonhuman primate model of pertussis. *Infection and immunity,* 80**,** 1530-1536.
WARFEL, J. M., ZIMMERMAN, L. I. & MERKEL, T. J. 2014. Acellular pertussis vaccines protect against disease but fail to prevent infection and transmission in a nonhuman primate model. *Proceedings of the National Academy of Sciences,* 111**,** 787-792.
WARFEL, J. M., ZIMMERMAN, L. I. & MERKEL, T. J. 2016. Comparison of three whole-cell pertussis vaccines in the baboon model of pertussis. *Clinical and Vaccine Immunology,* 23**,** 47-54.
WEIGAND, R. A., VINCI, K. D. & ROTHFIELD, L. I. 1976. Morphogenesis of the bacterial division septum: a new class of septation-defective mutants. *Proceedings of the National Academy of Sciences,* 73**,** 1882-1886.
WELSBY, P. 1985. The epidemiology of pertussis and pertussis immunisation in the united kingdom and the united states: a comparative study: Cherry, H. Curr Probl Pediatr February 1984. Year Book Medical Publishers Inc. *Journal of Infection,* 11**,** 183.
WENDELBOE, A. M., VAN RIE, A., SALMASO, S. & ENGLUND, J. A. 2005. Duration of immunity against pertussis after natural infection or vaccination. *The Pediatric infectious disease journal,* 24**,** S58-S61.
WESSEL, A. K., LIEW, J., KWON, T., MARCOTTE, E. M. & WHITELEY, M. 2013. Role of Pseudomonas aeruginosa peptidoglycan-associated outer membrane proteins in vesicle formation. *Journal of bacteriology,* 195**,** 213-219.
WHATMORE, A. M., CHUDEK, J. A. & REED, R. H. 1990. The effects of osmotic upshock on the intracellular solute pools of Bacillus subtilis. *Microbiology,* 136**,** 2527-2535.
WHITE, C. L., KITICH, A. & GOBER, J. W. 2010. Positioning cell wall synthetic complexes by the bacterial morphogenetic proteins MreB and MreD. *Molecular microbiology,* 76**,** 616-633.
WHO 2015. Pertussis vaccines: WHO position paper—August 2015. *Weekly Epidemiological Record= Relevé épidémiologique hebdomadaire.*
WICKHAM, H. 2016. ggplot2: Elegant Graphics for Data Analysis. Springer-Verlag, New York. ISBN 978-3-319-24277-4.
WILK, M. M., BORKNER, L., MISIAK, A., CURHAM, L., ALLEN, A. C. & MILLS, K. H. 2019. Immunization with whole cell but not acellular pertussis vaccines primes CD4 TRM cells that sustain protective immunity against nasal colonization with Bordetella pertussis. *Emerging microbes & infections,* 8**,** 169-185.
WILK, M. M., MISIAK, A., MCMANUS, R. M., ALLEN, A. C., LYNCH, M. A. & MILLS, K. H. 2017. Lung CD4 tissue-resident memory T cells mediate adaptive immunity induced by previous infection of mice with Bordetella pertussis. *The Journal of Immunology,* 199**,** 233-243.
WILLEMS, R. J., VAN DER HEIDE, H. G. & MOOI, F. R. 1992. Characterization of a Bordetella pertussis fimbrial gene cluster which is located directly downstream of the filamentous haemagglutinin gene. *Molecular microbiology,* 6**,** 2661-2671.

WILLIAMS, C. L., BOUCHER, P. E., STIBITZ, S. & COTTER, P. A. 2005. BvgA functions as both an activator and a repressor to control Bvgi phase expression of bipA in Bordetella pertussis. *Molecular microbiology,* 56**,** 175-188.

WILSON, R. P., RAFFATELLU, M., CHESSA, D., WINTER, S. E., TÜKEL, Ç. & BÄUMLER, A. J. 2008. The Vi-capsule prevents Toll-like receptor 4 recognition of Salmonella. *Cellular microbiology,* 10**,** 876-890.

WINTER, K., ZIPPRICH, J., HARRIMAN, K., MURRAY, E. L., GORNBEIN, J., HAMMER, S. J., YEGANEH, N., ADACHI, K. & CHERRY, J. D. 2015. Risk Factors Associated With Infant Deaths From Pertussis: A Case-Control Study. *Clin Infect Dis,* 61**,** 1099-106.

WORTHINGTON, Z. E. & CARBONETTI, N. H. 2007. Evading the proteasome: absence of lysine residues contributes to pertussis toxin activity by evasion of proteasome degradation. *Infection and immunity,* 75**,** 2946-2953.

XU, Z., OCTAVIA, S., LUU, L. D. W., PAYNE, M., TIMMS, V., TAY, C. Y., KEIL, A. D., SINTCHENKO, V., GUISO, N. & LAN, R. 2019. Pertactin-negative and filamentous hemagglutinin-negative Bordetella pertussis, Australia, 2013–2017. *Emerging infectious diseases,* 25**,** 1196.

YANCEY, P. H., CLARK, M. E., HAND, S. C., BOWLUS, R. D. & SOMERO, G. N. 1982. Living with water stress: evolution of osmolyte systems. *Science,* 217**,** 1214-1222.

YEH, Y.-C., COMOLLI, L. R., DOWNING, K. H., SHAPIRO, L. & MCADAMS, H. H. 2010. The Caulobacter Tol-Pal complex is essential for outer membrane integrity and the positioning of a polar localization factor. *Journal of bacteriology,* 192**,** 4847-4858.

YUK, M. H., COTTER, P. A. & MILLER, J. F. 1996. Genetic Regulation of Airway Colonization in Bordetella Species. *American journal of respiratory and critical care medicine,* 154**,** S150.

ZURITA, M. E., WILK, M. M., CARRIQUIRIBORDE, F., BARTEL, E., MORENO, G., MISIAK, A., MILLS, K. H. & HOZBOR, D. 2019. A pertussis outer membrane vesicle-based vaccine induces lung-resident memory CD4 T cells and protection against Bordetella pertussis, including pertactin deficient strains. *Frontiers in cellular and infection microbiology,* 9**,** 125.